学位論文

Research on lattice fermions based on graph theory and topology

グラフ理論とトポロジーに基づく格子フェルミオンの研究

令和5年度 博士（理学）申請

秋田大学大学院理工学研究科
総合理工学専攻

湯本 純

Research on lattice fermions based on graph theory and topology

Jun Yumoto

Abstract

In this thesis, we explore the relationship between lattice field theory and graph theory, placing special emphasis on two things: the interplay between Dirac lattice operators and matrices associated with graphs within the realm of spectral graph theory, and a new conjecture, which we propose, on the relation between the species of lattice fermions and the topology of the manifold the fermion is defined.

Beyond delving into fundamental concepts of spectral graph theory, such as degree and Laplacian matrices, we introduce a novel matrix named as "anti-symmetrized adjacency matrix", specifically tailored for cycle digraphs (T^1-lattice) and simple directed paths (B^1-lattice). The one of nontrivial relations between graph theory matrices and lattice operators is that the lattice action can be given by the bilinear form of an anti-symmetrized adjacency matrix and a vector of fermion fields. It means that the anti-symmetrized adjacency matrix, along with its extensions to higher dimensions, are equivalent to the matrix-representation of the naive lattice Dirac operators. Accordingly, we identify the number of "fermion species" as the number of zero-eigenvalues of the anti-symmetrized adjacency matrix. Furthermore, the number of fermion species is given by the topology of the weighted digraph. In particular, the maximum number of them is uniquely determined by the number of cycle digraphs in the whole digraph.

Our conjecture claims that a maximum number of fermion species on a finite lattice defined by discretizing D-dimensional manifold is equal to the summation of the Betti numbers of the manifold when the lattice fermion has several basic properties, including locality, γ_5-hermiticity, and hermiticity. For this conjecture, we can be provide rigorous proofs.

The maximum count of fermion species in a free lattice fermion operator is equivalent to the cumulative sum of all Betti numbers when the D-dimensional graph results from a cartesian product of cycle digraphs (T^1 lattice) and simple directed paths (B^1 lattice).

Contents

Chapter 1

Introduction

The lattice discretization of the field theory [1] is one of the most powerful tools to non-perturbative aspects of quantum gauge theories such as Quantum Chromo Dynamics (QCD). The lattice field theory are defined on the discrete euclidean space (or lattice) with a lattice constant $c_{\rm lat}$. Accordingly, the continuum field theory is equivalent to the quantum mechanics with uncountably infinite degrees of freedom while the lattice theory is equivalent to the quantum mechanics with countably infinite degrees of freedom. When we consider the finite volume of the lattice, the degrees of freedom are finite thus the lattice theory is equivalent to the quantum mechanics with finite degrees of freedom. In other words, the path integral can be calculated by using ab initio methods. In such a mathematically well-defined theory, we can calculate quantities in a non-perturbative way and there are no divergences in the lattice theory that occur in continuum theory. And one of outstanding advantages in the lattice field theory is that the gauge field is quantized in a gauge-invariant way: The gauge field on the lattice, which is called a link variable, is defined on the link of lattice sites as an element of the gauge group. The gauge-symmetric action is defined as a closed loop called a plaquette action. Non-perturbative physics has been investigated by lattice gauge field theory and use of the numerical Monte-Carlo simulation on lattice field theory [2].

However, there is a notorious problem called "Fermion doubling" in the lattice theory. This problem is that the chirally-symmetric fermion action on the lattice inevitably obtains degenerate degrees of freedom in a multiple number of two if we impose basic presuppositions as locality, translation symmetry and hermiticity. We call these multiple fermions "fermion species". This multiplicity of fermions on the lattice originates from the boundary condition for the finite volume lattice. The lattice with periodic boundary condition can be regarded as the D-dimensional torus spacetime. The no-go theorem by Nielsen and Ninomiya [3–5] uncovers the background of this multiplicity by relating the Dirac operator of lattice fermions to the Poincaré–Hopf theorem [6], which shows the relation between the Euler characteristic $\chi(M)$ of the compact and orientable differentiable manifold M and the index of the vector function defined on M. In the case of lattice fermions, the Dirac operator in the momentum space can be regarded as a vector function defined on the torus up to the γ-matrix where the Euler characteristic is zero. The index here stands for the net number of zeros of the vector function, counted with signs $\pm$ depending on the slope of the zero crossing. For the Dirac operator this index

is identified as the chiral charge for each species, which means the sign in front of γ_5 differently assigned to each zero. A conclusion from the Poincaré–Hopf theorem is that the index should be zero for the zero Euler characteristic. This means that the number of zeros of the Dirac operator with a positive chiral charge should be equal to the number of zeros with a negative chiral charge. Lattice fermions should therefore appear in a multiple number of two, half of which have a positive chiral charge or chirality and the others have a negative charge.

One of the methods to avoid fermion doubling is Wilson fermion [7]. In this formulation we add a chiral symmetry breaking term called the Wilson term to the naive fermion action, which assigns O(1/a) mass to doublers. In the classical continuum limit we acquire a single fermion mode because doublers are decoupled with infinite mass. As others methods, Domain-wall or overlap fermions [8–12], and staggered fermions [13–19] have been proposed to bypass the problems and have been broadly used in the lattice simulation. Apart from them, relatively new approaches have been proposed, including the generalized Wilson fermions [20–27], the staggered-Wilson fermions [17,24,28–39], the minimally doubled fermion [40–60] and the central-branch Wilson fermion [24,32,61,62]. However, we will not discuss these formulations in this thesis because it is a digression from the main point of the story.

In the our works [63,64], we figured out the non-trivial relation between spectral graph theory and lattice field theory, and investigated the number of zero-eigenvalues of lattice Dirac operators in terms of graph theory. We proposed a conjecture [64] claiming, "*under certain conditions, the maximal number of Dirac zero-modes of a free lattice fermion is equal to the sum of Betti numbers of the graph (lattice) on which the fermion is defined*". This conjecture is consistent with the known fact on naive lattice fermions: the species of the four-dimensional naive fermion is sixteen, which is interpreted as the sum of the Betti number of four-dimensional torus (T^4). This thesis organizes and systematically relates these works and adds recent work.

we investigate operators in lattice field theory using spectral graph theory and present partial evidence supporting the conjecture regarding the interplay between Dirac zero-modes and the Betti numbers of the graph [64]. Beyond fundamental concepts in graph theory, such as the adjacency matrix and Laplacian matrix, we introduce an "anti-symmetrized adjacency matrix" and explore its rank in relation to graph topology. It is noteworthy that the anti-symmetrized adjacency matrix, along with its higher-dimensional extensions, coincide with a naive Dirac operator for the free lattice theory. Leveraging this equivalences, we elucidate the counts of fermion species for free Dirac operators on the lattice, linking them to Betti numbers associated with graph topology: The maximal number of fermion species for a free fermion operator is equated to the sum of all Betti numbers of the graph (lattice). This holds true for D-dimensional graphs structured as cartesian products of cycle digraphs (T^1 lattice) and simple directed paths (B^1 lattice). We also discuss our result indicating that the naive and massless fermion on a certain graph corresponding to a D-dimensional sphere has two fermion species, which is consistent to the fact that the sum of Betti numbers of the D-dimensional sphere is two.

This thesis is constructed as follows: In Chapter. 2 we review lattice field theory. We review naive fermion and Wilson fermion. In Chapter. 3 we review graph theory and matrices defined in the theory. We review the basic theorems and show a novel theorem

regarding the anti-symmetrized adjacency matrix. In Chapter. 4 we study lattice Dirac fields in terms of graph theory, and derive the number of fermion species by use of the novel theorem. In Chapter. 5 we propose a new conjecture about the relation between fermion species and topology. And we prove the theorems on the femrion species. Chapter. 6 is devoted to the summary and discussion.

Chapter 2

Lattice field theory

In this chapter, we will review the lattice fermions. This chapter is divided into four sections. The fist section will review the naive fermion, placing special emphasis on the spectra of lattice Dirac operator and fermion species. And we will mention a problem in lattice field theory called "fermion doubling". Furthermore, we will review a theorem about fermion species. The theorem called as "Nielsen–Ninomiya no-go theorem", claims that multiple fermion species appear when the necessary physical conditions are imposed on the lattice fermion action. In the remaining two sections, we will review "Wilson fermion" and "Domain-wall fermion" as methods of avoiding the fermion doubling.

Before this discussion, we define the lattice field theory. Let Lat be a finite volume D-dimensional hypercubic lattice[1] bellow

$$Lat \equiv \left\{ n = c_{\text{lat}} \sum_{\mu=1}^{D} n_\mu \hat{\mu} \;\middle|\; n_\mu \in [1, N_\mu] \subset \mathbb{N} \right\} \tag{2.1}$$

where c_{lat} is the lattice constant, which is a minimum length between sites on each direction in the lattice. And $\hat{\mu}$ is the standard basis in D-dimensional hypercubic lattice, which is the object between the closest lattice sites. We term it as "μ-link". Its sites are represented by D integer as $n = (n_1, n_2, \cdots, n_D)$. For simplicity, we consider that the lattice constant is $c_{\text{lat}} = 1$. In this chapter, we consider the lattice with periodic boundary condition unless otherwise stated. The lattice is defined as

$$Lat_{\text{periodic}} \equiv \left\{ n = \sum_{\mu=1}^{D} n_\mu \hat{\mu} \;\middle|\; \begin{array}{c} \exists N_\mu \in \mathbb{N} \quad \text{s.t.} \quad n + N_\mu \hat{\mu} \sim n \,, \\ n_\mu \in [1, N_\mu] \subset \mathbb{N} \end{array} \right\} \tag{2.2}$$

where the added conditions are the periodic boundary condition.

In the lattice field theory, the field is defined on the lattice sites. It is given by ψ_n for $n \in Lat$. We mention one advantage of the lattice field theory. It is that the gauge field is quantized in a gauge invariant way. The gauge field on the lattice is defined on the link between lattice sites as an element in the compact gauge group such as the Lie group: $U(N)$ and $SU(N)$. It is given by $U_{n,\mu} = \exp\left[igc_{\text{lat}} A_\mu(n)\right]$ with the coupling constant

[1] Lattice field theory can be defined on Euclidean space. However, for convenience we define this theory restrictively to the finite volume D-dimensional hypercubic lattice in this these.

g and the gauge field A_μ. The gauge field A_μ is an element in the Lie algebra since $A_\mu \equiv \sum_a A^a_\mu(n) T^a \in \mathcal{SU}(N)$ where T^a is a generator of Lie algebra $\mathcal{SU}(N)$. Here, $\mathcal{SU}(N)$ is the Lie algebra $\mathcal{SU}(N)$ for $SU(N)$. The generator T^a is N-square matrix satisfying

$$\mathrm{tr}\, T^a = 0\,, \qquad (T^a)^\dagger = T^a \tag{2.3}$$

$$\mathrm{tr}\, T^a T^b = \frac{1}{2}\delta_{ab}\,, \qquad \left[T^a, T^b\right] = i f^{abc} T^c \tag{2.4}$$

where tr is the trace of the matrix and $[A, B]$ is $\left[T^a, T^b\right] \equiv AB - BA$. Furthermore, we introduce the gauge coupling g and the corresponding gauge field $A_\mu(n)$ in the continuum. The link variable is assumed to satisfy $U_{n+\hat{\mu},-\mu} = U^\dagger_{n,\mu}$. The case of two dimensions with the link variable is depicted in Fig. 2.1

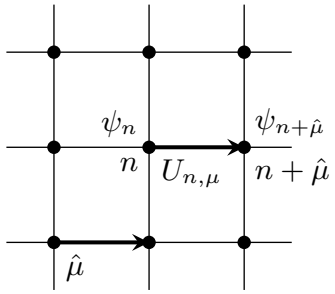

Figure 2.1: The two dimensional lattice and the fields defined on its sites. Here, ψ_n is the fields.

2.1 Naive fermon

In this section we will review the naive lattice fermion from the view points of the spectra of the lattice Dirac operator and the fermion species.

Firstly, we discuss about the lattice fermion action of the naive fermion. We consider the lattice as Lat_{periodic} since the translation invariance is imposed on the four-dimensional hyeprcubic lattice. In the later chapter, this lattice is equivalent to T^4-lattice. Then, a lattice action of naive fermion is given by

$$S_{\mathrm{nf}} = c^4_{\mathrm{lat}} \sum_n \sum_{\mu=1}^{4} \frac{1}{2c_{\mathrm{lat}}} \left[\bar{\psi}_n \gamma_\mu U_{n,\mu} \psi_{n+\hat{\mu}} - \bar{\psi}_{n+\hat{\mu}} \gamma_\mu U^\dagger_{n,\mu} \psi_n + m \bar{\psi}_n \psi_n\right] \tag{2.5}$$

where ψ_n, m are the fermionic fields and mass for fermions with a dimensions $1/c_{\mathrm{lat}}$, respectively. And $U_{n,\mu}$ is called the link variable. γ-matrices and $U_{n,\pm\mu}$ act on the fermionic fields ψ_n. The sum $\sum_n$ is the summation over lattice sites $n = (n_1, n_2, n_3, n_4)$ in the lattice. In lattice field theory we can nondimensionalize fermion actions by redefining fields and

mass as $c_{\rm lat}^{3/2}\psi_n \to \psi_n$ and $mc_{\rm lat} \to m$. The dimensionless actions are given by

$$\begin{aligned} S_{\rm nf} &= \sum_n \sum_{\mu=1}^{4} \frac{1}{2} \left[\bar{\psi}_n \gamma_\mu U_{n,\mu} \psi_{n+\hat{\mu}} - \bar{\psi}_{n+\hat{\mu}} \gamma_\mu U_{n,\mu}^\dagger \psi_n + m \bar{\psi}_n \psi_n \right] \\ &= \sum_n \sum_{\mu=1}^{4} \bar{\psi}_n \gamma_\mu D_\mu \psi_n \end{aligned} \tag{2.6}$$

where $D_\mu \equiv \left(T_{+\mu} - T_{-\mu}\right)/2$ with $T_{\pm\mu}\psi_n = U_{n,\pm\mu}\psi_{n\pm\hat{\mu}}$. We term D_μ as "lattice Dirac operator". In a free theory, we just set $U_{n,\mu} = \mathbf{1}$. If we consider the free naive fermion, the lattice fermion action is given by

$$S_{\rm nf}^{\rm free} = \frac{1}{2} \sum_n \sum_{\mu=1}^{4} \left[\bar{\psi}_n \gamma_\mu \psi_{n+\hat{\mu}} - \bar{\psi}_{n+\hat{\mu}} \gamma_\mu \psi_n + m \bar{\psi}_n \psi_n \right] \tag{2.7}$$

and 16 fermion species are known to occur in the theory. The case of two dimensions is depicted in Fig. 2.2.

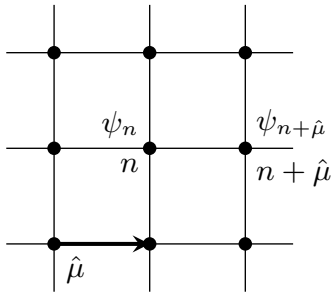

Figure 2.2: In the free theory, the two dimensional lattice and the fields defined on its sites.

Secondary, we discuss a notorious problem called a "doubling problem" in the lattice field theory. To show this problem, let us look into this by rewriting a free lattice fermion action in the momentum expression with the lattice spacing being explicit as

$$\begin{aligned} S_{\rm nf}^{\rm free} &= \int_{-\pi/c_{\rm lat}}^{\pi/c_{\rm lat}} \frac{d^4p}{(2\pi)^4} \, \bar{\psi}(-p) \left[i \sum_{\mu=1}^{4} \gamma_\mu \sin\left(c_{\rm lat} p_\mu\right) + m \right] \psi(p) \\ &= \int_{-\pi/c_{\rm lat}}^{\pi/c_{\rm lat}} \frac{d^4p}{(2\pi)^4} \, \bar{\psi}(-p) D(p) \psi(p) \end{aligned} \tag{2.8}$$

where we define the 4-vector momentum as p_μ for $\mu = 1, 2, 3, 4$. And $D(p)$ is the Dirac operator in the momentum space. The four-dimensional lattice (or discretization space time) results in restriction of the euclidean momentum space as $-\pi/c_{\rm lat} < p_\mu \leq \pi/c_{\rm lat}$, which is called the Brillouin zone. Then, a lattice fermion propagator obtained from this action is given by

$$G_{\rm nf}(p) = D^{-1}(p) = \frac{-is(p) + m}{s^2(p) + m^2} \tag{2.9}$$

where $s(p) \equiv \sum_{\mu=1}^{4} \gamma_\mu \sin(c_{\text{lat}} p_\mu)$. The zero point of the Dirac operator or the pole of the lattice fermion propagator in the momentum space $D(p) = s(p) + m = 0$ corresponds fermion degrees of freedom. In the massless case, this Dirac operator has 16 zeros within the Brillouin zone since the momentum p_μ takes 0 or π/c_{lat}. The spectra of Dirac operator in the case of four-dimensional lattice with 16^4 sites is depicted in Fig. 2.3. Then, the

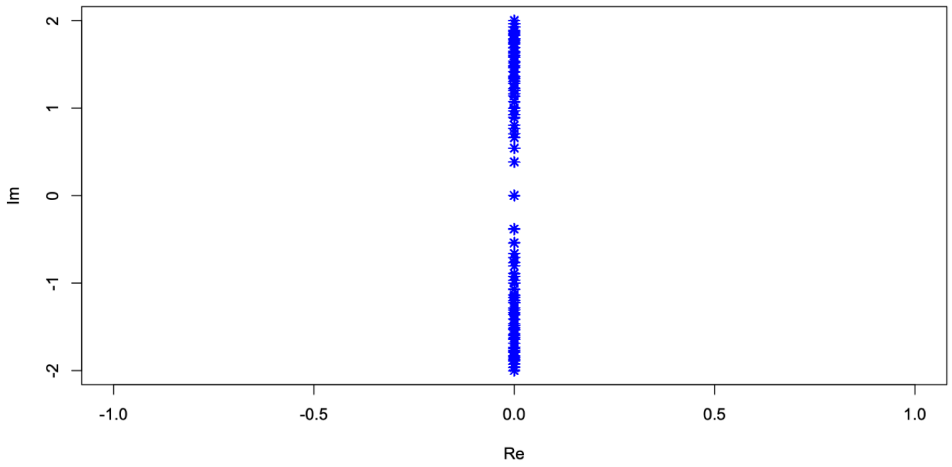

Figure 2.3: The spectra of Dirac operator in the case of four-dimensional lattice with 16^4 sites. 16 degeneracies exist at zero.

number of zeros is 16. In the D-dimensions, the Dirac operator has 2^D zeros since the D-dimensional Dirac operator in the momentum space is $D(p) = i \sum_{\mu=1}^{D} \gamma_\mu \sin(c_{\text{lat}} p_\mu) + m$. What multiple zeros appear in this way is called "fermion doubling". And these zeros are called "fermion species" (or doubler).

2.2 Nielsen–Ninomiya no-go theorem

In the previous section, we discussed about the naive fermion and fermion doubling. In particular, we showed how fermion doubling occurs in term of the spectra of Dirac operator.

This section is discussed about a notorious theorem about fermion doubling and its proof This theorem is called "Nielsen–Ninomiya no-go theorem" [3–5]. The theorem claims below.

Theorem 1 (Nielsen–Ninomiya no-go theorem)**.** *Let S be a free lattice fermion action on the finite volume four-dimensional hypercubic lattice. This action satisfies five conditions:*

(a) bilinear form of the fermion fields, (b) chiral symmetry,
(c) translation invariance, (d) hermiticity, (e) locality.

Then, the multiple fermion species appear in the lattice theory.

The proof is based on the work of Karsten [40].

Proof. For the assumed conditions, the lattice action have to satisfy as follows:

(a) The lattice fermion action is given by

$$S_{\rm f} = \sum_{x,y} \bar{\psi}(x) F(x,y) \psi(y) \tag{2.10}$$

where $\psi(x)$ is defined on the lattice sites and $F(x,y)$ is a function acting on the fermion fields $\psi(x)$ and depending two lattice site x, y.

(b) The lattice action must have the invariant for the chiral transformation defined as $\psi' = e^{i\theta\gamma_5}\psi$ and $\bar{\psi}' = \psi e^{i\theta\gamma_5}$. Accordingly, the lattice action can be written as

$$S_{\rm f} = \sum_{x,y} \sum_{\mu=1}^{D} \bar{\psi}(x) \gamma_\mu F_\mu(x,y) \psi(y) \tag{2.11}$$

where $F_\mu(x,y)$ are a function of the classical number, which corresponds the lattice Dirac operator. Indeed, this lattice action has the chiral symmetry since the lattice action performed the chiral transformation is

$$S'_{\rm f} = \sum_{x,y} \sum_{\mu=1}^{D} \bar{\psi}'(x) \gamma_\mu F_\mu(x,y) \psi'(y) = S_{\rm f} \tag{2.12}$$

where we used $\gamma_\mu\gamma_5 = -\gamma_5\gamma_\mu$. Note that what the mass term adds to the lattice action is forbidden since the lattice action with the mass term m breaks the chiral symmetry below

$$\begin{aligned} S'_{\rm f,m} &= \sum_{x,y} \sum_{\mu=1}^{D} \bar{\psi}'(x) \left\{ \gamma_\mu F_\mu(x,y) + m \right\} \psi'(y) \\ &= S_{\rm f} + m \sum_{x,y} \sum_{\mu=1}^{D} \bar{\psi}(x) e^{2i\theta\gamma_5} \psi(y) \,. \end{aligned} \tag{2.13}$$

(c) For this condition, the function $F(x,y)$ only depends on $x-y$, i.e. $F_\mu(x,y) = F_\mu(x-y)$. Meanshile, The lattice action can be rewritten as the action in the momentum space with a momentum p.

By use of the chiral symmetry and the bilinear form of the fermion fields, the lattice action is given by

$$S_{\rm f} = \sum_{x,y} \sum_{\mu=1}^{D} \bar{\psi}(x) \gamma_\mu F_\mu(x,y) \psi(y) \tag{2.14}$$

where $\psi(x)$ is defined on the lattice sites and $F_\mu(x,y)$ are a function of the classical number, which corresponds the lattice Dirac operator. Indeed, for the chiral transformation, which is defined as $\psi' = e^{i\theta\gamma_5}\psi$ and $\bar{\psi}' = \psi e^{i\theta\gamma_5}$, the lattice action is

$$S'_{\rm f} = \sum_{x,y} \sum_{\mu=1}^{D} \bar{\psi}'(x) \gamma_\mu F_\mu(x,y) \psi'(y) = S_{\rm f} \tag{2.15}$$

where we used $\gamma_\mu\gamma_5 = -\gamma_5\gamma_\mu$. For the translation invariance, the lattice action is rewritten as the action in the momentum space with a momentum p. Furthermore, the function $F(x,y)$ only depends on $x-y$, i.e. $F(x,y) = F_\mu(x-y)$. The hermiticity causes the function $F_\mu(x-y)$ to be a real function since $F^*(x-y) = F_\mu(x-y)$. To the function $F_\mu(x-y)$ satisfy the locality, we assume $|x-y|F_\mu(x-y) \to 0$ for $|x-y| \to \infty$. This means the Fourier transform of $F_\mu(x-y)$ is continuous.

As a result, the lattice action in the momentum space is given by

$$S_{\rm f} = \int_{-\pi/c_{\rm lat}}^{\pi/c_{\rm lat}} \frac{d^4p}{(2\pi)^4}\,\bar{\psi}(-p)\left[\, i\sum_\mu \gamma_\mu F_\mu(p)\right]\psi(p) \tag{2.16}$$

where $F_\mu(p)$ is the Fourier transform of $F_\mu(x-y)$. Furthermore, the function $F_\mu(p)$ is a continuous and real vector field defined on the four-dimensional torus. Since an inverse of propagator for this action in the Brillouin zone should be approximated to the Dirac operator, the inverse of propagator for this action in the Brillouin zone is

$$G^{-1}(p) = i\sum_\mu \gamma_\mu \tilde{p}_\mu + O(\tilde{p}^2) = i\sum_\mu \gamma_\mu F_\mu(p) \tag{2.17}$$

where $\tilde{p}$ is a physical momentum defined by $\tilde{p} \equiv (p-\bar{p})^2$. Accordingly, zeros of $F_\mu(p)$ corresponds to the zeros of Dirac operator. Here, by use of Poincaré–Hopf theorem multiple zeros of $F_\mu(p)$ appear since the Euler characteristic of the four-dimensional torus is zero. □

As an example of this theorem, we showed the naive fermion in the previous section. The latice action of naive fermion satisfies the bilinear form, the hermiticity, and locality. And it has the translation invariance and the chiral symmetry since this action has the periodicity of the lattice sites in each direction and no terms breaking the chiral symmetry (mass term). As shown in the previous section, the fermion doubling occurs in the naive fermion and the number of fermion species is sixteen.

In addition, an obtained important consequence of this theorem is that the fermion doubling can be avoided by breaking at least one of its conditions. In subsequent sections, we will review "Willson fermion" and "Domain-wall fermion" as ways to avoid fermion doubling.

2.3 Wilson fermion

In the previous sections, we showed the naive lattice femrion. In this and the following sections, we will introduce two methods to avoid fermion doubling. In particular, this section is discussed about Wilson fermoin.

Let us review about Wilson femrion. The Wilson fermion lifts degeneracy of sixteen species into five branches by introducing the species-splitting term called the Wilson term, which breaks the chiral symmetry explicitly. The free action for Wilson fermion in

four-dimensions is given by

$$\begin{aligned} S_{\rm Wf} &= \sum_n \sum_{\mu=1}^{4} \bar{\psi}_n \gamma_\mu D_\mu \psi_n + m \sum_n \bar{\psi}_n \psi_n + r \sum_n \sum_{\mu=1}^{4} \bar{\psi}_n \left(1 - C_\mu\right) \psi_n \\ &= S_{\rm nf} + S_{\rm W} \end{aligned} \tag{2.18}$$

where $D_\mu \equiv \left(T_{+\mu} - T_{-\mu}\right)/2$ and $C_\mu \equiv \left(T_{+\mu} + T_{-\mu}\right)/2$ with $T_{\pm\mu}\psi_n = U_{n,\pm\mu}\psi_{n\pm\hat{\mu}}$. m is a mass parameter and r is a Wilson parameter. $S_{\rm nf}$ is the naive lattice fermion action in Eq. (4.32) and $S_{\rm W}$ is the Wilson term. Note that the lattice on which this Wilson fermion is defined is T^4-lattice in Eq. (4.31). So, we consider the lattice with the periodic boundary condition in each direction. The Wilson term is explicitly expressed as

$$S_{\rm W} = m \sum_n \bar{\psi}_n \psi_n - \frac{r}{2} \sum_n \sum_{\mu=1}^{4} \left[\bar{\psi}_n U_{n,\mu} \psi_{n+\hat{\mu}} + \bar{\psi}_{n+\hat{\mu}} U^\dagger_{n,\mu} \psi_n - 2\bar{\psi}_n \psi_n \right] . \tag{2.19}$$

In a free theory, the Wilson term is

$$S_{\rm W}^{\rm free} = m \sum_n \bar{\psi}_n \psi_n - \frac{r}{2} \sum_n \sum_{\mu=1}^{4} \left[\bar{\psi}_n \psi_{n+\hat{\mu}} + \bar{\psi}_{n+\hat{\mu}} \psi_n - 2\bar{\psi}_n \psi_n \right] \tag{2.20}$$

because of $U_{n,\mu} = \mathbf{1}$. In the momentum space the free action is given by

$$S_{\rm Wf}^{\rm free} = \int_{-\pi}^{\pi} dp \left[\bar{\psi}(p) \left\{ \sum_{\mu=1}^{4} i\gamma_\mu \sin p_\mu + m + r \sum_{\mu=1}^{4} \left(1 - \cos p_\mu\right) \right\} \psi(p) \right] \tag{2.21}$$

since we take Fourier transform

$$\psi_n = \int_{-\pi}^{\pi} dp\, e^{-inp} \psi(p) \tag{2.22}$$

with $np \equiv \sum_{\mu=1}^{4} n_\mu p_\mu$. Accordingly, what was the fermion species in the naive fermion has the mass $M(p)$ which depends on the mass parameter and the Wilson parameter as follows:

$$M(p) = \begin{cases} m & \text{any } p_\mu = 1 \text{ in } p. \\ m + 2r & \text{one } p_\mu = \pi/c_{\rm lat} \text{ otherwise } p_\mu = 0 \text{ in } p. \\ m + 4r & \text{two } p_\mu = \pi/c_{\rm lat} \text{ otherwise } p_\mu = 0 \text{ in } p. \\ m + 6r & \text{three } p_\mu = \pi/c_{\rm lat} \text{ otherwise } p_\mu = 0 \text{ in } p. \\ m + 8r & \text{any } p_\mu = \pi/c_{\rm lat} \text{ in } p. \end{cases} . \tag{2.23}$$

By restoring the lattice spacing as $m \to m c_{\rm lat}$ and $M(p) \to c_{\rm lat} M(p)$, the mass is rewritten as

$$M(p) = \begin{cases} m & \text{any } p_\mu = 1 \text{ in } p. \\ m + 2r/c_{\rm lat} & \text{one } p_\mu = \pi/c_{\rm lat} \text{ otherwise } p_\mu = 0 \text{ in } p. \\ m + 4r/c_{\rm lat} & \text{two } p_\mu = \pi/c_{\rm lat} \text{ otherwise } p_\mu = 0 \text{ in } p. \\ m + 6r/c_{\rm lat} & \text{three } p_\mu = \pi/c_{\rm lat} \text{ otherwise } p_\mu = 0 \text{ in } p. \\ m + 8r/c_{\rm lat} & \text{any } p_\mu = \pi/c_{\rm lat} \text{ in } p. \end{cases} . \tag{2.24}$$

When we take the contium limit ($c_{\rm lat} \to 0$), the masses other than m diverge in the continuum limit. It means that for 16 fermion species of the naive fermion, 1 species is reserved and the other species are split as unphysical poles. The complex Dirac spectra of the free and $m = 0$, $r = 1$ case is depicted in Fig. 2.4. However if we take $m = -2$ and

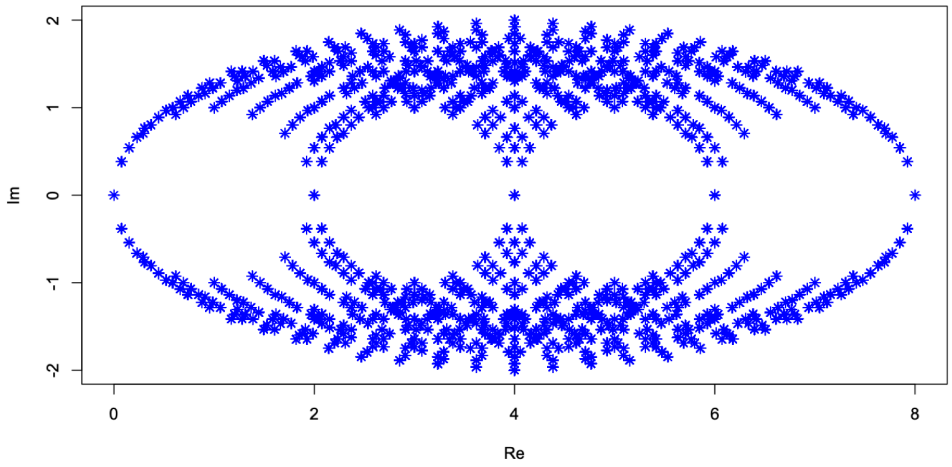

Figure 2.4: The complex Dirac spectra for Wilson fermion of the free and $m = 0$, $r = 1$. There are five branches where 1, 4, 6, 4 and 1 fermion modes correspond. The most left branch is called a physical branch.

$r = 1$, the of Dirac operator has 4 zeros since the Dirac operator is

$$D(p) = \sum_{\mu=1}^{4} \Big\{ i\gamma_\mu \sin p_\mu + (1 - \cos p_\mu) \Big\} - 2 \tag{2.25}$$

and the momentum of the zeros are

$$p = (\pi, 0, 0, 0)\,, (0, \pi, 0, 0)\,, (0, 0, \pi, 0)\,, (0, 0, 0, \pi) \tag{2.26}$$

where we assume $c_{\rm lat} = 1$ This choice of the mass parameter describe four fermions at least classically. Besides, for m $= -4$ we have six modes while we have four modes for m $= -6$. For m $= -8$ we again have a single mode. The sum of them are sixteen. Thus the fermion modes which we obtain from the Wilson fermion depends on the choice of the mass parameter. We call these five choices of the mass parameter "branches".

2.4 Domain-wall fermion

In the previous section, we introduced the Wilson fermion as one of methods to avoid the fermion doubling. This method made branching fermion species by adding a mass term called "Wilson term" into the lattice action. However, there is a breaking chiral symmetry in this lattice action. Since it conflicts with the conditions of no-go theorem, we can avoid fermion-doubling in a simple way.

In this section, we will review another method to avoid the problem called Domain-wall fermion. To construct the four dimensional fermion, this method starts with considering a five dimensional fermion with the mass depending a coordinate in the fifth direction. It was firstly proposed by Kaplan [8]. Subsequently, this method was applied to lattice fermion by Shamir and Furman [9, 10].

First, we will review Kaplan's way. For simplicity, we consider his idea in continuum theory. The five dimensional fermion action is given by

$$S_{\text{Kaplan}} = \int d^4x dx_5 \, \bar{\psi}(x, x_5) \left[\sum_{\mu=1}^{5} \gamma_\mu \partial_\mu - m(x_5) \right] \psi(x, x_5) \tag{2.27}$$

where x is the coordinate in the four-dimensional space and x_5 is the coordinate in the fifth direction. $m(x_5)$ is the mass parameter depending the coordinate x_5 and satisfies

$$m(x_5) = m_0 \epsilon(x_5) = \begin{cases} m_0 & x_5 > 0 \\ 0 & x_5 = 0 \\ -m_0 & x_5 < 0 \end{cases} \tag{2.28}$$

where $\epsilon(x_5)$ is the step function. By the mass parameter $m(x_5)$, the left-handed chiral fermion can be localized in the four-dimensional hyperplane ($x_5 = 0$). We can show it by solve the equation of motion for this action, i.e.

$$\left[\sum_{\mu=1}^{5} \gamma_\mu \partial_\mu - m(x_5) \right] \psi(x, x_5) = 0 \,. \tag{2.29}$$

To solve this equation, we consider $\psi(x, x_5) = \phi(x) f(x_5)$ where $\phi(x)$ is the four-dimensional fermion field and $f(x_5)$ is the scalar function. Now, we assume that the four-dimensional chiral fermion has the translation invariance in the four-dimensional hyperplane. By this assumption, the femrion fields $\phi(x)$ can be Fourier transformed as $\phi(x) = u(p) e^{ipx}$. Accordingly, the equation of motion is

$$\left[i \sum_{\mu=1}^{4} \gamma_\mu p_\mu \right] u(p) f(x_5) + \left[\gamma_5 \partial_5 f(x_5) - m(x_5) f(x_5) \right] u(p) = 0. \tag{2.30}$$

where ∂_5 is the partial differentiation with respect to the variable x_5. By assuming that $u(p)$ have to satisfy the massless Dirac equation below

$$\left[i \sum_{\mu=1}^{4} \gamma_\mu p_\mu \right] u(p) = 0 \,, \tag{2.31}$$

and $u(p)$ are the eigenmodes of γ_5 with $+1$ or -1 as eigenvalues, $u(p)$ and $f(s)$ are

$$\gamma_5 u(p) = \pm u(p) \tag{2.32}$$

$$f(x_5) = C \exp\left[\pm m_0 |x_5| \right] \tag{2.33}$$

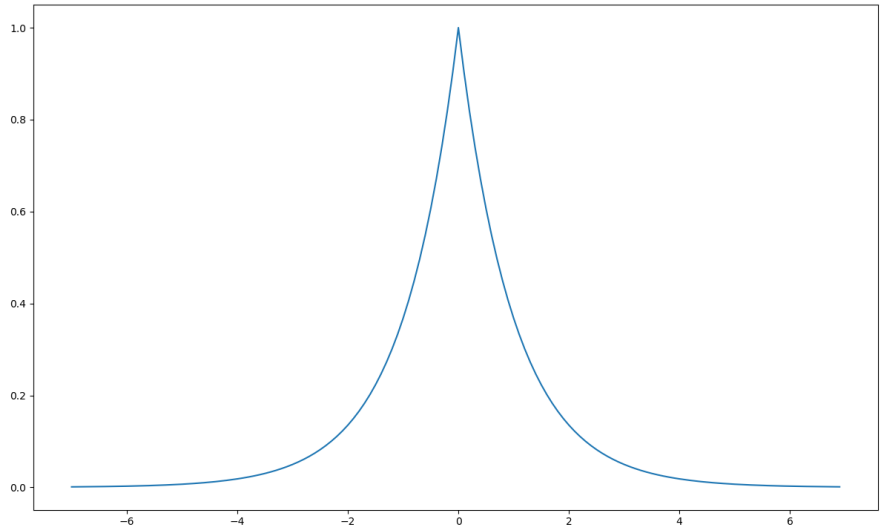

Figure 2.5: This figure plots $f(x_5) = C \exp[-m_0|x_5|]$ in the range -7 to 7 in the case of $C = 1$ and $m_0 = 1 > 0$.

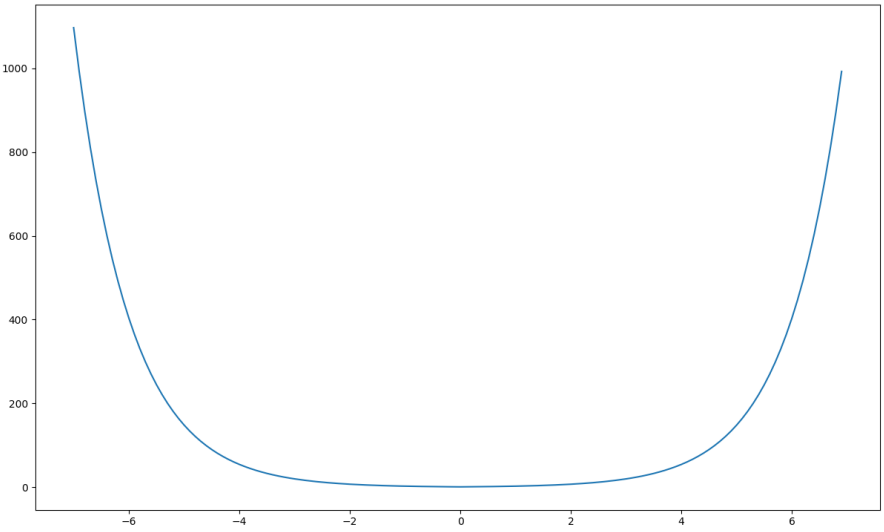

Figure 2.6: This figure plots $f(x_5) = C \exp[m_0|x_5|]$ in the range -7 to 7 in the case of $C = 1$ and $m_0 = 1 > 0$.

where C is the constant. These two equations imply that left-handed fermion be localized in the four-dimensional hyperplane ($x_5 = 0$) when the mass m_0 is positive, i.e. $m_0 > 0$. Indeed, we show it in the case of $m_0 > 0$. Then, $f(x_5)$ is chosen $f(x_5) = C \exp[-m_0|x_5|]$ as the normalizable solution since $\exp[m_0|x_5|]$ diverges in the range $-\infty$ to ∞ as shown in Fig. 2.5 and Fig. 2.6. And to satisfy Eq.2.31 and Eq.2.32, $u(p)$ is determined by the eigenmode of γ_5 with -1 as eigenvalue (left-handed fermion), i.e. $\gamma_5 u(p) = -u(p)$. For these results, $\psi(x, x_5) = Cu(p)f(x_5)e^{ipx}$ is localized in the four-dimensional hyperplane ($x_5 = 0$) for larger the mass m_0 as shown in Fig. 2.7. Thus, we can realize the left-handed

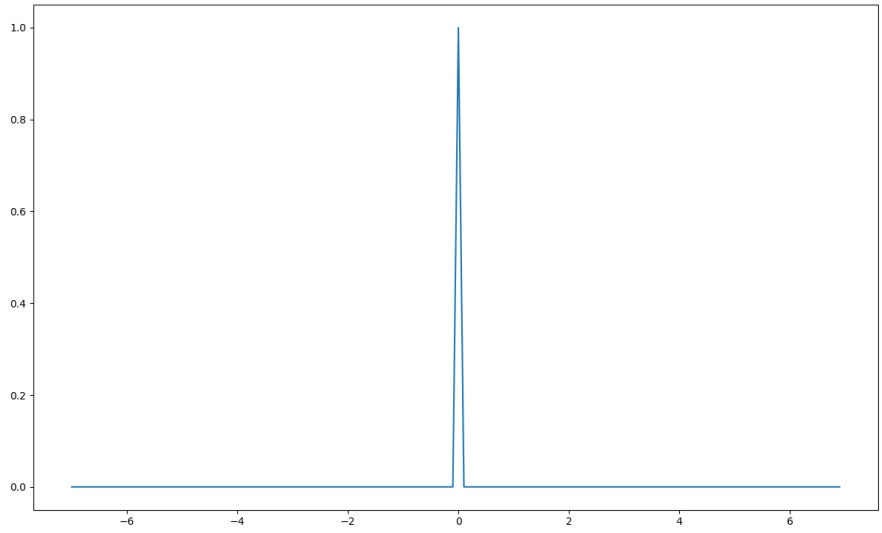

Figure 2.7: This figure plots $f(x_5) = C \exp[-m_0|x_5|]$ in the range -7 to 7 in the case of $C = 1$ and $m_0 = 10^{10} > 0$.

chiral fermion in the four-dimensional hyperplane by this way. By contrast, we can realize the left-handed chiral fermion in the four-dimensional hyperplane in the case of $m_0 < 0$.

However, this idea cannot be applied directly on the five dimensional finite volume hypercubic lattice since the boundary condition in the five dimensional direction makes a significant contribution to the function $f(x_5)$. For instance, we restrict the range in the five dimensional direction to $-N_5$ to N_5 and impose the periodic boundary condition. For this boundary condition, the mass parameter $m(x_5)$ is

$$m(x_5) = \begin{cases} m_0 & 0 < x_5 < N_5 \\ 0 & x_5 = 0, N_5, -N_5 \\ -m_0 & -N_5 < x_5 < 0 \end{cases} \tag{2.34}$$

as shown in Fig. 2.8. It means that there is the boundary where the mass changes in the four dimensional hyperplane ($x_5 = N_5$) boundary. And the change in its mass is opposite in sign to the change around $x_5 = 0$, i.e. $-m(x_5 - N_5) = m(x_5)$. Accordingly, the right-handed fermion is localized in the boundary ($x_5 = N_5$). Thus, in the five dimensional

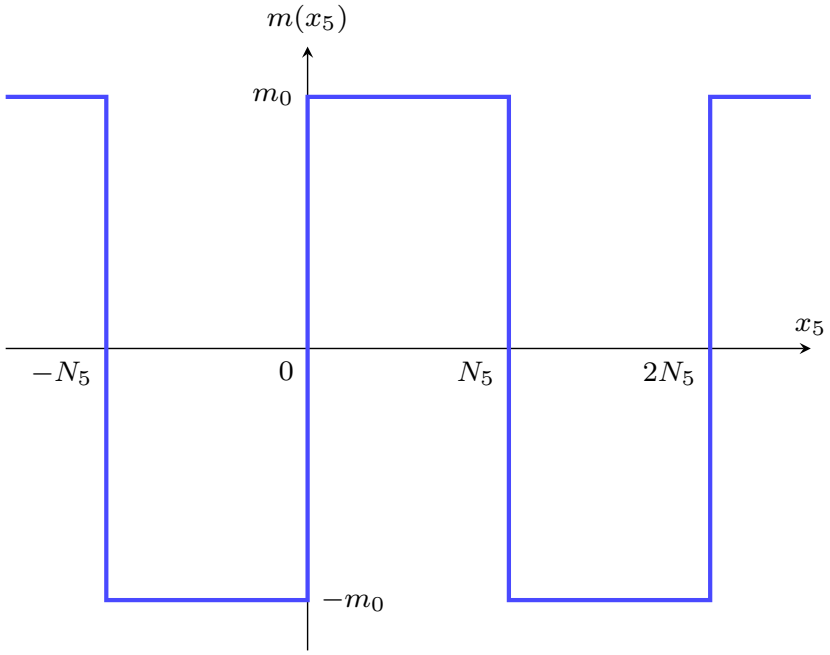

Figure 2.8: This figure plots the mass parameter $m(x_5)$ when imposed the periodic boundary condition $-N_5 \sim N_5$.

finite volume hypercubic lattice the whole is describing one Dirac fermion. And it is possible to avoid fermion doubling by adding the mass depending x_5.

Next, we review domain-wall fermion in the lattice theory. Specifically, we show a way in lattice of constructing zero-mass chiral fermions while avoiding fermion-doubling. We consider a finite volume five-dimensional hypercubic lattice imposed the Dirichlet boundary condition on the fifith direction and the periodic boundary condition on other directions. Namely,

$$L_{\mathrm{Dw}} \equiv \left\{ n = \sum_{\mu=1}^{4} n_\mu \hat{\mu} + n_5 \hat{\hat{5}} \;\middle|\; \begin{array}{c} \exists N_\mu \in \mathbb{N} \quad \text{s.t.} \quad n + N_\mu \hat{\mu} \sim n\,, \\ n_\nu \in [1, N_\nu] \subset \mathbb{N} \text{ for } \nu \in [1,5] \end{array} \right\} \tag{2.35}$$

where $\hat{\hat{5}}$ is the standard basis of the fifth direction. The domail-wall fermion action in this lattice is

$$\begin{aligned} S_{\mathrm{Dw}} = & \sum_{n,n_5} \bar{\psi}_{n,n_5} \left[\sum_{\mu=1}^{4} \gamma_\mu D_\mu + \gamma_5 D_5 \right] \psi_{n,n_5} \\ & + \sum_{n,n_5} \bar{\psi}_{n,n_5} \left[-M_0 + \sum_{\mu} (1 - C_\mu) + (1 - C_5) \right] \psi_{n,n_5} \end{aligned} \tag{2.36}$$

where $D_5 \psi_{n,n_5} \equiv (\psi_{n,n_5+1} - \psi_{n,n_5-1})/2$, $C_5 \psi_{n,n_5} \equiv (\psi_{n,n_5+1} + \psi_{n,n_5-1})/2$ and M_0 is a mass parameter. The sum $\sum_{n,n_5}$ is the summation over five-dimensional lattice sites $n, n_5 = (n_1, n_2, n_3, n_4; n_5)$. Note that there are two differences regarding boundary conditions and dynamical (or non-dynamical) variables between the fifth direction and other directions:

- On the fifth directions, ψ_{n,n_5} satisfies $\psi_{n,0} = \psi_{n,N_5+1} = 0$ since we impose the Dirichlet boundary condition, and its interval is $1 \leq n_5 \leq N_5$. On other directions, we impose the periodic boundary condition, and those intervals are $1 \leq n_\mu \leq N_\mu$.
- The link variables in the fifth direction are not dynamical while those in other directions can be dynamical. Accordingly, we can consider the coordinate of the fifth direction to be the flavour's degree of freedom.

Since there are non-dynamical variables in the fifith direction, we can rewrite the lattice action as

$$\begin{aligned} S_{\mathrm{Dw}} =& \sum_{n,n_5} \sum_{\mu=1}^{4} \bar{\psi}_{n,n_5} \gamma_\mu D_\mu \psi_{n,n_5} \\ &+ \sum_{m,n} \sum_{n_5,n_5'} \bar{\psi}_{m,n_5} \left[M P_L + M^\dagger P_R \right]^{mn}_{n_5 n_5'} \psi_{n,n_5'} \end{aligned} \tag{2.37}$$

where $P_R \equiv (\mathbf{1} + \gamma_5)/2$ and $P_L \equiv (\mathbf{1} - \gamma_5)/2$. The operator M, $M^\dagger$ are the mass terms given by

$$\begin{aligned} M^{mn}_{n_5 n_5'} \psi_{n,n_5'} \equiv& \left[1 + \sum_\mu (1 - C_\mu) - M_0 \right] \psi_{m,n_5} - \psi_{m,n_5+1} \\ =& W \psi_{m,n_5} - \psi_{m,n_5+1} \end{aligned} \tag{2.38}$$

and

$$\begin{aligned} (M^\dagger)^{mn}_{n_5 n_5'} \psi_{n,n_5'} \equiv& \left[1 + \sum_\mu (1 - C_\mu) - M_0 \right] \psi_{m,n_5} - \psi_{m,n_5-1} \\ =& W \psi_{m,n_5} - \psi_{m,n_5-1} \end{aligned} \tag{2.39}$$

respectively. As an example, the operators M, $M^\dagger$ in the case of $N_5 = 5$ are

$$M^{mn} = \begin{pmatrix} W & -1 & & & \\ & W & -1 & & \\ & & W & -1 & \\ & & & W & -1 \\ & & & & W \end{pmatrix} \tag{2.40}$$

and

$$(M^\dagger)^{mn} = \begin{pmatrix} W & & & & \\ -1 & W & & & \\ & -1 & W & & \\ & & -1 & W & \\ & & & -1 & W \end{pmatrix} \tag{2.41}$$

respectively. A difference between this action and Eq. 2.27 is that it has an off-diagonal and non-hermitian mass term with respect to coordinates in five directions. By deriving

zero-modes of this mass term, we realize the chiral fermion avoiding fermion doubling. Let ϕ_{n_5} be zero-modes of the operator M, i.e.

$$\sum_{n'_5} M_{n_5 n'_5} \phi_{n'_5} = W\phi_{n_5} - \phi_{n_5+1} = 0\,. \tag{2.42}$$

If $|W| < 1$ and $N_5 \to \infty$, there is a non-trivial solution obtained as $\phi_{n_5} = W^{n_5-1}\phi_1$. Indeed, this solution satisfies Eq. 2.42. And this mode can be normalized as $\phi_{n_5} = \sqrt{1-W^2}W^{n_5-1}$. By contrast, a solution for $\sum_{n'_5} M^\dagger_{n_5 n'_5}\phi_{n'_5} = 0$ is obtained as

$$\phi_{n_5} = \sqrt{1-W^2}W^{N_5-n_5} \tag{2.43}$$

if $|W| < 1$ and $N_5 \to \infty$.

And finally, we discuss the condition $|W| < 1$ necessary for the existence of zero-mode solutions. Because of $W = 1 + (1 - C_\mu) - M_0$ and Fourier transformation, the condition is

$$0 < M_0 - \sum_\mu (1 - \cos k_\mu) < 2\,. \tag{2.44}$$

Therefore, the relation between the momentum of k_μ, the range of mass parameter M_0, and the number of massless fermion are given in Table. 2.1. It indicates that this method can avoid fermion doubling.

Table 2.1: Classification of the number of massless fermion in DW fermion

momentum k_μ	the range of M_0	the number of massless fermion
any $k_\mu = 0$	$0 < M_0 < 2$	1
one $k_\mu = \pi$ otherwise $k_\mu = 0$	$2 < M_0 < 4$	4
two $k_\mu = \pi$ otherwise $k_\mu = 0$	$4 < M_0 < 6$	6
three $k_\mu = \pi$ otherwise $k_\mu = 0$	$6 < M_0 < 8$	4
any $k_\mu = \pi$	$8 < M_0 < 10$	1

Chapter 3

Spectral graph theory

In this chapter, we will introduce spectral graph theory in order to discuss lattice fermions in term of graph theory. This chapter is divided into three sections. In the first section, we will introduce some basic concepts about graph. Next section introduces matrices associated with graphs. The point of focus is that novel matrices called as anti-symmetrized adjacency matrices is defined. Final section mentions two theorems about the relationship between the nullity of matrices associated with graphs and the topology of the graphs. These theorems will be used in order to discuss the number of fermion species in later chapters.

3.1 Graphs

In this section, we will introduce some definieions of graphs and operation between graphs used in this paper.

We firstly introduce basic notions and definitions in graph theory. The definiitions of graph is given as bellow [65–68].

Definition 1 (graph)**.** *A graph G is a pair $G = (V, E)$, where V is a set of vertices of the graph and E is a set of edges of the graph.*

As examples, we can depict two graph in Fig. 3.1 with $V = \{1, 2, 3, 4\}$ and $E = \{\{1, 2\}, \{1, 3\}, \{1, 4\}, \{3, 4\}\}$. Here, we note that $\{i, j\}$ stands for an edge from i to j. If every adjacent vertices can be joined by an edge, the graph is referred to as "connected". Each of connected pieces of a graph is referred to as a "connected component". The two graphs in Fig. 3.1 are connected, where they have single connected components. They have no directed edge, which will be discussed next definition.

Definition 2 (directed graph or digraph)**.** *A directed graph (or digraph) is a pair (V, E) of sets of vertices and edges together with two maps* $\mathrm{init} : E \to V$ *and* $\mathrm{ter} : E \to V$*. The two maps are assigned to every edge e_{ij} with an initial vertex* $\mathrm{init}(e_{ij}) = v_i \in V$ *and a terminal vertex* $\mathrm{ter}(e_{ij}) = v_j \in V$*. The edge e_{ij} is said to be directed from* $\mathrm{init}(e_{ij})$ *to* $\mathrm{ter}(e_{ij})$*. If* $\mathrm{init}(e_{ij}) = \mathrm{ter}(e_{ij})$*, the edge e_{ij} is called a loop.*

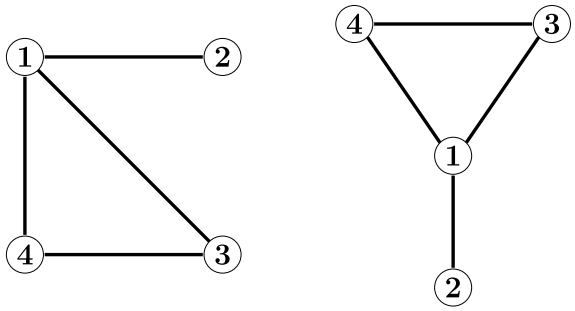

Figure 3.1: These examples are graphs having a pair $G = (V, E)$ with $V = \{1, 2, 3, 4\}$ and $E = \{\{1, 2\}, \{1, 3\}, \{1, 4\}, \{3, 4\}\}$.

As examples of directed graph, two graph in Fig. 3.2 are digraphs with $V = \{1, 2, 3, 4\}$ and $E = \{\{1, 2\}, \{1, 3\}, \{1, 4\}, \{3, 4\}\}$. Initial vertex and terminal vertices are assigned as $\mathrm{init}(\{i, j\}) = i, \mathrm{ter}(\{i, j\}) = j$.

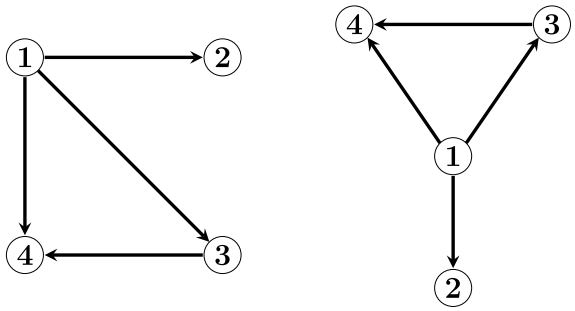

Figure 3.2: These examples are graphs having a pair (V, E) with $V = \{1, 2, 3, 4\}$ and $E = \{\{1, 2\}, \{1, 3\}, \{1, 4\}, \{3, 4\}\}$. The initial vertices of edges are $\mathrm{init}(\{1, 2\}) = 1, \mathrm{init}(\{1, 3\}) = 1, \mathrm{init}(\{1, 4\}) = 1, \mathrm{init}(\{3, 4\}) = 3$, while the terminal vertices are $\mathrm{init}(\{1, 2\}) = 2, \mathrm{init}(\{1, 3\}) = 3, \mathrm{init}(\{1, 4\}) = 4, \mathrm{init}(\{3, 4\}) = 4$.

Weighted graphs are defined as follows.

Definition 3 (weighted graph)**.** *The weighted graph has a value (the weight) for each edge in a graph or a digraph.*

We depict an example of weighted graphs in Fig. 3.3. It is a weighted and directed graph, each of whose edge has a weight as follows: $w(\{1, 2\}) = 1$, $w(\{2, 3\}) = 2$, $w(\{4, 1\}) = 3$, $w(\{2, 1\}) = -4$, $w(\{1, 4\}) = -1$, $w(\{4, 3\}) = -2$.

At the end of this section we introduce cartesian product which operations between graphs [69–71].

Definition 4 (cartesian product)**.** *The cartesian product of two simple graphs G_1 and G_2 is the graph $G = G_1 \square G_2$ with $V(G) = V(G_1) \times V(G_2)$ in which vertices (v_1, v_2) and (v_1', v_2') are adjacent iff either $v_2 = v_2'$ and v_1, v_1' are adjacent in G_1 or $v_1 = v_1'$ and v_2, v_2' are adjacent in G_2.*

As example of cartesian product, a graph $G = G_1 \square G_2$ in Fig. 3.4 has $V(G) = V(G_1) \times V(G_2)$ with $V(G_1) = \{v_1, v_2, v_3\}$ and $V(G_2) = \{v_1', v_2', v_3'\}$ where $E(G_1) = \{\{v_1, v_2\}, \{v_2, v_3\}\}$ and $E(G_2) = \{\{v_1', v_2'\}, \{v_2', v_3'\}\}$.

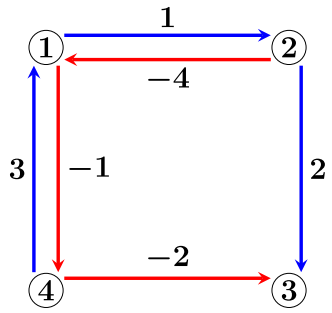

Figure 3.3: This digraph is weighted. Blue edges in the graph are those with positive weights, while red edges are those with negative weights.

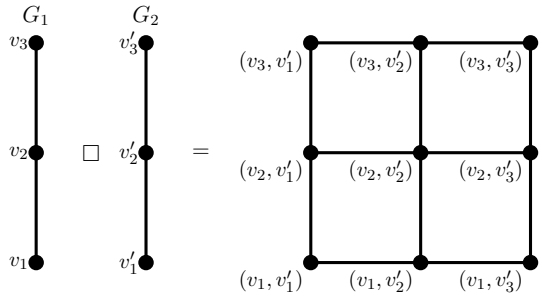

Figure 3.4: This graph is constructed by cartesian product of G_1 and G_2.

3.2 Matrices associated with graphs

For using later section, we here introduce definitions of matrices associated with graphs.

We introduce a definition of a degree matrix.

Definition 5 (Degree matrix)**.** *A degree matrix D of a graph is a $|V| \times |V|$ matrix defined as*

$$D_{ij} = \begin{cases} \deg(v_i) & i = j \\ 0 & \textit{otherwise} \end{cases} . \tag{3.1}$$

The degree $\deg(v_i)$ of a vertex v_i counts the number of times an edge terminates at that vertex. As an example we exhibit an degree matrix D of a graph in Fig. 3.1

$$D = \begin{pmatrix} 3 & 0 & 0 & 0 \\ 0 & 1 & 0 & 0 \\ 0 & 0 & 2 & 0 \\ 0 & 0 & 0 & 2 \end{pmatrix} . \tag{3.2}$$

On the other hand, the degree matrix D of a graph in Fig. 3.2 is

$$D = \begin{pmatrix} 0 & 0 & 0 & 0 \\ 0 & 1 & 0 & 0 \\ 0 & 0 & 1 & 0 \\ 0 & 0 & 0 & 2 \end{pmatrix} . \tag{3.3}$$

We next introduce a definition of an introduce matrix for undirected matrices.

Definition 6 (Incidence matrix (undirected))**.** *An incidence matrix B of a undirected graph is a $|V| \times |E|$ matrix defined as*

$$B_{ij} = \begin{cases} 1 & \textit{a vertex } v_i \textit{ is incident with edge } e_j \\ 0 & \textit{otherwise} \end{cases} . \tag{3.4}$$

As an example we exhibit an incidence matrix B of a graph in Fig. 3.1

$$B = \begin{pmatrix} 1 & 1 & 0 & 1 \\ 0 & 1 & 0 & 0 \\ 1 & 0 & 1 & 0 \\ 0 & 0 & 1 & 1 \end{pmatrix} , \tag{3.5}$$

where we define $e_{21} = e_2, e_{13} = e_1, e_{34} = e_3, e_{41} = e_4$.

Definition 7 (Incidence matrix (directed))**.** *An incidence matrix B of a directed graph is a $|V| \times |E|$ matrix defined as*

$$B_{ij} = \begin{cases} -1 & \textit{an edge } e_j \textit{ leaves a vertex } v_i \\ 1 & \textit{an edge } e_j \textit{ enters a vertex } v_i \\ 0 & \textit{otherwise} \end{cases} . \tag{3.6}$$

The incidence matrix B of a graph in Fig. 3.2 is

$$B = \begin{pmatrix} -1 & -1 & 0 & -1 \\ 0 & 1 & 0 & 0 \\ 1 & 0 & -1 & 0 \\ 0 & 0 & 1 & 1 \end{pmatrix} . \tag{3.7}$$

where we again define $e_{21} = e_2$, $e_{13} = e_1$, $e_{34} = e_3, e_{41} = e_4$.

We introduce a definition of an adjacency matrix. An adjacency matrix for wighted graphs is defined as follows.

Definition 8 (adjacency matrix)**.** *The adjacency matrix A of a graph is the $|V| \times |V|$ matrix given by*

$$A_{ij} = \begin{cases} w_{ij} & \textit{if there is a edge from } i \textit{ to } j \\ 0 & \textit{otherwise} \end{cases} , \tag{3.8}$$

where w_{ij} is the weight of an edge from i to j.

As examples, we exhibit an adjacency matrix A of a graph in Fig. 3.1 and Fig. 3.3

$$A(G) = \begin{pmatrix} 0 & 1 & 1 & 1 \\ 1 & 0 & 0 & 0 \\ 1 & 0 & 0 & 1 \\ 1 & 0 & 1 & 0 \end{pmatrix} . \tag{3.9}$$

$$A(G') = \begin{pmatrix} 0 & 1 & 0 & -1 \\ -4 & 0 & 2 & 0 \\ 0 & 0 & 0 & 0 \\ 3 & 0 & -2 & 0 \end{pmatrix} . \tag{3.10}$$

where G, G' denote the graph in Fig. 3.1 and Fig. 3.3 respectively. And we assumed that the weight of every edge in the graph G in Fig. 3.1 is 1, or $w(e \in G) = 1$. In general, the adjacency matrix of a directed graph is asymmetric since the existence of an edge from i to j does not necessarily imply that there is also an edge from j to i.

The Laplacian matrix is defined by the degree, adjacency and incidence matrices as follows.

Definition 9 (Laplacian matrix)**.** *The Laplacian matrix L of a graph is the $|V| \times |V|$ matrix given by*

$$L = D - A = BB^T \tag{3.11}$$

D, A are degree, adjacency matrices of a undirected and unweighted graph, while B is an incidence matrix of directed graph.

For a graph in Fig. 3.1, the Laplacian matrix is

$$L = \begin{pmatrix} 3 & -1 & -1 & -1 \\ -1 & 1 & 0 & 0 \\ -1 & 0 & 2 & -1 \\ -1 & 0 & -1 & 2 \end{pmatrix} . \tag{3.12}$$

One can easily check out $L = D - A = BB^T$.

In addition to the standard definitions of graph matrices, we introduce a specific adjacency matrix of directed graph as an "anti-symmetrized adjacency matrix" as follows.

Definition 10 (Anti-symmetrized adjacency matrix)**.** *The anti-symmetrized adjacency matrix A_{as} of a directed and weighted graph having no multiple edges is the $|V| \times |V|$ matrix given by -1*

$$(A_{\text{as}})_{ij} = \begin{cases} w_{ij} & i = \alpha \text{ and } j = \beta \text{ for edge } \{\alpha, \beta\} \\ -w_{ij}^{\dagger} & i = \beta \text{ and } j = \alpha \text{ for edge } \{\alpha, \beta\} \\ 0 & \text{otherwise} \end{cases} \tag{3.13}$$

where w_{ij} is the weight of an edge from i to j.

The anti-symmetrized adjacency matrix of a directed graph is anti-symmetric. As example, the anti-symmetrized adjacency matrix A_{as} of a graph in Fig. 3.2 is

$$A_{\text{as}} = \begin{pmatrix} 0 & 1 & 1 & 1 \\ -1 & 0 & 0 & 0 \\ -1 & 0 & 0 & 1 \\ -1 & 0 & -1 & 0 \end{pmatrix} . \tag{3.14}$$

3.3 Useful theorems of matrices associated with graphs

In this section, we will discuss useful theorems of Laplacian and anti-symmertized adjacency matrices. These theorems claim a non-trivial relationship between the nullity of matrices associated with graph and topology of the graph. In later section, these theorems will be used when we prove the relationship between the zero-modes of the difference matrix in lattice action and the topology of the graph.

3.3.1 Betti numbers and Laplacian

The topology of a graph is known to be detected by matrices associated with the graph.

Theorem 2 (Betti numbers and Laplacian)**.** *The zeroth Betti numbers $\beta_0(G)$ of the graph G are related to the rank of graph Laplacian.*

$$|V| - \operatorname{rank} L(G) = \beta_0(G) \tag{3.15}$$

where $\beta_0(G)$ is also the number of connected components of the graph G.

It means that the number of exact zero eigenvalues of the Laplacian matrix agrees with $\beta_0(G)$ which is equal to the number of connected components of the graph. A proof of this theorem refers to the proof on eigenvalues of Laplacian matrix [72]. The proof is given below.

Proof. Firstly, we prove it for a graph with a single connected component. The zeroth Betti number is $\beta_0(G) = 1$ since the graph has a single connected component. So, we will prove $|V| - \operatorname{rank} L(G) = \beta_0(G) = 1$. Let $\boldsymbol{v} \in \mathbb{C}^{|V|}$ be a vector, where $\boldsymbol{v} = \sum_{i=1}^{|V|} x_i \boldsymbol{e}_i$ with $\boldsymbol{e}_i$ is the standard basis. $|V|$ is the set of vertices in the graph G. The bilinear form $\boldsymbol{v}^\dagger L(G)\boldsymbol{v}$ is

$$\boldsymbol{v}^\dagger L(G)\boldsymbol{v} = \boldsymbol{v}^\dagger \big\{ D(G) - A(G) \big\} \boldsymbol{v} = \boldsymbol{v}^\dagger D(G)\boldsymbol{v} - \boldsymbol{v}^\dagger A(G)\boldsymbol{v}\,, \tag{3.16}$$

where $D(G)$ and $A(G)$ are the degree matrix of G and the adjacency matrix of G respectively. Based on the definitions of degree matrix and adjacency matrix,

$$\begin{aligned}
\boldsymbol{v}^\dagger L(G)\boldsymbol{v} &= \sum_{i=1}^{|V|} \deg(v_i)|x_i|^2 - \sum_{\{i,j\}\in E} (\bar{x}_i x_j + \bar{x}_j x_i) \\
&= \sum_{\{i,j\}\in E} \left(|x_i|^2 + |x_j|^2 \right) - \sum_{\{i,j\}\in E} (\bar{x}_i x_j + \bar{x}_j x_i) \\
&= \sum_{\{i,j\}\in E} (\bar{x}_i - \bar{x}_j)\,(x_i - x_j) \\
&= \sum_{\{i,j\}\in E} |x_i - x_j|^2
\end{aligned} \tag{3.17}$$

where $\{i, j\}$ stands for an edge between one vertex v_i and other vertex v_j. Furthermore, E is the set of edges in G.

If the vector $\boldsymbol{v}$ is a zero-mode (zero-eigenvector) of the Laplacian $L(G)$, the bilinear form $\boldsymbol{v}^\dagger L(G)\boldsymbol{v}$ satisfies the following equation,

$$\boldsymbol{v}^\dagger L(G)\boldsymbol{v} = \sum_{\{i,j\}\in E} |x_i - x_j|^2 = 0\,. \tag{3.18}$$

From this and $|x_i - x_j|^2 \geq 0$, $x_i = x_j$ for any edge $\{i,j\} \in E$ is obtained. Since we consider a graph with single connected component, the components of the zero-mode $\boldsymbol{v}$ must satisfy $x_1 = x_2 = \cdots = x_{|V|}$. If there is $x_i \neq x_j$ in components of zero-mode $\boldsymbol{v}$, the graph can be divided into G_1 and G_2 such that there is no edges between G_1 and G_2. But, this is inconsistent with the fact that the graph has single connected component. We then have that the zero-mode $\boldsymbol{v}$ for Laplacian $L(G)$ is unique and explicitly written as $\boldsymbol{v} = \alpha \sum_{i=1}^{|V|} \boldsymbol{e}_i$ with $\alpha \in \mathbb{C}$. Hence, $|V| - \operatorname{rank} L(G) = \beta_0(G) = 1$ holds for a graph G with single connected component since the rank of Laplacian is $L(G) = |V| - 1$.

Secondary, we prove it for a graph with $k > 1$ connected components. The zeroth Betti number for this graph is $\beta_0(G) = k$ since the zeroth Betti number is equal to the number of connected components. As a result, we will prove $|V| - \operatorname{rank} L(G) = \beta_0(G) = k$. The graph can be divided into k graphs with single component such that there are no edges between each two of graphs. They are denoted as G_ν for $\nu \in \{1, 2, \cdots, k\}$. These edges satisfy $E(G_\nu) \cap E(G_\rho) = \emptyset$ for $\nu \neq \rho$ since there are no edges between each two of connected graphs. Furthermore, the number of vertices of G_ν is denoted as $|V(G_\nu)|$ and $\sum_{\nu=1}^{k} |V(G_\nu)| = |V|$. Then, a Laplacian $L(G)$ is a block matrix as

$$L(G) = \begin{pmatrix} L(G_1) & & & \\ & L(G_2) & & \\ & & \ddots & \\ & & & L(G_k) \end{pmatrix} = \bigoplus_{\nu=1}^{k} L(G_\nu) \tag{3.19}$$

since $E(G_\nu) \cap E(G_\rho) = \emptyset$ for $\nu \neq \rho$. And $\oplus$ denotes the direct sum. The rank of Laplacian $L(G)$ is obtained as

$$\operatorname{rank} L(G) = \operatorname{rank} \left[\bigoplus_{\nu=1}^{k} L(G_\nu) \right] = \sum_{\nu=1}^{k} \operatorname{rank} L(G_\nu) \tag{3.20}$$

where we used the property of the direct sum. The rank of each matrix $L(G_\nu)$ is $\operatorname{rank} L(G_\nu) = |V(G_\nu)| - 1$ because each matrix $L(G_\nu)$ is a Laplacian for the graph G_ν with single component. Consequently, the rank of Laplacian $L(G)$ is

$$\operatorname{rank} L(G) = \sum_{\nu=1}^{k} \Big(|V(G_\nu)| - 1 \Big) = \sum_{\nu=1}^{k} |V(G_\nu)| - \sum_{\nu=1}^{k} 1 = |V| - k\,. \tag{3.21}$$

Hence, $|V| - \operatorname{rank} L(G) = \beta_0(G) = k$ holds for the graph G with k connected components. We now conclude that $|V| - \operatorname{rank}(G) = \beta_0(G)$ holds for generic graphs. □

3.3.2 Betti numbers and anti-symmetrized adjacency matices

We discuss a useful theorem of anti-symmetrized adjacency matrices. The theorem can be applied to anti-symmetrized adjacency matrix of only certain weighted digraphs. To discuss the theorem, we introduce the weighted digraph. Let G is the weighted digraph, which has γ-matrices as the weight and be constructed by a cartesian product of only the cycle digraph and the simple directed path. The cycle digraph and the simple directed path are denoted by $D^{(\text{cycle})}$ and $D^{(\text{path})}$ respectively. The digraph G is explicitly written as

$$\begin{aligned} G &\equiv G_1 \,\square\, G_2 \,\square\, \cdots \,\square\, G_D \\ w(e \in G_\mu) &= \gamma_\mu \end{aligned} \tag{3.22}$$

where $G_\mu \in \left\{ D_\mu^{(\text{cycle})}, D_\mu^{(\text{path})} \right\}$ for $\mu \in \{1, 2, \cdots, D\}$ and $w(e)$ denote the weight of edge e. The symbol $\square$ stands for the cartesian product, Furthermore, γ_μ is D-dimensional gamma matrices satisfying Clifford algebra as $\{\gamma_\mu, \gamma_\nu\} = 2\delta_{\mu\nu}$. The cycle digraph has a pair as

$$\begin{aligned} V(D_\mu^{(\text{cycle})}) &= \{1, 2, \cdots, |V|_\mu\} \\ E(D_\mu^{(\text{cycle})}) &= \{\{1,2\}, \{2,3\}, \cdots, \{|V|_\mu - 1, |V|_\mu\}, \{|V|_\mu, 1\}\} \ . \end{aligned} \tag{3.23}$$

where $V(D_\mu^{(\text{cycle})})$ is a set of vertices and $E(D_\mu^{(\text{cycle})})$ a set of edges. So, this digraph has $|V|_\mu$ vertices and $|V|_\mu$ directed edges. By contrast, the simple directed path has a pair as

$$\begin{aligned} V(D_\mu^{(\text{path})}) &= \{1, 2, \cdots, |V|_\mu\} \\ E(D_\mu^{(\text{path})}) &= \{\{1,2\}, \{2,3\}, \cdots, \{|V|_\mu - 1, |V|_\mu\}\} \end{aligned} \tag{3.24}$$

where $V(D_\mu^{(\text{path})})$ and $E(D_\mu^{(\text{path})})$ are a set of vertices and a set of edges respectively. So, this digraph has $|V|_\mu$ vertices and $|V|_\mu - 1$ directed edges unlike the cycle digraph. These digraph is depicted in Fig. 3.5. Then, the number of vertices of G is $|V| = \sum_{\mu=1}^{D} |V|_\mu$

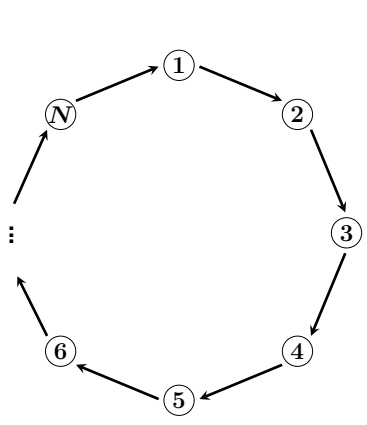

(a) $D^{(\text{cycle})}$ with N vertices.

(b) $D^{(\text{path})}$ with N vertices.

Figure 3.5: The two graphs correspond to a cycle digraph $D^{(\text{cycle})}$ and a simple directed path $D^{(\text{path})}$ respectively.

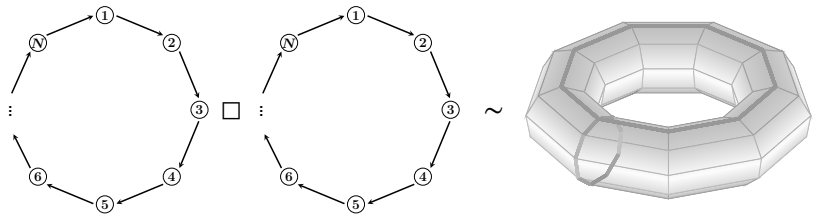

(a) $D_1^{(\mathrm{cycle})} \square D_2^{(\mathrm{cycle})}$ is identified as a two dimensional torus with directed edge.

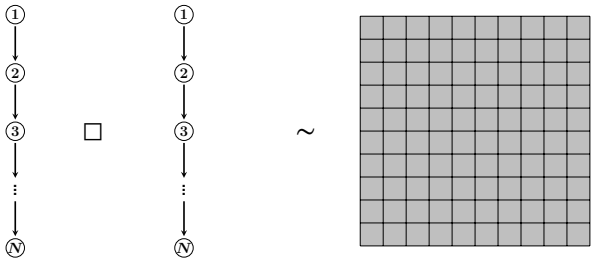

(b) $D_1^{(\mathrm{path})} \square D_2^{(\mathrm{path})}$ is identified as a two dimensional disk with directed edge.

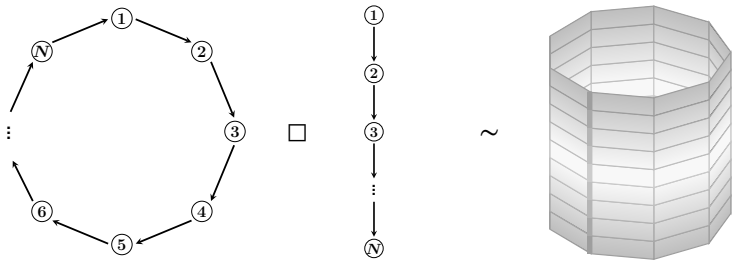

(c) $D_1^{(\mathrm{cycle})} \square D_2^{(\mathrm{path})}$ is identified as an cylinder with directed edge.

Figure 3.6: Three examples for G in Eq. (3.22) and manifolds corresponding to them are depicted.

where $|V|_\mu$ stands for the number of vertices of G_μ. Some examples are depicted in Fig. 3.6.

Next, we show the anti-symmetrized adjacency matrix for digraph G in Eq. (3.22). The anti-symmetrized adjacency matrix is $|V|$ square matrix constructed with tensor product (or Kronecker product) [69–71]. This matrix is exiplicitly written as

$$A_{\rm as}(G) = \sum_{\mu=1}^{D} \left\{ \left(\bigotimes_{\nu=1}^{D-\mu} \mathbf{1}_{|V|_{D+1-\nu}} \right) \otimes A'_{\rm as}(G_\mu) \otimes \left(\bigotimes_{\rho=1}^{\mu-1} \mathbf{1}_{|V|_\rho} \right) \right\} \otimes \gamma_\mu \tag{3.25}$$

where $\mathbf{1}_{|V|_\mu}$ is the identity matrix of size $|V|_\mu$ and $A'_{\rm as}(G_\mu)$ is an anti-symmetrized adjacency matrix for digraph G_μ with each component set to 1. The matrix $A'_{\rm as}(G_\mu)$ for the cycle digraph $G_\mu = D_\mu^{(\rm cycle)}$ is $|V|_\mu$ square matrix represented as

$$A'_{\rm as}(D_\mu^{(\rm cycle)}) = \begin{pmatrix} 0 & 1 & 0 & & 0 & 0 & -1 \\ -1 & 0 & 1 & \cdots & 0 & 0 & 0 \\ 0 & -1 & 0 & & 0 & 0 & 0 \\ & \vdots & & \ddots & & \vdots & \\ 0 & 0 & 0 & & 0 & 1 & 0 \\ 0 & 0 & 0 & \cdots & -1 & 0 & 1 \\ 1 & 0 & 0 & & 0 & -1 & 0 \end{pmatrix} \tag{3.26}$$

and the matrix $A'_{\rm as}(G_\mu)$ for the simple directed path $G_\mu = D_\mu^{(\rm path)}$ is $|V|_\mu$ square matrix represented as

$$A'_{\rm as}(D_\mu^{(\rm path)}) = \begin{pmatrix} 0 & 1 & 0 & & 0 & 0 & 0 \\ -1 & 0 & 1 & \cdots & 0 & 0 & 0 \\ 0 & -1 & 0 & & 0 & 0 & 0 \\ & \vdots & & \ddots & & \vdots & \\ 0 & 0 & 0 & & 0 & 1 & 0 \\ 0 & 0 & 0 & \cdots & -1 & 0 & 1 \\ 0 & 0 & 0 & & 0 & -1 & 0 \end{pmatrix} . \tag{3.27}$$

Note that the components of $A'_{\rm as}(D_1^{(\rm cycle)})$, $A'_{\rm as}(D_2^{(\rm path)})$ represent adjacent between vertices in each graph. In particular, the $(1, |V|_\mu)$ component and the $(|V|_\mu, 1)$ component in $A'_{\rm as}(D_\mu^{(\rm cycle)})$ represent the property of the cycle digraph $D_\mu^{(\rm cycle)}$, which has an edge leaving $|V|_\mu$ and entering 1. The matrix $A'_{\rm as}(D_\mu^{(\rm path)})$ also represents the property of the cycle digraph $D_\mu^{(\rm path)}$ as well as $A'_{\rm as}(D_\mu^{(\rm cycle)})$. As some examples of $A_{\rm as}(G)$, we show the anti-symmetrized adjacency matrices of $D_1^{(\rm cycle)} \square D_2^{(\rm cycle)}$, $D_1^{(\rm path)} \square D_2^{(\rm path)}$, and $D_1^{(\rm cycle)} \square D_2^{(\rm path)}$. These anti-symmetrized adjacency matrices are

$$A_{\rm as}(D_1^{(\rm cycle)} \square D_2^{(\rm cycle)}) = \mathbf{1}_{|V|_2} \otimes A'_{\rm as}(D_1^{(\rm cycle)}) \otimes \gamma_1 + A'_{\rm as}(D_2^{(\rm cycle)}) \otimes \mathbf{1}_{|V|_1} \otimes \gamma_2 \,, \tag{3.28a}$$

$$A_{\rm as}(D_1^{(\rm path)} \square D_2^{(\rm path)}) = \mathbf{1}_{|V|_2} \otimes A'_{\rm as}(D_1^{(\rm path)}) \otimes \gamma_1 + A_{\rm as}(D_2^{(\rm path)}) \otimes \mathbf{1}_{|V|_1} \otimes \gamma_2 \,, \tag{3.28b}$$

$$A_{\rm as}(D_1^{(\rm cycle)} \square D_2^{(\rm path)}) = \mathbf{1}_{|V|_2} \otimes A'_{\rm as}(D_1^{(\rm cycle)}) \otimes \gamma_1 + A'_{\rm as}(D_2^{(\rm path)}) \otimes \mathbf{1}_{|V|_1} \otimes \gamma_2 \tag{3.28c}$$

respectively.

At the end of this section, we will discuss an useful theorem related to the anti-symmetrized adjacency matrices. We claim the following theorem about the relationship between the rank of $A_{\rm as}(G)$ for the digraph in Eq. (3.22) and the topology of the digraph.

Theorem 3 (Betti numbers and anti-symmetrized adjacency matices)**.** *For the graphs G constructed a cartesian-product of only the cycle digraph and the simple directed path, the following equation holds;*

$$|V| \cdot \operatorname{rank}\gamma - \operatorname{rank} A_{\rm as}(G) \leq \operatorname{rank}\gamma \cdot \prod_{\mu=1}^{D} \Big\{ \beta_0(G_\mu) + \beta_1(G_\mu) \Big\}, \tag{3.29}$$

where $|V|$ is the number of vertices in G and $\operatorname{rank}\gamma$ is the rank of gamma matrices. When the graph G is constructed by d cycle digraphs and $(D-d)$ simple directed paths, this equation is rewritten as

$$\frac{\dim\left(\ker A_{\rm as}(G)\right)}{\operatorname{rank}\gamma} \leq 2^d \,. \tag{3.30}$$

It means that the maximum number of zero-eigenvalues of anti-symmetrized adjacency matrix $A_{\rm as}(G)$ divided by the rank of γ-matrices is determined by the zeroth Betti number and first Betti number of each digraph G_μ. The proof of this theorem is given below.

Proof. We consider four digraphs: the cycle digraph with even vertices, the one with odd vertices, the simple directed path with even vertices, and the one with odd vertices. The digraph G is constructed by a cartesian product of these digraphs. Then, the right side is Eq. (3.29) is obtained as

$$\begin{aligned}
&\operatorname{rank}\gamma \cdot \prod_{\mu=1}^{D} \Big\{ \beta_0(G_\mu) + \beta_1(G_\mu) \Big\} \\
&\quad = \operatorname{rank}\gamma \cdot \prod_{\mu^{\rm c}\in S^{\rm c}} \Big\{ \beta_0(D_{\mu^{\rm c}}^{(\rm cycle)}) + \beta_1(D_{\mu^{\rm c}}^{(\rm cycle)}) \Big\} \prod_{\mu^{\rm p}\in S^{\rm p}} \Big\{ \beta_0(D_{\mu^{\rm p}}^{(\rm path)}) + \beta_1(D_{\mu^{\rm p}}^{(\rm path)}) \Big\} \\
&\quad = \operatorname{rank}\gamma \cdot 2^{|S^{\rm c}|}
\end{aligned} \tag{3.31}$$

where $S^{\rm c} \equiv \left\{ \mu \;\middle|\; G_\mu = D_\mu^{(\rm cycle)} \right\}$ and $S^{\rm p} \equiv \left\{ \mu \;\middle|\; G_\mu = D_\mu^{(\rm path)} \right\}$. We used the known facts that $\beta_0(D_\mu^{(\rm cycle)}) + \beta_1(D_\mu^{(\rm cycle)}) = 2$ and $\beta_0(D_\mu^{(\rm path)}) + \beta_1(D_\mu^{(\rm path)}) = 1$ since the cycle digraph is homeomorphic to the circle S^1 and the simple directed path is homeomorphic to the line segment B^1. As a result, what we have to do is prove

$$|V| \cdot \operatorname{rank}\gamma - \operatorname{rank} A_{\rm as}(G) \leq \operatorname{rank}\gamma \cdot 2^{|S^{\rm c}|} \,. \tag{3.32}$$

To prove above inequality, we will derive the number of zero-eigenvalues of $A_{\rm as}(G)$. The diagonalization of $A_{\rm as}(G)$ can be derived as

$$\mathcal{U}^\dagger A_{\rm as}(G)\,\mathcal{U} = \sum_{\mu=1}^{D} \left\{ \left(\bigotimes_{\nu=1}^{D-\mu} \mathbf{1}_{|V|_{D+1-\nu}} \right) \otimes \left(U_\mu^\dagger A'_{\rm as}(G_\mu) U_\mu \right) \otimes \left(\bigotimes_{\rho=1}^{\mu-1} \mathbf{1}_{|V|_\rho} \right) \right\} \otimes \gamma_\mu \,, \tag{3.33}$$

where $\mathcal{U}$ is an unitary matrix defined as $\mathcal{U} \equiv \bigotimes_{\mu=1}^{D} U_\mu$ and U_μ is the unitary matrix for the diagonalization of $A'_{\rm as}(G_\mu)$. For later use, we define four sets as

$$\begin{aligned} S^{\rm c,e} &\equiv \left\{\mu \;\middle|\; G_\mu = D^{(\rm cycle)}, |V|_\mu = \text{even}\right\}, \quad S^{\rm c,o} \equiv \left\{\mu \;\middle|\; G_\mu = D^{(\rm cycle)}, |V|_\mu = \text{odd}\right\}, \\ S^{\rm p,e} &\equiv \left\{\mu \;\middle|\; G_\mu = D^{(\rm path)}, |V|_\mu = \text{even}\right\}, \quad S^{\rm p,o} \equiv \left\{\mu \;\middle|\; G_\mu = D^{(\rm path)}, |V|_\mu = \text{odd}\right\}. \end{aligned} \tag{3.34}$$

respectively. Consequently, the diagonalization of $A_{\rm as}(G)$ are obtained as

$$\begin{aligned} &\left(\mathcal{U}^\dagger A_{\rm as}(G)\mathcal{U}\right)_{mn} \\ &= 2i\left\{\sum_{\mu^{\rm c,e}\in S^{\rm c,e}} \gamma_{\mu^{\rm c,e}} \sin\left(\frac{2\pi(m_{\mu^{\rm c,e}}-1)}{|V|_{\mu^{\rm c,e}}}\right) + \sum_{\mu^{\rm c,o}\in S^{\rm c,o}} \gamma_{\mu^{\rm c,o}} \sin\left(\frac{2\pi(m_{\mu^{\rm c,o}}-1)}{|V|_{\mu^{\rm c,o}}}\right)\right. \\ &\quad \left. + \sum_{\mu^{\rm p,e}\in S^{\rm p,e}} \gamma_{\mu^{\rm p,e}} \cos\left(\frac{m_{\mu^{\rm p,e}}\pi}{|V|_{\mu^{\rm p,e}}+1}\right) + \sum_{\mu^{\rm p,o}\in S^{\rm p,o}} \gamma_{\mu^{\rm p,o}} \cos\left(\frac{m_{\mu^{\rm p,o}}\pi}{|V|_{\mu^{\rm p,o}}+1}\right)\right\}\delta_{mn}\,. \end{aligned} \tag{3.35}$$

as shown in Appendix. B

If the anti-symmetrized adjacency matrix $A_{\rm as}(G)$ has zero-eigenvalues, the diagonal components satisfy $\left(\mathcal{U}^\dagger A_{\rm as}(G)\mathcal{U}\right)_{mn} = 0$. This equation is exiplicitly written as

$$\begin{aligned} &\sum_{\mu^{\rm c,e}\in S^{\rm c,e}} \gamma_{\mu^{\rm c,e}} \sin\left(\frac{2\pi(m_{\mu^{\rm c,e}}-1)}{|V|_{\mu^{\rm c,e}}}\right) + \sum_{\mu^{\rm c,o}\in S^{\rm c,o}} \gamma_{\mu^{\rm c,o}} \sin\left(\frac{2\pi(m_{\mu^{\rm c,o}}-1)}{|V|_{\mu^{\rm c,o}}}\right) \\ &+ \sum_{\mu^{\rm p,e}\in S^{\rm p,e}} \gamma_{\mu^{\rm p,e}} \cos\left(\frac{m_{\mu^{\rm p,e}}\pi}{|V|_{\mu^{\rm p,e}}+1}\right) + \sum_{\mu^{\rm p,o}\in S^{\rm p,o}} \gamma_{\mu^{\rm p,o}} \cos\left(\frac{m_{\mu^{\rm p,o}}\pi}{|V|_{\mu^{\rm p,o}}+1}\right) = 0\,. \end{aligned} \tag{3.36}$$

However, since γ-matrices are linearly independent, the coefficient of each γ-matrices must be zero. Accordingly, the conditions for the matrix $A_{\rm as}(G)$ to have zero-eigenvalues are below

$$\begin{aligned} &\sin\left(\frac{2\pi(m_{\mu^{\rm p,e}}-1)}{|V|_{\mu^{\rm p,e}}}\right) = \sin\left(\frac{2\pi(m_{\mu^{\rm p,o}}-1)}{|V|_{\mu^{\rm p,o}}}\right) \\ &= \cos\left(\frac{m_{\mu^{\rm p,e}}\pi}{|V|_{\mu^{\rm p,e}}+1}\right) = \cos\left(\frac{m_{\mu^{\rm p,o}}\pi}{|V|_{\mu^{\rm p,o}}+1}\right) = 0\,, \end{aligned} \tag{3.37}$$

The solutions of this equation are

$$m_{\mu^{\rm c,e}} = 1\,, \quad m_{\mu^{\rm c,o}} = 0\,, \quad m_{\mu^{\rm p,o}} = \frac{|V|_{\mu^{\rm p,o}}+1}{2} \tag{3.38}$$

or

$$m_{\mu^{\rm c,e}} = \frac{|V|_{\mu^{\rm c,e}}}{2}+1\,, \quad m_{\mu^{\rm c,o}} = 0\,, \quad m_{\mu^{\rm p,o}} = \frac{|V|_{\mu^{\rm p,o}}+1}{2} \tag{3.39}$$

if $S^{\rm p,e} = \emptyset$. Then, the number of solutions is $2^{|S^{\rm c,e}|}$. Note that there are no solutions if $S^{\rm p,e} \neq \emptyset$ since there is no $m_{\mu^{\rm p,e}} \in \mathbb{N}$ satisfying Eq. (3.37). Because of them, the number of zero-eigenvalues of $A_{\rm as}(G)$ depends on the number of vertices in each digraph G_μ as shown in Table. 3.1. Hence, the rank of $A_{\rm as}(G)$ is obtain as

Table 3.1: Classification of the number of zero eigenvalues for $A_{\rm as}(G_\mu)$

	$\|V\|_\mu =$ even	$\|V\|_\mu =$ odd
$G_\mu = D^{(\rm cycle)}$	2	1
$G_\mu = D^{(\rm path)}$	0	1

$$\operatorname{rank} A_{\rm as}(G) = \begin{cases} \operatorname{rank}\gamma \cdot \left(|V| - 2^{|S^{\rm c,e}|}\right) & S^{\rm p,e} = \emptyset \\ \operatorname{rank}\gamma \cdot |V| & S^{\rm p,e} \neq \emptyset \end{cases} \tag{3.40}$$

since the diagonal components $\left(\mathcal{U}^\dagger A_{\rm as}(G)\,\mathcal{U}\right)_{mn}$ contain γ-matrices. Therefore, the following inequality has been prove

$$|V| \cdot \operatorname{rank}\gamma - \operatorname{rank} A_{\rm as}(G) \leq \operatorname{rank}\gamma \cdot 2^{|S^{\rm c}|} = \operatorname{rank}\gamma \cdot \prod_{\mu=1}^{D} \Big\{ \beta_0(G_\mu) + \beta_1(G_\mu) \Big\} \tag{3.41}$$

since $|S^{\rm c,e}| \leq S^{\rm c}$. With $|S^{\rm c}| = d$, the nullity of $A_{\rm as}(G)$ divided by the rank of γ-matrices satisfies an inequality below

$$\frac{\dim\left(\ker A_{\rm as}(G)\right)}{\operatorname{rank}\gamma} \leq 2^d \tag{3.42}$$

since $\dim\left(\ker A_{\rm as}(G)\right) = |V| \cdot \operatorname{rank}\gamma - \operatorname{rank} A_{\rm as}(G)$. □

In later chapter, we will use Thm. 3 in order to investigate the maximum number of zero-modes in the matrix-representation Dirac lattice operator.

Chapter 4

Lattice fermions and Graph theory

4.1 Lattice fermions as spectral graph theory

In this section, we will discuss lattice fermions on D-dimensional hypercubic lattices in term of spectral graph theory. Note that we assume periodic boundary condition or Dirichlet boundary condition as boundary condition on each direction in the lattices.

This section describes relationship between lattice fermions and graph theory and be divided into three parts. In the first part, we will discuss lattice fermions as graphs. Lattice fermions on the lattices can be represented as certain weighted digraphs. Next, we will refer to relationship between lattice action and matrices associated with the weighted digraphs. Lattice fermion action can be represented as the biliner form of anti-symmetrized adjacency matrix for the weighted digraphs. In other words, a matrix-representation of lattice Dirac operator can be written down by anti-symmetrized adjacency matrix for the digraphs corresponding to lattice fermions. Finally, we will show that the number of fermion species can be derived by the nullity of the anti-symmetrized adjacency matrix divided with the rank of γ-matrices.

4.1.1 Weighted digraphs corresponding to lattice fermions

In this discussion, we will show that lattice fermions on D-dimensional hypercubic lattices can be represented as certain directed and weighted graphs.

To discuss about the lattice fermions as graph theory, we firstly review the lattice fermions on D-dimensional hypercubic lattices. Let L be a finite volume D-dimensional hypercubic lattices as

$$L \equiv \left\{ n = \sum_{\mu=1}^{D} n_\mu \hat{\mu} = \sum_{\nu \in S^{\mathrm{PBC}}} n_\nu \hat{\nu} + \sum_{\rho \in S^{\mathrm{DBC}}} n_\rho \hat{\rho} \;\middle|\; \begin{array}{c} n_\mu \in [1, N_\mu] \subset \mathbb{Z}\,, \\ \exists N_\nu \in \mathbb{Z} \quad \text{s.t.} \quad n + N_\nu \hat{\nu} \sim n \end{array} \right\} \tag{4.1}$$

where $\hat{\mu}$ is standard basis in D-dimensional hypercubic lattice. Two set $S^{\mathrm{PBC}}, S^{\mathrm{DBC}}$ are defined as $S^{\mathrm{PBC}} \equiv \{\mu \mid n + N_\mu \hat{\mu} \sim n\}$ and $S^{\mathrm{DBC}} \equiv \left\{\mu \;\middle|\; \mu \notin S^{\mathrm{PBC}}\right\}$ respectively. These sets satisfy $|S^{\mathrm{PBC}}| + |S^{\mathrm{DBC}}| = D$. $n + N_\mu \hat{\mu} \sim n$ stands for Periodic Boundary Condition (PBC). By contrast, Dirichlet Boundary Condition (DBC) is $n_\mu \notin [1, N_\mu] \Rightarrow n = 0$. Note that the Dirichlet boundary condition is automatically imposed except on the direction

with periodic boundary condition since we consider the finite volume lattice. Then, lattice fermion action on this lattice is given as

$$S_L = \sum_{n\in L}\sum_{\mu=1}^{D} \bar{\psi}_n \gamma_\mu D_\mu \psi_n = \frac{1}{2}\sum_{n\in L}\sum_{\mu=1}^{D} \left[\bar{\psi}_n \gamma_\mu U_{n,\mu}\psi_{n+\hat{\mu}} - \bar{\psi}_{n+\hat{\mu}}\gamma_\mu U^\dagger_{n,\mu}\psi_n\right] \tag{4.2}$$

where $D_\mu \equiv (T_{+\mu} - T_{-\mu})/2$ with $T_{\pm\mu}\psi_n = U_{n,\pm\mu}\psi_{n\pm\hat{\mu}}$. D_μ is a difference operator called as lattice Dirac operator. ψ_n is the fermionic fields on which γ-matrices and $U_{n,\pm\mu}$ act. And $U_{n,\mu}$ is the gauge field, which is called the link variable satisfying $U_{n+\hat{\mu},-\mu} = U^\dagger_{n,\mu}$. In a free theory, we just set $U_{n,\mu} = \mathbf{1}$. The sum $\sum_{n\in L}$ is the summation over lattice sites $n = (n_1, \cdots, n_D) \in L$.

Next, we discuss lattice fermions on the lattice as graphs. We consider the weighted digraph G corresponding to the lattice fermions as

$$\begin{aligned} G &= G_1 \,\square\, G_2 \,\square\, \cdots \,\square\, G_D \\ w(e \in G_\mu) &= \gamma_\mu U_{n,\mu} \end{aligned} \tag{4.3}$$

where $G_\mu \in \left\{D^{(\text{cycle})}_\mu, D^{(\text{path})}_\mu\right\}$ for $\mu \in \{1, \cdots, D\}$ and $w(e)$ denote the weight of edge e. γ_μ is D-dimensional matrices, which was also described in the previous chapter. Note that the subscript n of the link variable stands for the vertices in the digraph, i.e. $n \in V(G)$. However, vertices in this digraph can be regarded as sites in the lattice L because $V(G)$ and the whole site are isomorphic as will be mentioned later. This weighted digraph is equal to the weighted digraph in Eq. (3.22) if we consider the case of a free theory. Some examples of G have shown in Fig. 3.6.

This digraph represents D-dimensional hypercubic lattice as graphs since vertices and edges in the digraph can be regarded as sites and links in the lattice. In particular, the set of vertices in the digraph G is isomorphic to the sites $n = (n_1, \cdots, n_D)$ in the lattice since the set of vertices is $V(G) = V(G_1) \times \cdots \times V(G_D)$ by definition of cartesian product in Def. 4. And any edge $\{m, n\}$ in the digraph can correspond to a link in the lattice by being represented as $n - m = \sum_{\mu=1}^{D}(n_\mu - m_\mu)\,\hat{\mu}$. Simultaneously, G_μ in the digraph G represents each boundary condition in D-dimensional hypercubic lattice as graph. Indeed, the cycle digraph $D^{(\text{cycle})}_\mu$ can be recognized as a graph represented periodic boundary condition $n + N_\mu\hat{\mu} \sim n$ as shown in Fig. 4.1. And the Dirichlet boundary condition corresponds to

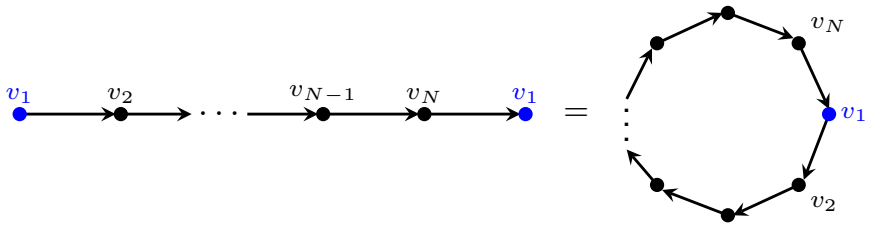

Figure 4.1: The periodic boundary condition can be represented as the cycle digraph since $v_n \sim v_{n+N}$ for a site v_n in 1-dim lattice.

the simple directed path since $n_\mu \notin [1, N_\mu] \Rightarrow n = 0$ for 1-dim lattice in each direction.

For these reasons, the digraph in Eq. (4.3) is recognized as a digraph representing D-dimensional hypercubic lattice with periodic boundary condition and Dirichlet boundary condition. In the next section, we will show that it is consistent to set $w(e \in G_\mu) = \gamma_\mu U_{n,\mu}$ as the weight on edges in digraph G.

4.1.2 Lattice action and anti-symmetrized adjacency matrix

In here, we will discuss relationship between lattice fermion action in Eq. (4.2) and anti-symmetrized adjacency matrix of the directed and weighted graph in Eq. (4.3).

Based on the definition of anti-symmetrized adjacency matrix in Def. 10, An anti-symmetrized adjacency matrix for the weighted digraph in Eq. (4.3) is obtained as

$$(A_{\rm as}(G))_{ij} = \begin{cases} \gamma_\mu U_{n,\mu} & i = n \text{ and } j = n+\hat{\mu} \text{ for edge } \{n, n+\hat{\mu}\} \\ -\gamma_\mu U^\dagger_{n,\mu} & i = n+\hat{\mu} \text{ and } j = n \text{ for edge } \{n, n+\hat{\mu}\} \\ 0 & \text{otherwise} \end{cases} \tag{4.4}$$

where use of $\gamma_\mu^\dagger = \gamma_\mu$ as the property of γ-matrices. Note that this anti-symmetrized adjacency matrix is equal to the anti-symmetrized adjacency matrix in Eq. (3.25) if we consider the case of a free theory. To represent lattice fermion action, we introduce a vector of fermion fields in D-dimensions. Namely, a vector $\boldsymbol{\psi}$ is $\boldsymbol{\psi} = \sum_n \psi_n \boldsymbol{e}_n$ where $\boldsymbol{e}_n \equiv \bigotimes_{\mu=1}^D \boldsymbol{e}_{n_{D+1-\mu}}$ are standard basis in $|V|$-dimensions which satisfy orthonormal $\boldsymbol{e}_m^\dagger \cdot \boldsymbol{e}_n = \delta_{mn} \equiv \prod_{\mu=1}^D \delta_{m_\mu n_\mu}$. δ_{kl} is the Kronecker delta. The component ψ_n is the fermion field on which γ-matrices and the link variable $U_{n,\mu}$ act. Here, we specify that the order of components ψ_n in the vector is $(1,1,\cdots,1) \to \cdots \to (N,1,\cdots,1) \to (1,2,\cdots,1) \to \cdots \to (N,N,\cdots,N)$ in descending order. Namely,

$$\boldsymbol{\psi} \equiv \begin{pmatrix} \psi_{(1,1,\cdots,1)} \\ \psi_{(2,1,\cdots,1)} \\ \vdots \\ \psi_{(N,1,\cdots,1)} \\ \psi_{(1,2,\cdots,1)} \\ \vdots \\ \psi_{(N,N,\cdots,N)} \end{pmatrix} \tag{4.5}$$

in term of the vector. By use of the anti-symmetrized adjacency matrix $A_{\rm as}(G)$ and the vector $\boldsymbol{\psi}$, the lattice fermion action in Eq. (4.2) can be represented as the bilinear form $\frac{1}{2}\bar{\boldsymbol{\psi}} A_{\rm as}(G) \boldsymbol{\psi}$. Because $\bar{\boldsymbol{\psi}} A_{\rm as}(G) \boldsymbol{\psi}$ is

$$\begin{aligned} \bar{\boldsymbol{\psi}} A_{\rm as}(G) \boldsymbol{\psi} &= \sum_{m,m' \in V} \bar{\psi}_m \big(A_{\rm as}(G) \big)_{mm'} \psi_{m'} \\ &= \sum_{m,m' \in V} \sum_{n \in V} \sum_{\mu=1}^D \bar{\psi}_m \gamma_\mu \big(U_{n,\mu} \delta_{mn} \delta_{m'\, n+\hat{\mu}} - U^\dagger_{n,\mu} \delta_{m\, n+\hat{\mu}} \delta_{mn} \big) \psi_{m'} \\ &= \sum_{n \in V} \sum_{\mu=1}^D \left[\bar{\psi}_n \gamma_\mu U_{n,\mu} \psi_{n+\hat{\mu}} - \bar{\psi}_{n+\hat{\mu}} \gamma_\mu U^\dagger_{n,\mu} \psi_n \right] , \end{aligned} \tag{4.6}$$

we can show $\frac{1}{2}\bar{\boldsymbol{\psi}} A_{\rm as}(G)\boldsymbol{\psi} = S_L$. As a result, we have also shown that it is consistent to set $w(e \in G_\mu) = \gamma_\mu U_{n,\mu}$ as the weight on edges in the digraph. It means that the lattice action for the directed and weighted graph in Eq. (3.22) is given as the bilinear form of the anti-semmetrized adjacency matrix for the digraph and vector of fermionic fields.

As an example of the bilinear form, we consider the case of $G = D_1^{(\rm cycle)} \square D_2^{(\rm path)}$ where $D_1^{(\rm cycle)}$ with three vertices and $D_2^{(\rm path)}$ with two vertices. This digraph is depicted in Fig. 4.2. Then, an anti-symmetrized adjacency matrix for this digraph is $|V| = 6$

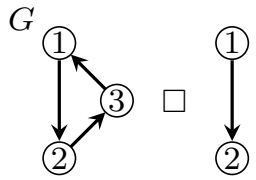

Figure 4.2: This directed and weighted graph illustrates $G = D_1^{(\rm path)} \square D_2^{(\rm cycle)}$ which has $D_1^{(\rm path)}$ with two vertices and $D_2^{(\rm path)}$ with three vertices.

square matrix with $\gamma_\mu U_{n,\mu}$ as components. It is explicitly written as

$$A_{\rm as}(G) = \begin{pmatrix} 0 & \gamma_1 U_{(1,1),1} & -\gamma_1 U^\dagger_{(3,1),1} & \gamma_2 U_{(1,1),2} & 0 & 0 \\ -\gamma_1 U^\dagger_{(1,1),1} & 0 & \gamma_1 U_{(2,1),1} & 0 & \gamma_2 U_{(2,1),2} & 0 \\ \gamma_1 U_{(3,1),1} & -\gamma_1 U^\dagger_{(2,1),1} & 0 & 0 & 0 & \gamma_2 U_{(3,1),2} \\ -\gamma_2 U^\dagger_{(1,1),2} & 0 & 0 & 0 & \gamma_1 U_{(1,2),1} & -\gamma_1 U^\dagger_{(3,2),1} \\ 0 & -\gamma_2 U^\dagger_{(2,1),2} & 0 & -\gamma_1 U^\dagger_{(1,2),1} & 0 & \gamma_1 U_{(2,2),1} \\ 0 & 0 & -\gamma_2 U^\dagger_{(3,1),2} & \gamma_1 U_{(3,2),1} & -\gamma_1 U^\dagger_{(2,2),1} & 0 \end{pmatrix} \tag{4.7}$$

in term of the matrix. As a result, the bilinear form $\bar{\boldsymbol{\psi}} A_{\rm as}(G)\boldsymbol{\psi}$ is obtained as

$$\begin{aligned} \bar{\boldsymbol{\psi}} A_{\rm as}(G)\boldsymbol{\psi} = & \sum_{n_2 \in V_2} \Big(\bar\psi_{(1,n_2)} \gamma_1 U_{(1,n_2),1} \psi_{(2,n_2)} - \bar\psi_{(2,n_2)} \gamma_1 U^\dagger_{(1,n_2),1} \psi_{(1,n_2)} \\ & \quad + \bar\psi_{(2,n_2)} \gamma_1 U_{(2,n_2),1} \psi_{(3,n_2)} - \bar\psi_{(3,n_2)} \gamma_1 U^\dagger_{(2,n_2),1} \psi_{(2,n_2)} \\ & \quad + \bar\psi_{(3,n_2)} \gamma_1 U_{(3,n_2),1} \psi_{(1,n_2)} - \bar\psi_{(1,n_2)} \gamma_1 U^\dagger_{(3,n_2),1} \psi_{(3,n_2)} \Big) \\ & + \sum_{n_1 \in V_1} \Big(\bar\psi_{(n_1,1)} \gamma_2 U_{(n_1,1),2} \psi_{(n_1,2)} - \bar\psi_{(n_1,2)} \gamma_2 U^\dagger_{(n_1,2),1} \psi_{(n_1,1)} \Big) \\ = & \sum_{n \in V} \sum_{\mu=1}^{2} \left[\bar\psi_n \gamma_\mu U_{n,\mu} \psi_{n+\hat\mu} - \bar\psi_{n+\hat\mu} \gamma_\mu U^\dagger_{n,\mu} \psi_n \right] \end{aligned} \tag{4.8}$$

where $V_1 \equiv V(D_1^{(\rm cycle)})$ and $V_2 \equiv V(D_2^{(\rm path)})$. As shown in these equations, each boundary condition is reflected in the components of the anti-symmetrized adjacency matrices. Even for $G = G_1 \square \cdots \square G_D$, components of the anti-symmetrized adjacency matrix reflects boundary conditions on each direction.

For this and previous discussions, the directed and weighted graph in Eq. (4.3) is recognized as the lattice fermions on finite volume D-dimensional hypercubic lattice with

periodic boundary condition and Dirichlet boundary condition in term of spectral graph theory. In the next discussion, we will show relationship between the number of fermion species and the nullity of anti-symmetrized adjacency matrices, and derive the number of fermion species for the lattices in Eq. (4.1)

4.1.3 Fermion species and the nullity of anti-symmetrized adjacency matrix

We will discuss about the relationship between the number of fermion species and anti-symmetrized adjacency matrices. This discussion is limited to the free theory. Thus, weighted digraph we are considering is the one in Eq. (3.22).

Before this discussion, let us mention about fermion species. The fermion species are given as zero-modes of lattice Dirac operator, i.e. φ_p such that $D_\mu \varphi_p = 0$. In other words, the fermion species are equivalent to zero-eigenvalues (or nullity) of the matrix-representation of lattice Dirac operator since zero-modes of lattice Dirac operator is elements in kernel space of the operator. Thus, the number of fermion species can be derived by the nullity of the matrix-representation of the lattice Dirac operator. Note that the number of fermion species is equal to the nullity of the matrix-representation of lattice Dirac operator divided with the rank of γ-matrices.

We discuss about the matrix-representation of the lattice Dirac operator and fermion species as spectral graph theory. In the previous discussion, the bilinear form of $A_{\text{as}}(G^{\text{free}})$ in the free theory is

$$\bar{\boldsymbol{\psi}} A_{\text{as}}(G^{\text{free}}) \boldsymbol{\psi} = \sum_{n \in V} \sum_{\mu=1}^{D} \left[\bar{\psi}_n \psi_{n+\hat{\mu}} - \bar{\psi}_{n+\hat{\mu}} \gamma_\mu \psi_n \right] \tag{4.9}$$

in term of spectral graph theory. Meanwhile, the free lattice fermion action on the lattice in Eq. (4.1) is given as

$$S_L^{\text{free}} = \frac{1}{2} \sum_{n \in L} \sum_{\mu=1}^{D} \left[\bar{\psi}_n \gamma_\mu \psi_{n+\hat{\mu}} - \bar{\psi}_{n+\hat{\mu}} \gamma_\mu \psi_n \right] = \bar{\boldsymbol{\psi}} \mathcal{D} \boldsymbol{\psi} \tag{4.10}$$

where $\mathcal{D}$ is the matrix-representation of the lattice Dirac operator and the vector $\boldsymbol{\psi}$ has assumed Eq. (4.5). Since $S_L^{\text{free}} = \bar{\boldsymbol{\psi}} A_{\text{as}}(G^{\text{free}}) \boldsymbol{\psi}/2$, the matrix-representation of the lattice Dirac operator is equal to the anti-symmetrized adjacency matrix with $1/2$ as the coefficient, i.e. $\mathcal{D} = A_{\text{as}}(G^{\text{free}})/2$. Since the number of fermion species can be derived by the matrix-representation of lattice Dirac operator, it can be derived by the nullity of anti-symmetrized adjacency matrix for the digraph in Eq. (3.22). Furthermore, the number of fermion species is equal to the nullity of the anti-symmetrized adjacency matrix divided with the rank of γ-matrices. As a result, the number of fermion species is expressed as

$$\#\text{species} = \frac{\dim \left(\ker A_{\text{as}}(G^{\text{free}}) \right)}{\operatorname{rank} \gamma} \tag{4.11}$$

where #species denotes the number of fermion species.

Next, we actually derive the number of fermion species on the weighted digraph in the free theory. The anti-symmetrized adjacency matrix $A_{\rm as}(G^{\rm free})$ in the case of free theory is the matrix in Eq. (3.25) since the directed and weighted graph is the one in Eq. (3.22). For this reason, we can use the theorem in Thm. 3 and results obtained in its proof to derive the number of fermion species. The maximum number of fermion species is given by the topology of graphs based on the theorem. The reason for discussing the maximum number is that the number of fermion species depends on vertices in each digraph G_μ, but the maximum number is uniquely determined by the topology. Thus, the maximum number of fermion species in the digraph $G^{\rm free}$ is

$$\max\left[\,\#\text{species}\,\right] = \max\left[\frac{\dim\left(\ker A_{\rm as}(G^{\rm free})\right)}{\operatorname{rank}\gamma}\right] = 2^{|S^{\rm c}|} \tag{4.12}$$

where $|S^{\rm c}|$ is the number of the cycle digraphs in $G^{\rm free}$. Meanwhile, the number of fermion species can be derived for the results obtained in the proof of the theorem. It is expressed as

$$\#\text{species} = \begin{cases} 2^{|S^{\rm c,e}|} & |S^{\rm p,e}| = 0 \\ 0 & |S^{\rm p,e}| \neq 0 \end{cases} \tag{4.13}$$

where $|S^{\rm c,e}|$, $|S^{\rm p,e}|$ are the number of the cycle digraphs with even vertices in $G^{\rm free}$ and the number of the simple directed paths with even vertices in $G^{\rm free}$, respectively.

As some examples, we consider two weighted digraphs: $D_1^{(\rm cycle)} \,\square\, D_2^{(\rm path)}$ where $D_1^{(\rm cycle)}$ with three vertices and $D_2^{(\rm path)}$ with two vertices, $D_1^{(\rm path)} \,\square\, D_2^{(\rm cycle)}$ with three vertices each, $D_1^{(\rm cycle)} \,\square\, D_2^{(\rm cycle)}$ with three vertices each, $D_1^{(\rm cycle)} \,\square\, D_2^{(\rm cycle)}$ with four vertices each. These weighted digraphs are denoted as

$$G^{(1)} = D_1^{(\rm cycle)} \,\square\, D_2^{(\rm path)}\,, \qquad |V(D_1^{(\rm cycle)})| = 3\,, \qquad |V(D_2^{(\rm path)})| = 2 \tag{4.14a}$$

$$G^{(2)} = D_1^{(\rm path)} \,\square\, D_2^{(\rm cycle)}\,, \qquad |V(D_1^{(\rm path)})| = 3\,, \qquad |V(D_2^{(\rm cycle)})| = 3 \tag{4.14b}$$

$$G^{(3)} = D_1^{(\rm cycle)} \,\square\, D_2^{(\rm cycle)}\,, \qquad |V(D_1^{(\rm cycle)})| = 3\,, \qquad |V(D_2^{(\rm cycle)})| = 3 \tag{4.14c}$$

$$G^{(4)} = D_1^{(\rm cycle)} \,\square\, D_2^{(\rm cycle)}\,, \qquad |V(D_1^{(\rm cycle)})| = 4\,, \qquad |V(D_2^{(\rm cycle)})| = 4 \tag{4.14d}$$

The first digraph has shown in Fig. 4.2, and the other digraphs are depicted in Fig. 4.3. The number of fermion species for each digraph is as follows:

- $G^{(1)}$; The number of fermion species is #species $= 0$ since $|S^{\rm p,e}| \neq 0$. For Eq. (3.35), the diagonalization of the anti-symmetrized adjeecency matrix $A_{\rm as}(G^{(1)})$ is obtained as

$$\begin{aligned} \mathcal{U}^\dagger A_{\rm as}(G^{(1)})\,\mathcal{U} = i\,\mathrm{Diag}\Big[\, & \gamma_2\,,\ \sqrt{3}\gamma_1 + \gamma_2\,,\ -\sqrt{3}\gamma_1 + \gamma_2\,, \\ & -\gamma_2\,,\ \sqrt{3}\gamma_1 - \gamma_2\,,\ -\sqrt{3}\gamma_1 - \gamma_2 \Big]\,. \end{aligned} \tag{4.15}$$

  An inequality #species $< 2^{|S^{\rm c}|} = 2$ holds since $|S^{\rm c}| = 1$.

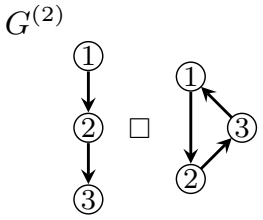

(a) $G^{(2)} = D_1^{(\mathrm{path})} \square D_2^{(\mathrm{cycle})}$.

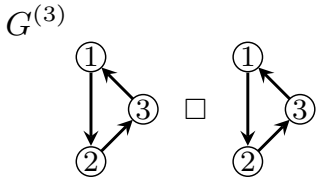

(b) $G^{(3)} = D_1^{(\mathrm{cycle})} \square D_2^{(\mathrm{cycle})}$.

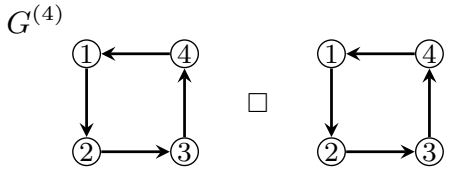

(c) $G^{(4)} = D_1^{(\mathrm{cycle})} \square D_2^{(\mathrm{cycle})}$.

Figure 4.3: These digraphs depict three examples $G^{(2)}, G^{(3)}, G^{(4)}$.

- $G^{(2)}$; The number of fermion species is #species $= 1$ since $|S^{\mathrm{p,e}}| = 0$ and $|S^{\mathrm{c,e}}| = 0$. The diagonalization of the anti-symmetrized adjeecency matrix $A_{\mathrm{as}}(G^{(2)})$ is obtained as

$$\begin{aligned}\mathcal{U}^\dagger A_{\mathrm{as}}(G^{(2)})\mathcal{U} = i\,\mathrm{Diag}\Big[&\sqrt{2}\gamma_1\,,\ 0\,,\ -\sqrt{2}\gamma_1\,,\\ &\sqrt{2}\gamma_1+\sqrt{3}\gamma_2\,,\ \sqrt{3}\gamma_2\,,\ -\sqrt{2}\gamma_1+\sqrt{3}\gamma_2\,,\\ &\sqrt{2}\gamma_1-\sqrt{3}\gamma_2\,,\ -\sqrt{3}\gamma_2\,,\ -\sqrt{2}\gamma_1-\sqrt{3}\gamma_2\Big]\,.\end{aligned} \tag{4.16}$$

  An inequality #species $< 2^{|S^{\mathrm{c}}|} = 2$ holds since $|S^{\mathrm{c}}| = 1$.

- $G^{(3)}$; The number of fermion species is #species $= 1$ since $|S^{\mathrm{p,e}}| = 0$ and $|S^{\mathrm{c,e}}| = 0$. The diagonalization of the anti-symmetrized adjeecency matrix $A_{\mathrm{as}}(G^{(3)})$ is obtained as

$$\begin{aligned}\mathcal{U}^\dagger A_{\mathrm{as}}(G^{(3)})\mathcal{U} = \sqrt{3}i\,\mathrm{Diag}\Big[&0\,,\ \gamma_1\,,\ -\gamma_1\,,\\ &\gamma_2\,,\ \gamma_1+\gamma_2\,,\ -\gamma_1+\gamma_2\,,\\ &-\gamma_2\,,\ \gamma_1-\gamma_2\,,\ -\gamma_1-\gamma_2\Big]\,.\end{aligned} \tag{4.17}$$

  An inequality #species $< 2^{|S^{\mathrm{c}}|} = 4$ holds since $|S^{\mathrm{c}}| = 2$.

- $G^{(4)}$; The number of fermion species is #species $= 4$ since $|S^{\mathrm{p,e}}| = 0$ and $|S^{\mathrm{c,e}}| = 2$. The diagonalization of the anti-symmetrized adjeecency matrix $A_{\mathrm{as}}(G^{(4)})$ is obtained as

$$\begin{aligned}\mathcal{U}^\dagger A_{\mathrm{as}}(G^{(4)})\mathcal{U} = i\,\mathrm{Diag}\Big[&0\,,\ \gamma_1\,,\ 0\,,\ -\gamma_1\,,\ \gamma_2\,,\ \gamma_1+\gamma_2\,,\ \gamma_2\,,\ -\gamma_1+\gamma_2\,,\\ &0\,,\ \gamma_1\,,\ 0\,,\ -\gamma_1\,,\ -\gamma_2\,,\ \gamma_1-\gamma_2\,,\ -\gamma_2\,,\ -\gamma_1-\gamma_2\Big]\,.\end{aligned} \tag{4.18}$$

An equation #species $= 2^{|S^{\rm c}|} = 4$ holds since $|S^{\rm c}| = 2$.

As these examples show, the number of fermion species depends on either even or odd vertices for each digraph G_μ in the weighted digraph $G^{\rm free}$. And the number of them determines upper bound by the topology of graphs.

In later sections, we will discuss in the cases of D-dimensional hypercubic lattice with only periodic boundary condition (T^D-lattice) and one with only Dirichlet boundary condition (B^D-lattice).

4.2 Lattice fermions on torus

In the previous section, we discussed lattice fermions on D-dimensional hypercubic lattices with periodic boundary condition or Dirichlet boundary condition in each direction in term of spectral graph theory. In this section, we will discuss lattice fermions on T^D-lattice in term of spectral graph theory. This section is divided into two parts. Fist, we will discuss in D-dimensions. In here, we will introduce a directed and weighted graph representing lattice fermions in D-dimensions and show that lattice fermion action is given by the bilinear form of matrices for the weighted digraph. Furthermore, we will discuss the number of fermion species. The second part will be discussed about lattice fermions on T^4-lattice. The lattice fermions on this lattice are the well-known naive lattice fermions. We will show that the results of this discussion are consistent with the known results.

Before this discussion, we will mention the T^D-lattice and lattice fermions on it. The T^D-lattice is a finite volume D-dimensional hypercubic lattice with only periodic boundary condition, and be expressed as

$$T^D\text{-lattice} \equiv \left\{ n = \sum_{\mu=1}^{D} n_\mu \hat{\mu} \;\middle|\; \begin{array}{c} n_\mu \in [1, N_\mu] \subset \mathbb{Z}\,, \\ \exists N_\mu \in \mathbb{Z} \quad \text{s.t.} \quad n + N_\mu \hat{\mu} \sim n \end{array} \right\} \tag{4.19}$$

where $\hat{\mu}$ is the standard basis in D-dimensional hypercubic lattice. As previously mentioned, the periodic boundary condition is represented as $n + N_\mu \hat{\mu} \sim n$. An illustrated boundary condition is shown in Fig. 4.1. Then, a lattice fermion action on T^D-lattice is given as

$$S_{T^D} = \sum_n \sum_{\mu=1}^{D} \bar{\psi}_n \gamma_\mu D_\mu \psi_n = \frac{1}{2} \sum_n \sum_{\mu=1}^{D} \left[\bar{\psi}_n \gamma_\mu U_{n,\mu} \psi_{n+\hat{\mu}} - \bar{\psi}_{n+\hat{\mu}} \gamma_\mu U^\dagger_{n,\mu} \psi_n \right] \tag{4.20}$$

where $D_\mu \equiv (T_{+\mu} - T_{-\mu})/2$ with $T_{\pm\mu}\psi_n = U_{n,\pm\mu}\psi_{n\pm\hat{\mu}}$. D_μ is a difference operator called as lattice Dirac operator. ψ_n is the fermionic fields on which γ-matrices and $U_{n,\pm\mu}$ act. And $U_{n,\mu}$ is the gauge field, which is called the link variable satisfying $U_{n+\hat{\mu},-\mu} = U^\dagger_{n,\mu}$. In a free theory, we just set $U_{n,\mu} = \mathbf{1}$. The sum $\sum_n$ is the summation over lattice sites $n = (n_1, \cdots, n_D)$ in T^D-lattice. The difference between this action and the action in Eq. (4.2) is that there are no terms representing Dirichlet boundary condition. In the free and four-dimensional case, the lattice fermion action is given by

$$S^{\rm free}_{\rm nf} = \frac{1}{2} \sum_n \sum_{\mu=1}^{D} \left[\bar{\psi}_n \gamma_\mu \psi_{n+\hat{\mu}} - \bar{\psi}_{n+\hat{\mu}} \gamma_\mu \psi_n \right] \tag{4.21}$$

and 16 fermion species are known to occur in the theory.

4.2.1 Lattice fermions on any dimensional torus

In this subsection, we will discuss lattice fermions on T^D-lattice in term of spectral graph theory. This subsection is divided into three parts. In the first and second part, we will discuss a directed and weighted graph representing lattice fermion on T^D-lattice and its lattice action as spectral graph theory. The final part describes about the number of fermion species and the nullity of matrices associated with the weighted digraph.

Firstly, we discuss a directed and weighted graph representing lattice fermions on T^D-lattice. For the previous section, let G_{T^D} be the directed and weighted graph corresponding to the T^D-lattice. It is expressed as

$$\begin{aligned} G_{T^D} &= D_1^{(\text{cycle})} \square D_2^{(\text{cycle})} \square \cdots \square D_D^{(\text{cycle})} \\ w(e \in G_\mu) &= \gamma_\mu U_{n,\mu} \end{aligned} \tag{4.22}$$

where $D_\mu^{(\text{cycle})}$ is the cycle digraph with $|V|_\mu$ vertices. Note that the subscript n of the link variable stands for the vertices in the digraph, i.e. $n \in V$ where V is the set of vertices in G_{T^D}. However, vertices in this digraph can be regarded as sites in the T^D-lattice because V and the whole site are isomorphic by definition of cartesian product in Def 4. In particular, since the set of vertices in G_{T^D} is $V = V(D_1^{(\text{cycle})}) \times \cdots \times V$ by cartesian product, a map $f : V \to T^D$-lattice is isomorphism. Each digraph $D_\mu^{(\text{cycle})}$ is a digraph representing periodic boundary condition $n + N_\mu \hat{\mu} \sim n$ since the cycle digraph is equivalent to the boundary condition by setting $N_\mu = |V|_\mu$. The case of $D = 2$ is depicted in Fig. 4.4 Based on the definition in Def. 10, an anti-symmetrized adjacency matrix for

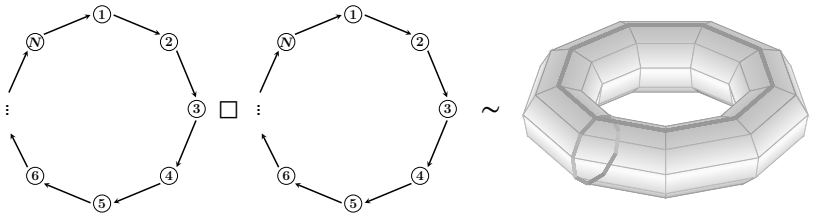

Figure 4.4: The digraph G_{T^2} is identified as a two dimensional torus with directed edges.

the weighted digraph G_{T^D} is obtain as

$$(A_{\text{as}}(G_{T^D}))_{ij} = \begin{cases} \gamma_\mu U_{n,\mu} & i = n \text{ and } j = n + \hat{\mu} \text{ for edge } \{n, n + \hat{\mu}\} \\ -\gamma_\mu U_{n,\mu}^\dagger & i = n + \hat{\mu} \text{ and } j = n \text{ for edge } \{n, n + \hat{\mu}\} \\ 0 & \text{otherwise} \end{cases} \tag{4.23}$$

where use of $\gamma_\mu^\dagger = \gamma_\mu$ as the property of γ-matrices. In the free theory, which sets $U_{n,\mu} = \mathbf{1}$, this anti-symmetrized adjacency matrix is written as the following simple expression by use of tensor product,

$$A_{\text{as}}(G_{T^D}^{\text{free}}) = \sum_{\mu=1}^{D} \left\{ \left(\bigotimes_{\nu=1}^{D-\mu} \mathbf{1}_{|V|_{D+1-\nu}} \right) \otimes A'_{\text{as}}(D_\mu^{(\text{cycle})}) \otimes \left(\bigotimes_{\rho=1}^{\mu-1} \mathbf{1}_{|V|_\rho} \right) \right\} \otimes \gamma_\mu \tag{4.24}$$

where $A'_{\rm as}(D^{(\rm cycle)}_\mu)$ is $|V|_\mu$-square matrix in Eq.(3.26).

Secondary, we show that the bilinear form $\bar{\boldsymbol{\psi}} A_{\rm as}(G_{T^D})\boldsymbol{\psi}$ is equivalent to the lattice femrion action on T^D-lattice. To discuss it, we use the vector of fermion fields in D-dimensions that is expressed as $\boldsymbol{\psi} = \sum_{n\in V}\psi_n \boldsymbol{e}_n$ where $\boldsymbol{e}_n \equiv \bigotimes_{\mu=1}^D \boldsymbol{e}_{n_{D+1-\mu}}$. Note that $\boldsymbol{e}_n$ are the standard basis in $|V|$-dimensions which satisfy orthonormal $\boldsymbol{e}^\dagger_m \cdot \boldsymbol{e}_n = \delta_{mn} \equiv \prod_{\mu=1}^D \delta_{m_\mu n_\mu}$. And γ-matrices and the link variable $U_{n,\mu}$ act on the fermionic field ψ_n in the vector. By use of this vector, the bilinear form of the anti-symmetrized adjacency matrix $A_{\rm as}(G_{T^D})$ and the vector $\boldsymbol{\psi}$ is

$$\begin{aligned}\bar{\boldsymbol{\psi}} A_{\rm as}(G_{T^D})\boldsymbol{\psi} &= \sum_{m,m'\in V} \bar\psi_m \big(A_{\rm as}(G_{T^D}) \big)_{mm'} \psi_{m'} \\ &= \sum_{n\in V}\sum_{\mu=1}^D \big[\bar\psi_n \gamma_\mu U_{n,\mu}\psi_{n+\hat\mu} - \bar\psi_{n+\hat\mu}\gamma_\mu U^\dagger_{n,\mu}\psi_n \big]\end{aligned} \tag{4.25}$$

for Eq. (4.23). As shown in Eq. (4.20), we can show $S_{T^D} = \bar{\boldsymbol{\psi}} A_{\rm as}(G_{T^D})\boldsymbol{\psi}/2$. And by the vector $\boldsymbol{\psi}$ the lattice action S_{T^D} can be rewritten as

$$S_{T^D} = \sum_{n\in V}\sum_{\mu=1}^D \big[\bar\psi_n \gamma_\mu U_{n,\mu}\psi_{n+\hat\mu} - \bar\psi_{n+\hat\mu}\gamma_\mu U^\dagger_{n,\mu}\psi_n \big] = \bar{\boldsymbol{\psi}} \mathcal{D}_{T^D}\boldsymbol{\psi} \tag{4.26}$$

where $\mathcal{D}_{T^D}$ is the matrix-representation of lattice Dirac operator on T^D-lattice. As a result, we obtain that the matrix-representation of lattice Dirac operator is equal to the anti-symmetrized adjacency matrix for the digraph G_{T^D} with $1/2$ as the coefficient, i.e. $\mathcal{D}_{T^D} = A_{\rm as}(G_{T^D})/2$. In the case of free theory, the free lattice fermion action is also equal to $\bar{\boldsymbol{\psi}} A_{\rm as}(G^{\rm free}_{T^D})\boldsymbol{\psi}/2$ since the bilinear form $\bar{\boldsymbol{\psi}} A_{\rm as}(G^{\rm free}_{T^D})\boldsymbol{\psi}/2$ is

$$\begin{aligned}\frac{1}{2}\bar{\boldsymbol{\psi}} A_{\rm as}(G^{\rm free}_{T^D})\boldsymbol{\psi} &= \frac{1}{2}\sum_{m,n\in V}\sum_{\mu=1}^D \bar\psi_m\gamma_\mu\psi_n \Big\{ \boldsymbol{e}^\dagger_{m_\mu} A'_{\rm as}(D^{(\rm cycle)}_\mu)\boldsymbol{e}_{n_\mu}\Big\} \prod_{\nu=1}^{D-\mu}\prod_{\rho=1}^{\mu-1}\delta_{m_{D+1-\nu}n_{D+1-\nu}}\delta_{m_\rho n_\rho} \\ &= \frac{1}{2}\sum_{m,n\in V}\sum_{\mu=1}^D \bar\psi_m\gamma_\mu\psi_n \Big\{ \delta_{m_\mu+1\, n_\mu} - \delta_{m_\mu\, n_\mu+1}\Big\} \prod_{\nu=1}^{D-\mu}\prod_{\rho=1}^{\mu-1}\delta_{m_{D+1-\nu}n_{D+1-\nu}}\delta_{m_\rho n_\rho} \\ &= \frac{1}{2}\sum_{m,n\in V}\sum_{\mu=1}^D \bar\psi_m\gamma_\mu\psi_n \Big\{ \delta_{m+\hat\mu\, n} - \delta_{m\, n+\hat\mu}\Big\} \\ &= \frac{1}{2}\sum_{n}\sum_{\mu=1}^D \big[\bar\psi_n\gamma_\mu\psi_{n+\hat\mu} - \bar\psi_{n+\hat\mu}\gamma_\mu\psi_n \big] = S^{\rm free}_{T^D}\end{aligned} \tag{4.27}$$

where we used $\boldsymbol{e}^\dagger_{m_\mu} A'_{\rm as}(D^{(\rm cycle)}_\mu)\boldsymbol{e}_{n_\mu} = \delta_{m_\mu+1\, n_\mu} - \delta_{m_\mu\, n_\mu+1}$ for Eq. (3.26). Since the free lattice action can be written as $S^{\rm free}_{\rm nf} = \bar{\boldsymbol{\psi}}\mathcal{D}^{\rm free}_{T^D}\boldsymbol{\psi}$, the matrix-representation of free lattice Dirac operator results in $\mathcal{D}^{\rm free}_{T^D} = A_{\rm as}(G^{\rm free}_{T^D})/2$.

Finally, we discuss the number of fermion species for the weighted digraph in the free theory. For the theorem in Thm. 3, the maximum number of fermion species is uniquely

determined by the topology of graphs, and be expressed as

$$\max\left[\,\#\text{species}\,\right] = \prod_{\mu=1}^{D}\left\{\beta_0(D_\mu^{(\text{cycle})}) + \beta_1(D_\mu^{(\text{cycle})})\right\} = 2^D \tag{4.28}$$

where $\beta_0(D_\mu^{(\text{cycle})}) + \beta_1(D_\mu^{(\text{cycle})}) = 2$. On the other hands, the number of fermion species is given by the number of the cycle digraphs with even vertices in $G_{T^D}^{\text{free}}$. It is expressed as

$$\#\text{species} = 2^{|S^{\text{c,e}}|} \tag{4.29}$$

where $|S^{\text{c,e}}|$ is the number of the cycle digraphs with even vertices in $G_{T^D}^{\text{free}}$. We can confirm this result by examining the nullity of the anti-symmetrized adjacency matrix for the weighted digraph $G_{T^D}^{\text{free}}$. For Eq. (3.35), the diagonalization of the anti-symmetrized adjacency matrix for the weighted digraph $G_{T^D}^{\text{free}}$ is

$$\left(\mathcal{U}^\dagger A_{\text{as}}(G_{T^D}^{\text{free}})\,\mathcal{U}\right)_{mn} = 2i\delta_{mn}\sum_{\mu=1}^{D}\gamma_\mu \sin\left(\frac{2\pi\,(m_\mu - 1)}{|V|_\mu}\right) \tag{4.30}$$

for $m, n \in V$. Since the linear independence of γ-matrices and $m_\mu \in \mathbb{Z}$, there are $2^{|S^{\text{c,e}}|}$ ways in which $m = (m_1, \cdots, m_D)$ satisfies $\left(\mathcal{U}^\dagger A_{\text{as}}(G_{T^D}^{\text{free}})\,\mathcal{U}\right)_{mn} = 0$. Thus, we have shown Eq. (4.29) by the anti-symmetrized adjacency matrix for the weighted digraph $G_{T^D}^{\text{free}}$.

We comment on the meaning of m_μ. This m_μ can be interpreted as a "shifted momentum" in this case. However, it is not necessarily equivalent to the momentum since it can be defined also on the lattice in which the momentum cannot be defined. Thus, m_μ should be simply interpreted as an index for the modes in general.

In the next subsection, we will discuss in four-dimensions. This lattice fermion is the well-known lattice fermion as naive lattice fermion.

4.2.2 Lattice fermions on four-dimensional torus

In this section, we will discuss lattice fermons on four-dimensional torus lattice, which is as a physically significant case, in term of spectral graph theory. This lattice fermion is known as the naive fermion. We will show that the results of this discussion are consistent with the known results.

Before this discussion, we review the four-dimansional torus lattice and the lattice fermion on it. The four-dimansional torus lattice is given by

$$T^4\text{-lattice} \equiv \left\{ n = \sum_{\mu=1}^{4} n_\mu \hat{\mu} \;\middle|\; \begin{array}{c} n_\mu \in [1, N_\mu] \subset \mathbb{Z}\,, \\ \exists N_\mu \in \mathbb{Z} \quad \text{s.t.} \quad n + N_\mu \hat{\mu} \sim n \end{array} \right\} \tag{4.31}$$

based on Eq. (4.19). Then, a lattice fermion action on four-dimensions is given as

$$S_{\text{nf}} = \sum_n \sum_{\mu=1}^{4} \bar{\psi}_n \gamma_\mu D_\mu \psi_n = \frac{1}{2}\sum_n \sum_{\mu=1}^{4}\left[\bar{\psi}_n \gamma_\mu U_{n,\mu}\psi_{n+\hat{\mu}} - \bar{\psi}_{n+\hat{\mu}}\gamma_\mu U_{n,\mu}^\dagger \psi_n\right] \tag{4.32}$$

where $D_\mu \equiv (T_{+\mu} - T_{-\mu})/2$ with $T_{\pm\mu}\psi_n = U_{n,\pm\mu}\psi_{n\pm\hat{\mu}}$. D_μ, ψ_n are the lattice Dirac operator and the fermionic fields respectively. And $U_{n,\mu}$ is called the link variable. γ-matrices and $U_{n,\pm\mu}$ act on the fermionic fields ψ_n. In a free theory, we just set $U_{n,\mu} = \mathbf{1}$. The sum $\sum_n$ is the summation over lattice sites $n = (n_1, n_2, n_3, n_4)$ in four-dimensional torus lattice. In the free and four-dimensional case, the lattice fermion action is given by

$$S_{\rm nf}^{\rm free} = \frac{1}{2}\sum_n \sum_{\mu=1}^{4} \left[\bar{\psi}_n \gamma_\mu \psi_{n+\hat{\mu}} - \bar{\psi}_{n+\hat{\mu}} \gamma_\mu \psi_n\right] \tag{4.33}$$

and 16 fermion species are known to occur in the theory.

First, we discuss a directed and weighted graph representing lattice fermions in four-dimensions. The weighted digraph representing lattice fermions on four-dimensional torus lattice (T^4-lattice) is

$$\begin{gathered} G_{T^4} = D_1^{(\rm cycle)} \square D_2^{(\rm cycle)} \square D_3^{(\rm cycle)} \square D_4^{(\rm cycle)} \\ w(e \in G_\mu) = \gamma_\mu U_{n,\mu} \end{gathered} \tag{4.34}$$

where $D_\mu^{(\rm cycle)}$ is the cycle digraph with $|V|_\mu$ vertices. This digraph G_{T^4} is depicted in Fig. 4.5. The subscript n of the link variable stands for the vertices in the digraph, i.e.

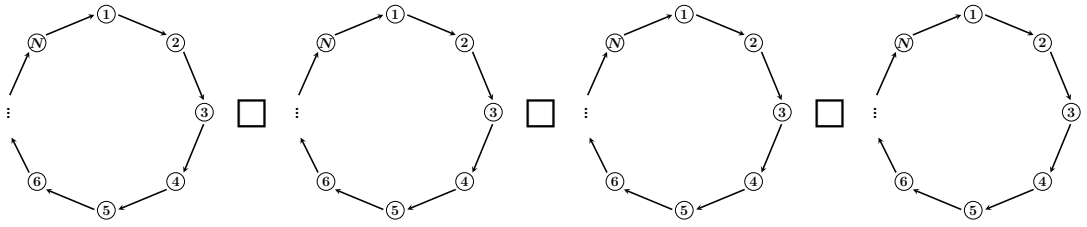

Figure 4.5: This digraph constructed cartesian-product $\square$ of four cycle digraphs $D^{(\rm cycle)}$ with $|V|_\mu = N$ vertices each.

$n \in V$ where V is the set of vertices in G_{T^D}. For Def. 10, an anti-symmetrized adjacency matrix of the weighted digraph G_{T^4} is obtained as

$$(A_{\rm as}(G_{T^4}))_{ij} = \begin{cases} \gamma_\mu U_{n,\mu} & i = n \text{ and } j = n+\hat{\mu} \text{ for edge } \{n, n+\hat{\mu}\} \\ -\gamma_\mu U_{n,\mu}^\dagger & i = n+\hat{\mu} \text{ and } j = n \text{ for edge } \{n, n+\hat{\mu}\} \\ 0 & \text{otherwise} \end{cases} \tag{4.35}$$

where use of $\gamma_\mu^\dagger = \gamma_\mu$. If we consider the free theory, which sets $U_{n,\mu} = \mathbf{1}$, this anti-symmetrized adjacency matrix is written as

$$\begin{aligned} A_{\rm as}(G_{T^4}^{\rm free}) &= \sum_{\mu=1}^{4} \left\{ \left(\bigotimes_{\nu=1}^{4-\mu} \mathbf{1}_{|V|_{5-\nu}} \right) \otimes A'_{\rm as}(D_\mu^{(\rm cycle)}) \otimes \left(\bigotimes_{\rho=1}^{\mu-1} \mathbf{1}_{|V|_\rho} \right) \right\} \otimes \gamma_\mu \\ &= \mathbf{1}_{|V|_4} \otimes \mathbf{1}_{|V|_3} \otimes \mathbf{1}_{|V|_2} \otimes A'_{\rm as}(D_1^{(\rm cycle)}) \otimes \gamma_1 \\ &\quad + \mathbf{1}_{|V|_4} \otimes \mathbf{1}_{|V|_3} \otimes A'_{\rm as}(D_2^{(\rm cycle)}) \otimes \mathbf{1}_{|V|_1} \otimes \gamma_2 \\ &\quad + \mathbf{1}_{|V|_4} \otimes A'_{\rm as}(D_3^{(\rm cycle)}) \otimes \mathbf{1}_{|V|_2} \otimes \mathbf{1}_{|V|_1} \otimes \gamma_3 \\ &\quad + A'_{\rm as}(D_4^{(\rm cycle)}) \otimes \mathbf{1}_{|V|_4} \otimes \mathbf{1}_{|V|_2} \otimes \mathbf{1}_{|V|_1} \otimes \gamma_4 \end{aligned} \tag{4.36}$$

where $A'_{\rm as}(D^{(\rm cycle)}_\mu)$ is $|V|_\mu$-square matrix in Eq.(3.26).

Next, we show that the lattice fermion action on four-dimensional torus lattice is equivalent to the bilinear form $\bar{\boldsymbol{\psi}} A_{\rm as}(G_{T^D})\boldsymbol{\psi}/2$. We introduce a vector of fermion fields in four-dimensions that is $\boldsymbol{\psi} = \sum_{n\in V}\psi_n \boldsymbol{e}_n$ where $\boldsymbol{e}_n \equiv \bigotimes_{\mu=1}^4 \boldsymbol{e}_{n_{5-\mu}}$. Note that $\boldsymbol{e}_n$ are the standard basis in $|V|$-dimensions. By use of this vector, the bilinear form $\bar{\boldsymbol{\psi}} A_{\rm as}(G_{T^D})\boldsymbol{\psi}/2$ is equal to the lattice fermion action on four-dimensional torus lattice since

$$\begin{aligned}\frac{1}{2}\bar{\boldsymbol{\psi}} A_{\rm as}(G_{T^4})\boldsymbol{\psi} &= \frac{1}{2}\sum_{m,m'\in V}\bar{\psi}_m\big(\, A_{\rm as}(G_{T^4})\,\big)_{mm'}\psi_{m'} \\ &= \frac{1}{2}\sum_{n\in V}\sum_{\mu=1}^4\left[\bar{\psi}_n\gamma_\mu U_{n,\mu}\psi_{n+\hat{\mu}} - \bar{\psi}_{n+\hat{\mu}}\gamma_\mu U^\dagger_{n,\mu}\psi_n\right] = S_{\rm nf}\end{aligned} \tag{4.37}$$

for Eq. (4.23). In the free theory, the free lattice fermion action on four-dimensional torus lattice is equal to $\bar{\boldsymbol{\psi}} A_{\rm as}(G^{\rm free}_{T^4})\boldsymbol{\psi}/2$ since each term in the bilinear form is equivalent to the difference term for each direction in the action. In particular, the first term in the bilinear form is

$$\begin{aligned}&\frac{1}{2}\bar{\boldsymbol{\psi}}\left(\mathbf{1}_{|V|_4}\otimes\mathbf{1}_{|V|_3}\otimes\mathbf{1}_{|V|_2}\otimes A'_{\rm as}(D^{(\rm cycle)}_1)\otimes\gamma_1\right)\boldsymbol{\psi} \\ &\quad= \frac{1}{2}\sum_{m,n\in V}\bar{\psi}_m\gamma_1\psi_n\Big\{\boldsymbol{e}^\dagger_{m_1}A'_{\rm as}(D^{(\rm cycle)}_1)\boldsymbol{e}_{n_1}\Big\}\delta_{m_4n_4}\delta_{m_3n_3}\delta_{m_2n_2} \\ &\quad= \frac{1}{2}\sum_{m,n\in V}\bar{\psi}_m\gamma_1\psi_n\Big\{\delta_{m_1+1\,n_1}-\delta_{m_1\,n_1+1}\Big\}\delta_{m_4n_4}\delta_{m_3n_3}\delta_{m_2n_2} \\ &\quad= \frac{1}{2}\sum_{m,n\in V}\bar{\psi}_m\gamma_1\psi_n\Big\{\delta_{m+\hat{1}\,n}-\delta_{m\,n+\hat{1}}\Big\} \\ &\quad= \frac{1}{2}\sum_n\left[\bar{\psi}_n\gamma_\mu\psi_{n+\hat{1}} - \bar{\psi}_{n+\hat{1}}\gamma_\mu\psi_n\right]\end{aligned} \tag{4.38}$$

where $\boldsymbol{e}^\dagger_{m_1}A'_{\rm as}(D^{(\rm cycle)}_1)\boldsymbol{e}_{n_1} = \delta_{m_1+1\,n_1}-\delta_{m_1\,n_1+1}$ for Eq. (3.26). Accordingly, the summation of each term in the bilinear form is obtain as

$$\frac{1}{2}\bar{\boldsymbol{\psi}} A_{\rm as}(G^{\rm free}_{T^4})\boldsymbol{\psi} = \frac{1}{2}\sum_{n\in V}\sum_{\mu=1}^4\left[\bar{\psi}_n\gamma_\mu\psi_{n+\hat{\mu}} - \bar{\psi}_{n+\hat{\mu}}\gamma_\mu\psi_n\right] = S^{\rm free}_{\rm nf}\,. \tag{4.39}$$

Thus, we have shown that the lattice fermion action on four-dimensional torus lattice is equivalent to the bilinear form of $\bar{\boldsymbol{\psi}} A_{\rm as}(G_{T^4})\boldsymbol{\psi}/2$ even if it is not the free theory. Furthermore, by rewriting the lattice action as $S_{\rm nf} = \bar{\boldsymbol{\psi}}\mathcal{D}_{T^4}\boldsymbol{\psi}$, the matrix-representation of four-dimensional lattice Dirac operator is equal to the anti-symmetrized adjacency matrix for the weighted digraph G_{T^4} with $1/2$ as the coeffient, i.e. $\mathcal{D}_{T^4} = A_{\rm as}(G_{T^4})/2$.

And finally, we discuss the number of fermion species for the weighted digraph $G^{\rm free}_{T^4}$. Since the fermion species are equivalent to the nullity of the matrix-representation of lattice Dirac operator, the number of fermion species can be derived by the nullity of the anti-symmetrized adjacency matrix for $G^{\rm free}_{T^4}$. It is expressed as

$$\#\text{species} = 2^{|S^{\rm c,e}|} \tag{4.40}$$

where $|S^{\mathrm{c,e}}|$ is the number of cycle digraphs with even vertices. As this equation shows, the number of fermion species depends on the number of vertices in each digraph $D_\mu^{(\mathrm{cycle})}$. It can be classified as shown in Table. 4.1. However, the maximum number of them is

Table 4.1: Classification of the number of fermion species

	$\lvert S^{\mathrm{c,e}}\rvert = 0$	$\lvert S^{\mathrm{c,e}}\rvert = 1$	$\lvert S^{\mathrm{c,e}}\rvert = 2$	$\lvert S^{\mathrm{c,e}}\rvert = 3$	$\lvert S^{\mathrm{c,e}}\rvert = 4$
#species	1	2	4	8	16

uniquely determined by the topology of graphs as

$$\max\left[\,\#\text{species}\,\right] = \prod_{\mu=1}^{4}\left\{\beta_0(D_\mu^{(\mathrm{cycle})}) + \beta_1(D_\mu^{(\mathrm{cycle})})\right\} = 2^4 \tag{4.41}$$

for Thm. 3. It is consistent with the well-known result that 16 fermion species appear in the theory.

4.3 Lattice fermions on ball

In the previous section, we discussed the lattice fermions on torus lattice in term of spectral graph theory. We showed three facts as follows:

- The lattice fermion on torus lattice can be represented as the directed and weighted graph constructed by the cartesian product of only the cycle digraph with γ-matrices and link variable as the weight.
- The lattice action as spectral graph theory is given by the bilinear form of the anti-symmetrized adjacency matrix and the vector of fermion fields. It holds even if it is the free theory.
- The number of fermion species is derived by the number of cycle digraphs with even vertices. However, the maximum number of them is uniquely determined by the topology of graphs (or the number of cycle digraph).

In this section, we will discuss lattice fermions on D-dimensional hyperball lattice (B^D-lattice) in term of spectral graph theory. This section is divided into two subsections. The first subsection will be discussed in D-dimensions. Next, we will discuss in four-dimensions.

Before this discussion begins, we mention the D-dimenional hyperball lattice and lattice fermion action on it. We define the D-dimensional hyperball lattice as a finite volume D-dimensional hypercubic lattice with only Dirichlet boundary condition. It is expressed as

$$B^D\text{-lattice} \equiv \left\{ n = \sum_{\mu=1}^{D} n_\mu \hat{\mu} \;\middle|\; n_\mu \in [1, N_\mu] \subset \mathbb{Z} \right\} . \tag{4.42}$$

The Dirichlet boundary condition is automatically imposed on each direction since we consider a finite volume lattice and the boundary condition is $n_\mu \in [1, N_\mu] \Rightarrow n = 0$. Then, a lattice fermion action on B^D-lattice is given as

$$S_{B^D} = \sum_n \sum_{\mu=1}^{D} \bar{\psi}_n \gamma_\mu D_\mu \psi_n = \frac{1}{2} \sum_n \sum_{\mu=1}^{D} \left[\bar{\psi}_n \gamma_\mu U_{n,\mu} \psi_{n+\hat{\mu}} - \bar{\psi}_{n+\hat{\mu}} \gamma_\mu U^\dagger_{n,\mu} \psi_n \right] \tag{4.43}$$

where $D_\mu \equiv (T_{+\mu} - T_{-\mu})/2$ with $T_{\pm\mu}\psi_n = U_{n,\pm\mu}\psi_{n\pm\hat{\mu}}$. D_μ, ψ_n are the lattice Dirac operator and the fermionic fields respectively. And $U_{n,\mu}$ is the gauge field called the link variable. The sum $\sum_n$ is the summation over lattice sites $n = (n_1, \cdots, n_D)$ in the D-dimensional hyperball lattice. The difference between this action and the action in Eq. (4.20) is that there are no terms representing periodic boundary condition. In a free theory, this lattice fermion action is written as

$$S^{\text{free}}_{B^D} = \frac{1}{2} \sum_n \sum_{\mu=1}^{D} \left[\bar{\psi}_n \gamma_\mu \psi_{n+\hat{\mu}} - \bar{\psi}_{n+\hat{\mu}} \gamma_\mu \psi_n \right] \tag{4.44}$$

because we only set $U_{n,\mu} = \mathbf{1}$.

4.3.1 Lattice fermions on any dimensional hyperball

In this section, we will discuss lattice fermions on D-dimensional hyperball lattice in term of spectral graph theory.

Firstly, we discuss a directed and weighted graph representing the lattice fermions and a matrix associated the graph. For the graph in Eq. (3.22), the weighted digraph representing the lattice fermions on B^D-lattice is given by

$$\begin{gathered} G_{B^D} = D_1^{(\text{path})} \square D_2^{(\text{path})} \square \cdots \square D_D^{(\text{path})} \\ w(e \in G_\mu) = \gamma_\mu U_{n,\mu} \end{gathered} \tag{4.45}$$

where $D_\mu^{(\text{path})}$ is the simple directed path with $|V|_\mu$ vertices. The subscript n of $U_{n,\mu}$ is the vertex in the digraph, i.e. $n \in V$ where V is the set of vertices in G_{B^D}. However, vertices in this digraph can be regarded as sites in the any dimensional hyperball lattice since V and the whole sites are isomorphic. And each digraph $D_\mu^{(\text{path})}$ is a graph representing Dirichlet boundary condition since the vertices in each digraph only run from 1 to $|V|_\mu$. As an example, the case of $D = 2$ is depicted in Fig. 4.6. By definition in Def. 10, an anti-symmetrized adjacency matrix for the weighted digraph is obtain as

$$(A_{\text{as}}(G_{B^D}))_{ij} = \begin{cases} \gamma_\mu U_{n,\mu} & i = n \text{ and } j = n + \hat{\mu} \text{ for edge } \{n, n+\hat{\mu}\} \\ -\gamma_\mu U^\dagger_{n,\mu} & i = n + \hat{\mu} \text{ and } j = n \text{ for edge } \{n, n+\hat{\mu}\} \\ 0 & \text{otherwise} \end{cases} \tag{4.46}$$

where we used the property of γ-matrices that is $\gamma_\mu^\dagger = \gamma_\mu$. If we consider in a free theory that is we set $U_{n,\mu} = \mathbf{1}$, this anti-symmetrized adjacency matrix is written as a simple

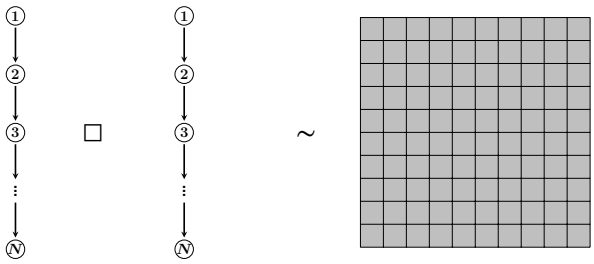

Figure 4.6: G_{B^2} is identified as a two dimensional disk with directed edge.

expression constructed by tensor product. Is is expressed as

$$A_{\rm as}(G^{\rm free}_{B^D}) = \sum_{\mu=1}^{D} \left\{ \left(\bigotimes_{\nu=1}^{D-\mu} \mathbf{1}_{|V|_{D+1-\nu}} \right) \otimes A'_{\rm as}(D^{\rm (path)}_{\mu}) \otimes \left(\bigotimes_{\rho=1}^{\mu-1} \mathbf{1}_{|V|_{\rho}} \right) \right\} \otimes \gamma_{\mu} \tag{4.47}$$

where $A'_{\rm as}(D^{\rm (path)}_{\mu})$ is $|V|_{\mu}$-square matrix in Eq.(3.27).

Secondary, we show that the bilinear form $\bar{\boldsymbol{\psi}} A_{\rm as}(G_{B^D})\boldsymbol{\psi}$ is equivalent to the lattice fermion action on B^D-lattice. $\boldsymbol{\psi}$ is the vector of fermion fields in D-dimensions that is expressed as $\boldsymbol{\psi} = \sum_{n\in V} \psi_n \boldsymbol{e}_n$ where $\boldsymbol{e}_n \equiv \bigotimes_{\mu=1}^{D} \boldsymbol{e}_{n_{D+1-\mu}}$. The components ψ_n is the fermionic fields in D-dimensions on which the weight $\gamma_\mu U_{n,\mu}$ act. The vectors $\boldsymbol{e}_n$ are the standard basis in $|V|$-dimensions which satisfy orthonormal $\boldsymbol{e}^{\dagger}_m \cdot \boldsymbol{e}_n = \delta_{mn} \equiv \prod_{\mu=1}^{D} \delta_{m_\mu n_\mu}$. By use of this vector, the bilinear form is

$$\begin{aligned} \bar{\boldsymbol{\psi}} A_{\rm as}(G_{B^D})\boldsymbol{\psi} &= \sum_{m,m'\in V} \bar{\psi}_m \big(A_{\rm as}(G_{B^D}) \big)_{mm'} \psi_{m'} \\ &= \sum_{n\in V} \sum_{\mu=1}^{D} \left[\bar{\psi}_n \gamma_\mu U_{n,\mu} \psi_{n+\hat{\mu}} - \bar{\psi}_{n+\hat{\mu}} \gamma_\mu U^{\dagger}_{n,\mu} \psi_n \right] \end{aligned} \tag{4.48}$$

for Eq. (4.46). As the action in Eq. (4.43) shows, we can prove that the bilinear form with the coefficient $1/2$ is equal to the lattice fermion action on B^D-lattice, i.e. $S_{B^D} = \bar{\boldsymbol{\psi}} A_{\rm as}(G_{B^D})\boldsymbol{\psi}/2$. If we consider in the free theory, the bilinear form with the coefficient $1/2$ is the free lattice action, or

$$\frac{1}{2}\bar{\boldsymbol{\psi}} A_{\rm as}(G^{\rm free}_{B^D})\boldsymbol{\psi} = \sum_{n\in V} \sum_{\mu=1}^{D} \left[\bar{\psi}_n \gamma_\mu \psi_{n+\hat{\mu}} - \bar{\psi}_{n+\hat{\mu}} \gamma_\mu \psi_n \right] = S^{\rm free}_{B^D} \tag{4.49}$$

because of $U_{n,\mu} = \mathbf{1}$. Therefore, the lattice fermion action for any dimensional hyperball lattice is given by the bilinear form of the matrix $A_{\rm as}(G_{B^D})$ and the vector $\boldsymbol{\psi}$, regardless of whether it is a free theory.

Finally, we discuss about the number of fermion species for the directed and weighted graph G_{B^D} in the free theory. The number of fermion species is given by the number of the simple directed paths with even vertices in $G^{\rm free}_{B^D}$. It is expressed as

$$\#\text{species} = \begin{cases} 1 & |S^{\rm p,e}| = 0 \\ 0 & |S^{\rm p,e}| \neq 0 \end{cases} \tag{4.50}$$

where $|S^{\mathrm{p,e}}|$ is the number of the simple directed paths with even vertices. This equation means that there is single fermion species if there is no simple directed paths with even vertices in the weighted digraph $G^{\mathrm{free}}_{B^D}$. We can confirm this result by examining the nullity of the anti-symmetrized adjacency matrix for the weighted digraph. From Eq. (3.35), the anti-symmetrized adjacency matrix for $G^{\mathrm{free}}_{B^D}$ is

$$\left(\mathcal{U}^\dagger A_{\mathrm{as}}(G^{\mathrm{free}}_{T^D})\mathcal{U}\right)_{mn} = 2i\delta_{mn}\sum_{\mu=1}^{D}\gamma_\mu \cos\left(\frac{m_\mu \pi}{|V|_\mu + 1}\right) \tag{4.51}$$

for $m_\mu \in V(D^{(\mathrm{path})}_\mu)$ and $m, n \in V = V(D^{(\mathrm{path})}_1) \times \cdots \times V(D^{(\mathrm{path})}_D)$. There is only one way in which m satisfies $\left(\mathcal{U}^\dagger A_{\mathrm{as}}(G^{\mathrm{free}}_{T^D})\mathcal{U}\right)_{mn} = 0$ when there are no simple directed paths with even vertices in $G^{\mathrm{free}}_{T^D}$. Otherwise, there are no ways in which m satisfies $\left(\mathcal{U}^\dagger A_{\mathrm{as}}(G^{\mathrm{free}}_{T^D})\mathcal{U}\right)_{mn} = 0$. Accordingly, the number of fermion species depends on the vertices in the weighted digraph $G^{\mathrm{free}}_{T^D}$. Meanwhile, the maximum number of fermion species is uniquely determined by the topology of graphs, and be expressed as

$$\max\left[\,\#\mathrm{species}\,\right] = \prod_{\mu=1}^{D}\left\{\beta_0(D^{(\mathrm{path})}_\mu) + \beta_1(D^{(\mathrm{path})}_\mu)\right\} = 1 \tag{4.52}$$

because of $\beta_0(D^{(\mathrm{path})}_\mu)+\beta_1(D^{(\mathrm{path})}_\mu) = 1$. It is consistent with the number of fermion species when $|S^{\mathrm{p,e}}| = 0$. Therefore, there is one physical pole on the bulk of any dimensional hyperball when the number of sites in each direction is the odd number. If we take a thermodynamical limit for $|V|_\mu =$ even vertices, one of the non-zero eigenvalue approaches to zero. Thus, lattice fermions on the finite-volume lattice of d-dimensional hyperball B^d have one physical pole on the bulk.

We comment the reasonableness of the existence of a single fermion species on the bulk. As well-known, the lattice fermion defined on a lattice with boundaries can have edge modes on the boundaries. Therefore, the edge mode works to cancel the gauge anomaly at the boundary when we introduce gauge fields or link variables. The existence of a single fermion species on the bulk in the present lattice fermion with boundaries is reasonable as with the case of the domain-wall fermion.

The results we have obtained in this discussion are again not so novel. However, we have shown that we can easily find the number of fermion species by obtaining the weighted digraph corresponding to the lattice fermions and using the theorem in Thm. 3.

4.3.2 Lattice fermions on four-dimensional hyperball

In this subsection, we will show four-dimensional hyperball as a concrete example of B^D-lattice. This subsection is divided into three parts. The first part is discussed

Before this discussion, we review the four-dimensional hyperball lattice and the lattice fermions on it. The four-dimensional hyperball lattice is expressed as

$$B^4\text{-lattice} \equiv \left\{ n = \sum_{\mu=1}^{4} n_\mu \hat{\mu} \;\middle|\; n_\mu \in [1, N_\mu] \subset \mathbb{Z} \right\}. \tag{4.53}$$

Then, a lattice fermion action on B^4-lattice is given as

$$S_{B^4} = \sum_n \sum_{\mu=1}^{4} \bar{\psi}_n \gamma_\mu D_\mu \psi_n = \frac{1}{2} \sum_n \sum_{\mu=1}^{4} \left[\bar{\psi}_n \gamma_\mu U_{n,\mu} \psi_{n+\hat{\mu}} - \bar{\psi}_{n+\hat{\mu}} \gamma_\mu U^\dagger_{n,\mu} \psi_n \right] \tag{4.54}$$

where $D_\mu \equiv (T_{+\mu} - T_{-\mu})/2$ with $T_{\pm\mu}\psi_n = U_{n,\pm\mu}\psi_{n\pm\hat{\mu}}$. D_μ, ψ_n are the lattice Dirac operator and the fermionic fields respectively. And $U_{n,\mu}$ is the gauge field called the link variable. The sum $\sum_n$ is the summation over lattice sites $n = (n_1, n_2, n_3, n_4)$ in the four-dimensional hyperball lattice. In a free theory, this lattice fermion action is written as

$$S^{\text{free}}_{B^4} = \frac{1}{2} \sum_n \sum_{\mu=1}^{4} \left[\bar{\psi}_n \gamma_\mu \psi_{n+\hat{\mu}} - \bar{\psi}_{n+\hat{\mu}} \gamma_\mu \psi_n \right] \tag{4.55}$$

because we only set $U_{n,\mu} = \mathbf{1}$.

Firstly, we discuss about a weighted digraph representing the lattice fermions on B^4-lattice and an anti-symmetrized adjacency matrix for it. The weighted digraph is

$$\begin{gathered} G_{B^4} = D_1^{(\text{path})} \square D_2^{(\text{path})} \square D_3^{(\text{path})} \square D_4^{(\text{path})} \\ w(e \in G_\mu) = \gamma_\mu U_{n,\mu} \end{gathered} \tag{4.56}$$

where $D_\mu^{(\text{path})}$ is the simple directed path with $|V|_\mu$ vertices and n is the vertex in the digraph. Note that vertices in this digraph can be regarded as sites in the any dimensional hyperball lattice since V and the whole sites are isomorphic. This digraph is depicted in Fig. 4.7. By definition in Def. 10, an anti-symmetrized adjacency matrix for the weighted

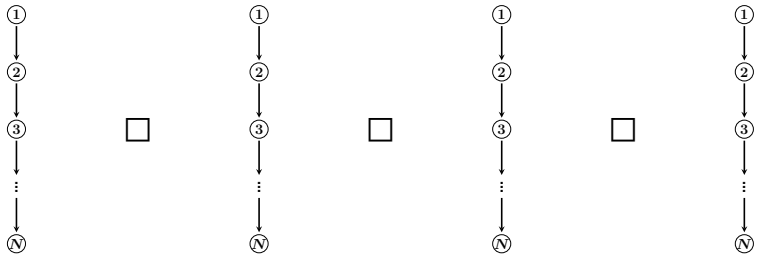

Figure 4.7: This digraph constructed cartesian-product $\square$ of four simple directed paths $D^{(\text{path})}$ with $|V|_\mu = N$ vertices each.

digraph is obtained as

$$(A_{\text{as}}(G_{B^4}))_{ij} = \begin{cases} \gamma_\mu U_{n,\mu} & i = n \text{ and } j = n + \hat{\mu} \text{ for edge } \{n, n+\hat{\mu}\} \\ -\gamma_\mu U^\dagger_{n,\mu} & i = n + \hat{\mu} \text{ and } j = n \text{ for edge } \{n, n+\hat{\mu}\} \\ 0 & \text{otherwise} \end{cases} \tag{4.57}$$

where use of $\gamma_\mu^\dagger = \gamma_\mu$. The difference between this matrix and the matrix for G_{T^4} in Eq. (4.35) is that there are no components representing an edge leaving $|V|_\mu$ and entering

1. If we consider the free theory, which sets $U_{n,\mu} = \mathbf{1}$, this anti-symmetrized adjacency matrix is written as

$$\begin{aligned} A_{\rm as}(G^{\rm free}_{T^4}) &= \sum_{\mu=1}^{4} \left\{ \left(\bigotimes_{\nu=1}^{4-\mu} \mathbf{1}_{|V|_{5-\nu}} \right) \otimes A'_{\rm as}(D^{(\rm path)}_{\mu}) \otimes \left(\bigotimes_{\rho=1}^{\mu-1} \mathbf{1}_{|V|_{\rho}} \right) \right\} \otimes \gamma_{\mu} \\ &= \mathbf{1}_{|V|_4} \otimes \mathbf{1}_{|V|_3} \otimes \mathbf{1}_{|V|_2} \otimes A'_{\rm as}(D^{(\rm path)}_{1}) \otimes \gamma_1 \\ &\quad + \mathbf{1}_{|V|_4} \otimes \mathbf{1}_{|V|_3} \otimes A'_{\rm as}(D^{(\rm path)}_{2}) \otimes \mathbf{1}_{|V|_1} \otimes \gamma_2 \\ &\quad + \mathbf{1}_{|V|_4} \otimes A'_{\rm as}(D^{(\rm path)}_{3}) \otimes \mathbf{1}_{|V|_2} \otimes \mathbf{1}_{|V|_1} \otimes \gamma_3 \\ &\quad + A'_{\rm as}(D^{(\rm path)}_{4}) \otimes \mathbf{1}_{|V|_4} \otimes \mathbf{1}_{|V|_2} \otimes \mathbf{1}_{|V|_1} \otimes \gamma_4 \end{aligned} \tag{4.58}$$

where $A'_{\rm as}(D^{(\rm path)}_{\mu})$ is $|V|_{\mu}$-square matrix in Eq.(3.27).

Secondary, we show that the lattice action on four-dimensional hyperball lattice is equivalent to the bilinear form $\bar{\boldsymbol{\psi}} A_{\rm as}(G_{B^4})\boldsymbol{\psi}/2$. A vector $\boldsymbol{\psi}$ is $\boldsymbol{\psi} = \sum_{n\in V} \psi_n \boldsymbol{e}_n$ where $\boldsymbol{e}_n \equiv \bigotimes_{\mu=1}^{4} \boldsymbol{e}_{5-\mu}$ are the standard basis in $|V|$-dimensions. Accordingly, the bilinear form $\bar{\boldsymbol{\psi}} A_{\rm as}(G_{B^4})\boldsymbol{\psi}$ is

$$\begin{aligned} \frac{1}{2}\bar{\boldsymbol{\psi}} A_{\rm as}(G_{B^4})\boldsymbol{\psi} &= \frac{1}{2} \sum_{m,m'\in V} \bar{\psi}_m \big(A_{\rm as}(G_{B^4}) \big)_{mm'} \psi_{m'} \\ &= \frac{1}{2} \sum_{n\in V} \sum_{\mu=1}^{4} \left[\bar{\psi}_n \gamma_{\mu} U_{n,\mu} \psi_{n+\hat{\mu}} - \bar{\psi}_{n+\hat{\mu}} \gamma_{\mu} U^{\dagger}_{n,\mu} \psi_n \right] = S_{B^4} \end{aligned} \tag{4.59}$$

for Eq. (4.46). In the case of free theory, the free lattice fermion action on four-dimensional torus lattice is equal to $\bar{\boldsymbol{\psi}} A_{\rm as}(G^{\rm free}_{B^4})\boldsymbol{\psi}/2$ since we only set $U_{n,\mu} = \mathbf{1}$. In particular, the bilinear form is obtain as

$$\frac{1}{2}\bar{\boldsymbol{\psi}} A_{\rm as}(G^{\rm free}_{B^4})\boldsymbol{\psi} = \frac{1}{2} \sum_{n\in V} \sum_{\mu=1}^{4} \left[\bar{\psi}_n \gamma_{\mu} \psi_{n+\hat{\mu}} - \bar{\psi}_{n+\hat{\mu}} \gamma_{\mu} \psi_n \right] = S^{\rm free}_{B^4} \,. \tag{4.60}$$

Furthermore, there are no terms, which represent edges leaving $|V|_{\mu}$ and entering 1 in each digraph $D^{(\rm path)}_{\mu}$, in the bilinear unlike $\bar{\boldsymbol{\psi}} A_{\rm as}(G^{\rm free}_{B^4})\boldsymbol{\psi}$ form since there are no components representing the edges. Thus, we have shown that the lattice fermion action on four-dimensional hyperball lattice is equivalent to the bilinear form of $\bar{\boldsymbol{\psi}} A_{\rm as}(G_{B^4})\boldsymbol{\psi}/2$ even if it is not the free theory. Furthermore, by rewriting the lattice action as $S_{B^4} = \bar{\boldsymbol{\psi}} \mathcal{D}_{B^4} \boldsymbol{\psi}$, the matrix-representation of four-dimensional lattice Dirac operator is equal to the anti-symmetrized adjacency matrix for the weighted digraph G_{B^4} with $1/2$ as the coeffient, i.e. $\mathcal{D}_{B^4} = A_{\rm as}(G_{B^4})/2$ as well as the case of T^4-lattice.

Finally, we discuss about the number of fermion species for the directed and weighted graph $G^{\rm free}_{B^4}$. The number of fermion species is given by the nullity of the anti-symmetrized adjacency matrix for $G^{\rm free}_{B^4}$ since the fermion species are equivalent to the nullity of the matrix-representation lattice Dirac operator. Accordingly, the number of fermion species is given by

$$\#\text{species} = \begin{cases} 1 & |S^{\rm p,e}| = 0 \\ 0 & |S^{\rm p,e}| \neq 0 \end{cases} \tag{4.61}$$

where $|S^{\mathrm{p,e}}|$ is the number of simple directed paths with even vertices. Thus, the number of fermion species depends on the number of vertices in each simple directed path $D_\mu^{(\mathrm{path})}$. Meanwhile, the maximum number of them is uniquely determined by the topology of graphs. For Thm. 3, the maximum number of them is obtained as

$$\max\left[\,\#\text{species}\,\right] = \prod_{\mu=1}^{4}\left\{\beta_0(D_\mu^{(\mathrm{path})}) + \beta_1(D_\mu^{(\mathrm{path})})\right\} = 1\,. \tag{4.62}$$

It is consistent with the maximum number of them for G_{B^D}. Therefore, there is at most one physical pole on the bulk of four-dimensional hyperball lattice.

4.4 Lattice fermions on hypersphere

In the previous sections, we discuss about the lattice fermions for the directed and weighted graph constructed by cartesian product of only the cycle digraphs and the simple directed paths. As an example outside of this graph, we will discuss about lattice fermion on a weighted digraph which can be considered as discretized sphere.

In the continuum field theory, the fermion action on spheres gives massive fermionic degrees of freedom since the curvature works as effective mass. It is, however, not the case on the discretized sphere.

In this section, we will study the number of fermion species on the discretized sphere, where we perform discretization and put a fermion on the lattice in a special manner. We empirically show that the maximum number of fermion species on the discretized sphere is equal to two. This section is divided into two parts. First, we will discuss about the two-dimensional cases. The next subsection mentions the higher dimensional cases.

We begin with the two-dimensional cases. We firstly consider the following discretized spherical coordinate system for 2-sphere, labeled by two integers (M, N):

$$x_3 = r\cos\theta_2, \qquad x_2 = r\sin\theta_2\cos\theta_1, \qquad x_1 = r\sin\theta_2\sin\theta_1, \tag{4.63}$$

$$\theta_1 \equiv \frac{2m\pi}{M}, \quad \theta_2 \equiv \frac{(N-n)\,\pi}{N-1} \tag{4.64}$$

where r is a radial distance and $m \in [1, M] \in \mathbb{N}$, $n \in [1, N] \in \mathbb{N}$. For simplicity, we fix a radial distance as $r = 1$. We label lattice sites as $v = (m, n)$. Note that there are two special points $(m, 1)$, (m, N) who ignore the hopping in m-direction. We call the two points the south pole, relabeled as $(0, 1)$, and the north pole, relabeled as $(0, N)$, respectively. For convenience, we call this lattice as S^2-lattice.

To obtain the naive-fermion-like action on S^2-lattice, we consider a directed and weighted graph representing lattice fermions on the lattice. The weighted digraph is

$$G_{S^2}^{(M,N)} = G_1 \cup G_2 \tag{4.65}$$

$$w(e \in G_\mu) = \sigma_\mu \tag{4.66}$$

for $\mu = 1, 2$. Each digraph $G_1 = (V, E_1), G_2 = (V, E_2)$ are given by

$$V = \{\, (1,2),\, (2,2),\, \cdots,\, (M,2),\, (1,3),\, \cdots,\, (M,N-1),\, (0,1),\, (0,N) \,\}, \tag{4.67}$$

$$\begin{aligned} E_1 = \{\, &\{(1,2),(2,2)\},\, \cdots,\, \{(M,2),(1,2)\}, \{(1,3),(2,3)\},\, \cdots,\, \{(M,3),(1,3)\}, \\ &\cdots,\, \{(1,N-1),(2,N-1)\},\, \cdots,\, \{(M,N-1),(1,N-1)\} \,\}, \end{aligned} \tag{4.68}$$

and

$$\begin{aligned} E_1 = \{\, &\{(0,N),(1,N-1)\},\, \cdots,\, \{(0,N),(M,N-1)\}, \\ &\{(1,N-1),(1,N-2)\},\, \cdots,\, \{(M,N-1),(M,N-2)\}, \\ &\cdots \{(1,2),(0,1)\},\, \cdots,\, \{(M,2),(0,1)\} \,\}. \end{aligned} \tag{4.69}$$

As an example, the digraph in the case of $(M, 3)$ is depicted in Fig. 4.8. σ_μ is the two-

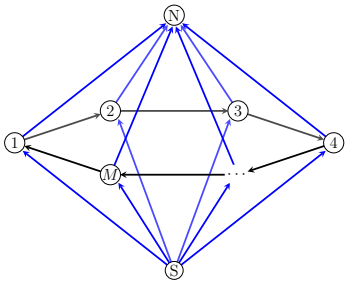

(a) $G_{S^2}^{(M,N)}$

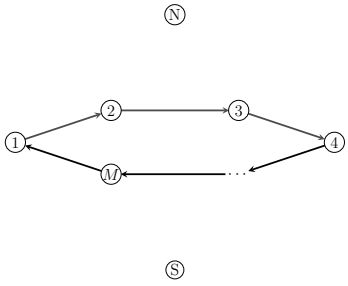

(b) G_1.

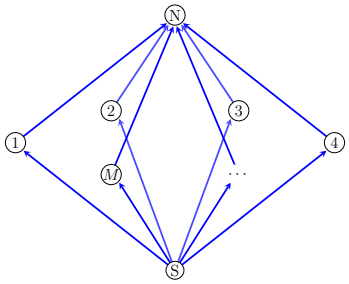

(c) G_2.

Figure 4.8: These digraphs depict $G_{S^2}^{(M,N)}$, G_1, G_2 in the case of $(M, 3)$, . In these digraph, the south pole and the north pole are written as S and N, respectively

dimensional gamma matrices which are called "Pauli matrices". These matrices satisfy Clifford algebra as $\{\sigma_\mu, \sigma_\nu\} = 2\delta_{\mu\nu}$. Note that we include no link variables in the weight because the present case is considered in a free theory. By definition in Def. 10, an anti-symmetrized adjacency matrix for the digraph $G_{S^2}^{(M,N)}$ is obtained as

$$A_{\rm as}(G_{S^2}^{(M,N)}) = \begin{pmatrix} \mathbf{1}_{N-2} \otimes A'_{\rm as}(D^{(\rm cycle)}) & \\ & O_2 \end{pmatrix} \otimes \sigma_1 + \begin{pmatrix} A'_{\rm as}(D^{(\rm path)}) & V_{M(N-2),2} \\ -V^\dagger_{M(N-2),2} & O_2 \end{pmatrix} \otimes \sigma_2 \tag{4.70}$$

where O_k is the k-dimensional null matrix. $A'_{\rm as}(D^{(\rm cycle)})$, $A'_{\rm as}(D^{(\rm path)})$ are the M-square matrix in Eq. (3.26) and the $(N-2)$-square matrix in Eq. (3.27) respectively. And

$V_{M(N-2),2}$ is given by

$$V_{M(N-2),2} \equiv \begin{pmatrix} 1 & 0 \\ 0 & 0 \\ & \vdots \\ 0 & 0 \\ 0 & -1 \end{pmatrix}_{N-2,2} \otimes \begin{pmatrix} 1 \\ 1 \\ \vdots \\ 1 \\ 1 \end{pmatrix}_{M,1} , \tag{4.71}$$

where the subscripts j, k of the matrix $(\ )_{j,k}$ stand for the row and column sizes. Furthermore, we introduce $\boldsymbol{\psi}$ as a vector of fermion fields in two-dimensions. It is defined as $\boldsymbol{\psi} \equiv \sum_{v \in V} \boldsymbol{e}_v$ with the standard basis $\boldsymbol{e}_v$ in $|V|$ dimensions. And ψ_v is the fermion fields in two-dimensions on which the Pauli matrices act. Here, we specify the order of components ψ_v in the vector as $(1,2) \to (2,2) \to \cdots \to (M,2) \to (1,3) \to \cdots \to (M, N-1) \to (0,1) \to (0,N)$. Namely, it is expressed as

$$\boldsymbol{\psi} = \begin{pmatrix} \psi_{(1,2)} \\ \psi_{(2,2)} \\ \vdots \\ \psi_{(M,2)} \\ \psi_{(1,3)} \\ \vdots \\ \psi_{(M,N-1)} \\ \psi_{(0,1)} \\ \psi_{(0,N)} \end{pmatrix} . \tag{4.72}$$

For the results in the previous sections, the lattice action for the weighted digraph is given by the anti-symmetrized adjacency matrix and the vector of fermion fields. Accordingly, the the naive-fermion-like action on S^2-lattice is given by the bilinear form

$$S_{S^2}^{(M,N)} = \frac{1}{2} \bar{\boldsymbol{\psi}} A_{\mathrm{as}}(G_{S^2}^{(M,N)}) \boldsymbol{\psi} \, . \tag{4.73}$$

Since the matrix-representation of lattice Dirac operator is equal to the anti-symmetrized adjacency matrix with $1/2$ as coefficient, the matrix-representation of lattice Dirac operator for $G_{S^2}^{(M,N)}$ is

$$\mathcal{D}_{S^2}^{(M,N)} = \frac{1}{2} A_{\mathrm{as}}(G_{S^2}^{(M,N)}) \, . \tag{4.74}$$

Finally, we discuss about the number of fermion species on S^2-lattice. In here, we show the number of fermion species on S^2-lattice $(M, 3)$. Then, the anti-symmetrized adjacency matrix for $G_{S^2}^{(M,3)}$ is

$$A_{\mathrm{as}}(G_{S^2}^{(M,3)}) = \begin{pmatrix} A'_{\mathrm{as}}(D^{(\mathrm{cycle})}) & \\ & O_2 \end{pmatrix} \otimes \sigma_1 + \begin{pmatrix} \mathbf{1}_M & V_{m,2} \\ -V_{m,2}^\dagger & O_2 \end{pmatrix} \otimes \sigma_2 \, . \tag{4.75}$$

Since the fermion species can be derived by the nullity of the anti-symmetrized adjacency matrix for the digraph corresponding to lattice fermion, we analyze the diagonalization of the matrix. The matrix $A_{\mathrm{as}}(G_{S^2}^{(M,3)})$ can be diagonalized by the unitary matrix

$$\mathcal{U} \equiv U \otimes \mathbf{1}_2 \tag{4.76}$$

where U is the unitary matrix below

$$U = \frac{1}{\sqrt{M}} \begin{pmatrix} 1 & 1 & & 1 & 0 & \chi & \bar{\chi} \\ \xi & \xi^2 & \cdots & \xi^{M-1} & 0 & \chi & \bar{\chi} \\ \xi^2 & \xi^4 & & \xi^{2(M-1)} & 0 & \chi & \bar{\chi} \\ \vdots & \vdots & \ddots & \vdots & \vdots & \vdots & \vdots \\ \xi^{M-1} & \xi^{2(M-1)} & & \xi^{(M-1)^2} & 0 & \chi & \bar{\chi} \\ 0 & 0 & \cdots & 0 & \sqrt{\frac{M}{2}} & -\sqrt{M}|\chi|^2 & -\sqrt{M}|\chi|^2 \\ 0 & 0 & & 0 & \sqrt{\frac{M}{2}} & \sqrt{M}|\chi|^2 & \sqrt{M}|\chi|^2 \end{pmatrix}, \tag{4.77}$$

with $\xi \equiv e^{\frac{-2\pi i}{M}}$ and $\chi \equiv i/\sqrt{2}$. Then, the spectra of the anti-symmetrized adjacency matrix $A_{\rm as}(G^{(M,N)}_{S^2})$ is obtain as

$$\begin{aligned} &\mathcal{U}^\dagger A_{\rm as}(G^{(M,N)}_{S^2})\mathcal{U} \\ &= 2i\mathrm{Diag}\left[\sigma_1 \sin\left[\frac{2\pi}{M}\right], \sigma_1 \sin\left[\frac{4\pi}{M}\right], \cdots, \sigma_1 \sin\left[\frac{2\pi\,(M-1)}{M}\right], 0, -i\sigma_2\sqrt{\frac{M}{2}}, i\sigma_2\sqrt{\frac{M}{2}}\right]. \end{aligned} \tag{4.78}$$

From Eq. 4.78, one finds that the number of fermion species is analytically two for even M since there is a certain j satisfying $j = \frac{M}{2} + 1 \in \mathbb{N}$ and $\sin\left[\frac{2\pi(j-1)}{M}\right] = 0$. On the other hand, the number of fermion species is one for odd M since there is no j satisfies $\sin\left[\frac{2\pi(j-1)}{M}\right] = 0$ for this case.

These results indicate that there are up to two fermion species on the S^2-lattice $(M, 3)$. We show that the maximal number of fermion species are two also in other cases including $(M, N) = (4, 4), (5, 4), (5, 5), (4, 5), (6, 9)$ by numerical calculations as shown in Appendix. C.1. The results are summarized in Table. C.1.

In higher dimensions, we discuss the naive-fermion-like action on the cellular decomposed sphere in a parallel manner. We show that there are up to two fermion species on the discretized 4-sphere (S^4-lattice) labeled by four integers (N_1, N_2, N_3, N_4) by numerical calculation in Appendix. C.2.

It is notable that the lattice fermion action on the spherical lattice has been studied in the literature in the different context [73–75]. Our result is consistent with the observations obtained in the literature.

In the end of this section, we make a comment on possible zero-mode (zero-eigenvalue) difference giving the quantum anomaly in gravitational background. In curved space, the difference of the numbers of left-handed and right-handed zero-modes are related to the anomaly resulting from the gravitational background. Our argument of the existence of two exact zero modes is not inconsistent to this difference of the numbers of zero-modes. For example, the case with two right-handed zero-modes and zero left-handed zero-modes are consistent with both arguments. This kind of fixing of zero modes may be due to the specific choice of the sphere discretization or due to the lattice artifact, but there is no contradiction so far.

Chapter 5

The number of fermion species based on topology

In the previous chapter, we have discussed that the lattice fermions on the various lattices. In particular, the maximum number of fermion species is determined by the number of cycle digraphs as follows:

- For $G = G_1 \square \cdots \square G_D$ with $G_\mu \in \left\{ D_\mu^{(\text{cycle})}, D_\mu^{(\text{path})} \right\}$, the maximum number of fermion species is
$$\max [\, \#\text{species} \,] = 2^{|S^{\text{c}}|} \tag{5.1}$$
where $|S^{\text{c}}|$ is the number of cycle digraphs.

- For $G = D_1^{(\text{cycle})} \square \cdots \square D_D^{(\text{cycle})}$ (or T^D-lattice), the maximum number of fermion species is
$$\max [\, \#\text{species} \,] = 2^D \tag{5.2}$$
since the digraph G is constructed by D cycle digraphs.

- For $G = D_1^{(\text{path})} \square \cdots \square D_D^{(\text{path})}$ (or B^D-lattice), the maximum number of fermion species is
$$\max [\, \#\text{species} \,] = 1 \tag{5.3}$$
since the digraph G is constructed by only the simple directed paths.

It means that the maximum number of fermion species is given by the topology of graphs. Meanwhile, in this chapter we will discuss about the relationship between the maximum number of them and the topology of manifolds. The first half of this chapter is mentioned about a new conjecture we propose. Later in this chapter is devoted to proving this conjecture for certain manifolds.

5.1 New conjecture about the maximal number of the species

In this section, we will discuss about the relationship between the maximum number of fermion species and the topology of manifolds. We predict that the maximum number

of them is equal to the summation of the Betti numbers for the continuum manifold. As one of the circumstantial evidences, we show that the maximum number of them on the digraph $G^{\rm free}_{T^4}$ is equal to the summation of the four-dimensional torus. There are 2^4 fermion species on the digraph $G^{\rm free}_{T^4}$ for Thm. 3. Meanwhile, the summation of the Betti number is $\sum_{r=0}^{4}\beta_r(T^4)=16$ since these Betti number are

$$\beta_0(T^4)=\beta_4(T^4)=1\,,\quad \beta_1(T^4)=\beta_3(T^4)=4\,,\quad \beta_2(T^4)=6\,. \tag{5.4}$$

As a result, the maximum number of them is equal to the summation of the Betti numbers for T^4. In Table. 5.1, we summarize the relation of the sum of the Betti numbers and the maximum number of fermion species for the weighted digraph. Here, the manifold

Table 5.1: Betti numbers and Maximum numbers of fermion species

manifold M	sum of $\beta_r(M)$	maximal # of fermion species
1-d torus	$1+1$	2
2-d torus	$1+2+1$	4
3-d torus	$1+3+3+1$	8
4-d torus	$1+4+6+4+1$	16
Torus T^D	$(1+1)^D$	2^D
Hyperball B^D	$1+0+0+\cdots$	1
Sphere S^D	$1+0+0+\cdots+1$	2
$T^D\times B^d$	$2^D\times 1$	2^D

$T^D\times B^d$ can be regarded as the weighted digraph below

$$\begin{gathered} G^{\rm free}_{T^D\times B^d}=D_1^{(\rm cycle)}\,\square\,\cdots\,\square\,D_D^{(\rm cycle)}\,\square\,D_{D+1}^{(\rm path)}\,\square\,\cdots\,\square\,D_{D+d}^{(\rm path)} \\ w(e\in G_\mu)=\gamma_\mu \end{gathered} \tag{5.5}$$

for $G_\mu\in\left\{D_\mu^{(\rm cycle)},D_\mu^{(\rm path)}\right\}$. For Thm. 3, the maximum number of fermion species is $\max\left[\,\#\text{species}\,\right]=2^D$.

From these facts, we propose a new conjecture on the number of fermion species on the discretized torus, hyperball, their direct-product space, and hypersphere. Hereafter, we denote these manifolds as $\mathcal{M}$. The conjecture is as follows:

Conjecture 1. *We firstly impose the following five conditions on the free fermion action of the discretized manifolds ${}^*\mathcal{M}$:*

i. Difference operator; we adopt the anti-symmetrized adjacency matrix as the matrix-representation of lattice Dirac operator. For this reason, the lattice action is given by the bilinear form of the anti-symmetrized adjacency matrix and the vector of fermion fields.

ii. γ_{D+1} hermiticity or axis-symmetric Dirac spectrum; we only consider lattice fermions with real-axis-symmetric Dirac eigenvalue spectrum. This condition is satisfied by γ_{D+1} hermiticity in even dimensions. For this condition, we can exclude the cases of the unphysical system.

iii. $2^{D/2}$ *or* $2^{(D+1)/2}$ *spinors; this condition assures the linear independence of the lattice action for each direction. When* D *is even(odd), we consider* $2^{D/2}$*(*$2^{(D+1)/2}$*) spinors. This condition prohibits deliberately reducing the number of fermion species.*

iv. Locality; this condition leads to finite-hopping actions.

v. Finite volume lattice; Since taking the infinite volume limit changes the maximum number of fermion species and differs from our conjecture, we discuss the finite volume case. In other words, we consider only the case of the digraphs with finite vertices.

Our conjecture claims that, as long as these conditions hold, the maximum number of species of free fermions on the digraph regarded as the lattice-discretized D*-dimensional manifold is equal to the summation of Betti numbers* $\beta_r(\mathcal{M})$ *over* $0 \leq r \leq D$ *for the continuum manifold* $\mathcal{M}$*. It is expressed as*

$$\max\left[\,\#\text{species}({}^*\mathcal{M})\,\right] = \sum_{r=0}^{D} \beta_r(\mathcal{M})\,, \tag{5.6}$$

where $\#\text{species}({}^*\mathcal{M})$ *is the number of fermion species on the weighted digraph regarded as the lattice-discretized manifold* ${}^*\mathcal{M}$*.*

5.2 The theorem for the maximum number of fermion species

In the previous section, we proposed the conjecture claiming the relationship between the maximum number of fermion species and the topology of manifolds. In the restricted manifolds, this conjecture can be proved. This section will mention about a theorem which claims the non-trivial relation between the maximum number of them and the sum of the Betti numbers for the restricted manifolds, and we will prove the theorem.

Before this discussion, we prove a novel topological lemma.

Lemma 1. *For the manifold* $\mathcal{M} = M_1 \times M_2 \times \cdots \times M_D$ *with* $M_\mu \in \{S^1, I\}$*, the sum of all Betti numbers for the manifold* $\mathcal{M}$ *is equal to the product of the summation of zeroth and first Betti numbers in each manifold* M_μ*, i.e.*

$$\sum_{r=0}^{D} \beta_r(\mathcal{M}) = \prod_{\mu=1}^{D} \Big\{ \beta_0(M_\mu) + \beta_1(M_\mu) \Big\}\,. \tag{5.7}$$

When the manifold $\mathcal{M}$ *is constructed by* d *circle and* $(D-d)$ *line segments, this equation is rewritten as*

$$\sum_{r=0}^{D} \beta_r(\mathcal{M}) = \prod_{\mu=1}^{D} \Big\{ \beta_0(M_\mu) + \beta_1(M_\mu) \Big\} = 2^d\,. \tag{5.8}$$

It means that the sum of all Betti numbers for the manifold $\mathcal{M} = M_1 \times M_2 \times \cdots \times M_D$ with $M_\mu \in \{S^1, I\}$ is given by the number of the circles. This theorem can be proved using a topological theorem called the Künneth theorem.

Proof. Firstly, we show the case of $D = 2$. The manifold is $\mathcal{M} = M_1 \times M_2$ with $M_\mu \in \{S^1, I\}$. Accordingly, what we have to do is to prove

$$\begin{aligned}\sum_{r=0}^{2} \beta_r(\mathcal{M}) &= \prod_{\mu=1}^{2} \Big\{ \beta_0(M_\mu) + \beta_1(M_\mu) \Big\} \\ &= \Big\{ \beta_0(M_1) + \beta_1(M_2) \Big\} \Big\{ \beta_0(M_2) + \beta_1(M_2) \Big\} .\end{aligned} \tag{5.9}$$

From the Künneth theorem, the r-th homology of the manifold $\mathcal{M}$ is written down as

$$H_r(\mathcal{M}) = H_r(M_1 \times M_2) \simeq \bigoplus_{r_1+r_2=r} H_{r_1}(M_1) \otimes H_{r_2}(M_2) . \tag{5.10}$$

where $H_r(M)$ stands for the r-th homology of manifold M. Since the r-th Betti number is defined as the rank of the r-th homology, the sum of all Betti numbers is

$$\begin{aligned}\sum_{r=0}^{2} \beta_r(\mathcal{M}) &= \sum_{r=0}^{2} \operatorname{rank} H_r(\mathcal{M}) \\ &= \sum_{r=0}^{2} \left[\sum_{r_1+r_2=r} \Big\{ \operatorname{rank} H_{r_1}(M_1) \cdot \operatorname{rank} H_{r_2}(M_2) \Big\} \right] \\ &= \sum_{r=0}^{2} \left[\sum_{r_1+r_2=r} \beta_{r_1}(M_1) \beta_{r_2}(M_2) \right] .\end{aligned} \tag{5.11}$$

Now, we can restrict r_μ in $\beta_{r_\mu}(M_\mu)$ to $0 \le r_\mu \le 1$ since the Betti number of circle S^1 or the line segment I are

$$\beta_{r_\mu}(S^1) = \begin{cases} 1 & r_\mu = 0 \\ 1 & r_\mu = 1 \\ 0 & \text{otherwise} \end{cases} , \qquad \beta_{r_\mu}(I) = \begin{cases} 1 & r_\mu = 0 \\ 0 & \text{otherwise} \end{cases} , \tag{5.12}$$

respectively Accordingly, the right-hand side in Eq. (5.11) is

$$\begin{aligned}&\sum_{r=0}^{2} \left[\sum_{r_1+r_2=r} \beta_{r_1}(M_1) \beta_{r_2}(M_2) \right] \\ &\quad = \beta_0(M_1)\beta_0(M_2) + \beta_0(M_1)\beta_1(M_2) + \beta_1(M_1)\beta_0(M_2) + \beta_1(M_1)\beta_1(M_2) \\ &\quad = \Big\{ \beta_0(M_1) + \beta_1(M_2) \Big\} \Big\{ \beta_0(M_2) + \beta_1(M_2) \Big\}\end{aligned} \tag{5.13}$$

because of $0 \le r = r_1 + r_2 \le 2$. As a result, we can prove that the equation in Eq. (5.9) holds.

Secondary, we show the case of $D > 2$. Here, we assume the summation of Betti numbers over $0 \le r \le D-1$ satisfies the following equation,

$$\sum_{r=0}^{D-1} \beta_r(M_1 \times \cdots \times M_{D-1}) = \prod_{\mu=1}^{D-1} \Big\{ \beta_0(M_\mu) + \beta_1(M_\mu) \Big\} . \tag{5.14}$$

The sum of all Betti numbers for the manifold $\mathcal{M} = M_1 \times \cdots \times M_D$ is obtained as

$$\begin{aligned}\sum_{r=0}^{D} \beta_r(\mathcal{M}) &= \sum_{r=0}^{D} \left[\sum_{r_1+r'=r} \beta_{r_1}(M_1)\beta_{r'}(M_2 \times \cdots \times M_D) \right] \\ &= \beta_0(M_1) \sum_{r'=0}^{D-1} \beta_{r'}(M_2 \times \cdots \times M_D) + \beta_1(M_1) \sum_{r'=0}^{D-1} \beta_{r'}(M_2 \times \cdots \times M_D)\end{aligned} \tag{5.15}$$

since $\beta_D(M_2 \times \cdots \times M_D) = 0$ and $\beta_{-1}(M_2 \times \cdots \times M_D) = 0$. By use of the assumption, the sum of all Betti numbers results in

$$\begin{aligned}\sum_{r=0}^{D} \beta_r(\mathcal{M}) &= \beta_0(M_1) \sum_{r'=0}^{D-1} \beta_{r'}(M_2 \times \cdots \times M_D) + \beta_1(M_1) \sum_{r'=0}^{D-1} \beta_{r'}(M_2 \times \cdots \times M_D) \\ &= \beta_0(M_1) \prod_{\mu=2}^{D} \Big\{ \beta_0(M_\mu) + \beta_1(M_\mu) \Big\} + \beta_1(M_1) \prod_{\mu=2}^{D} \Big\{ \beta_0(M_\mu) + \beta_1(M_\mu) \Big\} \\ &= \prod_{\mu=1}^{D} \Big\{ \beta_0(M_\mu) + \beta_1(M_\mu) \Big\} .\end{aligned} \tag{5.16}$$

Therefore, Eq. (5.7) holds for the manifold $\mathcal{M} = M_1 \times \cdots \times M_D$ with $M_\mu \in \{S^1, I\}$.

Finally, we show the equation in Eq. (5.8). When the manifold $\mathcal{M}$ is constructed by d circles and $(D-d)$ line segments, the right side in Eq. (5.7) is

$$\begin{aligned}\prod_{\mu=1}^{D} \Big\{ \beta_0(M_\mu) + \beta_1(M_\mu) \Big\} &= \prod_{\mu \in S^{\text{circle}}} \Big\{ \beta_0(S^1) + \beta_1(S^1) \Big\} \prod_{\mu \in S^{\text{line}}} \Big\{ \beta_0(I) + \beta_1(I) \Big\} \\ &= 2^{|S^{\text{circle}}|}\end{aligned} \tag{5.17}$$

where $S^{\text{circle}} \equiv \{\mu \mid M_\mu = S^1\}$ and $S^{\text{line}} \equiv \{\mu \mid M_\mu = I\}$. Since $|S^{\text{circle}}| = d$, we have shown Eq. (5.8). □

In our conjecture, we assumed arbitrary manifolds. However, we consider the restricted manifolds, which constructed by the directed product of only the circle S^1 and the line segment $I = [0, 1]$. It is expressed as

$$\mathcal{M} = M_1 \times M_2 \times \cdots \times M_D \tag{5.18}$$

for $M_\mu \in \{S^1, I\}$. Furthermore, the circle and the cycle digraph are homeomorphic, and the line segment is homeomorphic to the simple directed path, i.e. $S^1 \simeq D^{(\text{cycle})}$ and $I \simeq D^{(\text{path})}$. These facts will be used in the later proof. We obtain the following theorem.

Theorem 4 (lattice fermion and topology)**.** *The number of fermion species of the free, massless and naive lattice Dirac operator is equivalent to the sum of all the Betti numbers of the manifolds, which is $\mathcal{M} = M_1 \times M_2 \times \cdots \times M_D$ with $M_\mu \in \{S^1, I\}$, on which the lattice fermion is defined:*

$$\max\left[\, \#\text{species}({}^*\mathcal{M}) \,\right] \;=\; \max\left[\frac{\dim\left(\ker A_{\text{as}}({}^*\mathcal{M})\right)}{\operatorname{rank}\gamma} \right] \;=\; \sum_{r=0}^{D} \beta_r(\mathcal{M}) \tag{5.19}$$

where the lattice-discretized manifold ${}^*\mathcal{M}$ as ${}^*\mathcal{M} = {}^*M_1 \times \cdots \times {}^*M_D$ with ${}^*M_\mu \in \{{}^*S^1, {}^*I\}$. For generic case of the number of vertices (lattice sites) in G, we have

$$\#\text{species}({}^*\mathcal{M}) \;=\; \frac{\dim\left(\ker A_{\text{as}}({}^*\mathcal{M})\right)}{\text{rank}\,\gamma} \;\leq\; \sum_{r=0}^{D} \beta_r(\mathcal{M})\,. \tag{5.20}$$

It means that the number of fermion species on the lattice-discretized manifold ${}^*\mathcal{M}$ determines upper bound by the topology of the digraph corresponding to the continuum manifold $\mathcal{M}$.

We speculate that the theorem holds for massive fermions or other lattice fermion formulations since the introduction of mass or the modification of fermion actions never increase the number of femrion species of free fermions.

Proof. By use of Thm. 3, $S^1 \simeq D^{(\text{cycle})}$, and $I \simeq D^{(\text{path})}$, the maximum number of femrion species on the directed and weighted graph G in Eq. (3.22) is

$$\begin{aligned}
\max\left[\,\#\text{species}(G)\,\right] &= \max\left[\frac{\dim\left(\ker A_{\text{as}}(G)\right)}{\text{rank}\,\gamma}\right] \\
&= \prod_{\mu=1}^{D}\Big\{\beta_0(G_\mu) + \beta_1(G_\mu)\Big\} \\
&= \prod_{\mu=1}^{D}\Big\{\beta_0(M_\mu) + \beta_1(M_\mu)\Big\} = \sum_{r=0}^{D}\beta_r(\mathcal{M})\,.
\end{aligned} \tag{5.21}$$

Furthermore, by taking the weighted digraph G to be equal to the 2-skeleton (only vertices and edges) of the the lattice-discretized manifold ${}^*\mathcal{M}$, we can prove

$$\max\left[\,\#\text{species}({}^*\mathcal{M})\,\right] = \max\left[\frac{\dim\left(\ker A_{\text{as}}({}^*\mathcal{M})\right)}{\text{rank}\,\gamma}\right] = \sum_{r=0}^{D}\beta_r(\mathcal{M})\,. \tag{5.22}$$

Furthermore, we can also prove

$$\#\text{species}({}^*\mathcal{M}) \leq \sum_{r=0}^{D}\beta_r(\mathcal{M}) \tag{5.23}$$

Since $\#\text{species} \leq \prod_{\mu=1}^{D}\{\beta_0(G_\mu) + \beta_1(G_\mu)\}$. □

Chapter 6

Summary and discussion

In this chapter, this thesis summarizes my research on fermion species of lattice fermions in three parts. First, I will summarized Next, I will summarize the new formulations of lattice fermions using spectral graph theory and discuss further application of this formulation. And finally, I will summarize the non-trivial relation between lattice fermions and the topology and discuss very rich understanding of this this relation.

6.1 Lattice fermions as spectral graph theory

In this thesis, we have studied the novel formulation of lattic field theory using spectral graph theory and the relation between the fermion species and the Betti numbers of graphs. We had shown that the lattice fermion on the finite volume D-dimensional hypercubic lattice with the periodic boundary condition and Dirichlet boundary condition can be represented as the directed and weighted graph constructed by the cartesian product of the cycle digraphs and the simple directed paths below

$$\begin{aligned} G &= G_1 \,\square\, G_2 \,\square\, \cdots \,\square\, G_D \\ w(e \in G_\mu) &= \gamma_\mu U_{n,\mu} \end{aligned} \tag{6.1}$$

for $G_\mu \in \left\{ D_\mu^{(\text{cycle})}, D_\mu^{(\text{path})} \right\}$. In particular, the lattice fermion on torus lattice (with only the periodic boundary condition) can be represented as the directed and weighted graph constructed by the cartesian product of only the cycle digraph,

$$\begin{aligned} G &= D_1^{(\text{cycle})} \,\square\, D_2^{(\text{cycle})} \,\square\, \cdots \,\square\, D_D^{(\text{cycle})} \\ w(e \in D_\mu^{(\text{cycle})}) &= \gamma_\mu U_{n,\mu}\,. \end{aligned} \tag{6.2}$$

And the lattice fermion on hyperball lattice (with only the Dirichlet boundary condition) can be represented as the directed and weighted graph constructed by the cartesian product of only the simple directed path,

$$\begin{aligned} G &= D_1^{(\text{path})} \,\square\, D_2^{(\text{path})} \,\square\, \cdots \,\square\, D_D^{(\text{path})} \\ w(e \in D_\mu^{(\text{path})}) &= \gamma_\mu U_{n,\mu}\,. \end{aligned} \tag{6.3}$$

For the weighted digraph G, we have introduced a novel matrix associated with the graph, called as "anti-symmetrized adjacency matrix" $A_{\rm as}(G)$. By use of this matrix, the lattice fermion action for the weighted digraph is given by the bilinear form of the matrix and the vector of fermion fields, i.e. $S = \bar{\boldsymbol{\psi}} A_{\rm as}(G) \boldsymbol{\psi}$. We had shown that it holds even if it is a free theory. Furthermore, the number of fermion species is derived by the cycle digraphs with even vertices. However, the maximum number of them is uniquely determined by the topology of graphs (or the number of cycle digraph). We had shown the number of fermion species on varous lattice as follows:

- Product space of T^1-lattice and B^1-lattice (or the weighted digraph in Eq. (6.1)):

  The number of fermion species is given by the number of the cycle digraphs with even vertices and the number of the simple directed paths with even vertices. If the weighted digraph contains the simple directed paths with even vertices, there are no fermion species in the theory. Meanwhile, if the weighted digraph contains no simple directed paths with even vertices, the number of fermion species is the cycle digraphs with even vertices powers of two. It is expressed as

  $$\#\text{species} = \begin{cases} 2^{|S^{\rm c,e}|} & |S^{\rm p,e}| = 0 \\ 0 & |S^{\rm p,e}| \neq 0 \end{cases} \tag{6.4}$$

  where $|S^{\rm c,e}|$, $|S^{\rm p,e}|$ are the number of the cycle digraphs with even vertices in the weighted digraph and the number of the simple directed paths with even vertices in the weighted digraph, respectively. The maximum number of fermion species can be derived by the number of the cycle digraphs. The expressed equation is

  $$\max\left[\,\#\text{species}\,\right] = 2^{|S^{\rm c}|} \tag{6.5}$$

  where $S^{\rm c}$ is the number of the cycle digraphs.

- Torus lattice:

  The number of fermion species on torus lattice is given by the number of the cycle digraph with even vertices below

  $$\#\text{species} = 2^{|S^{\rm c,e}|}\,. \tag{6.6}$$

  And the maximum number of them is equal to the number of cycle digraphs powers of two. It other words, it is equal to 2 to the number of dimensions. It is expressed as

  $$\max\left[\,\#\text{species}\,\right] = 2^{|S^{\rm c}|} = 2^D \tag{6.7}$$

  where D is the number of dimensions.

- Hyperball lattice:

  The number of fermion species for the hyperball lattice depends on whether the simple directed path with even vertices is included in the whole weighted digraph below

  $$\#\text{species} = \begin{cases} 1 & |S^{\rm p,e}| = 0 \\ 0 & |S^{\rm p,e}| \neq 0 \end{cases}\,. \tag{6.8}$$

As this equation shows, there is one fermion species as the maximum number of them.

In addition to these lattices, we had shown the lattice fermion on the discretized sphere, where we perform discretization and put a fermion on the lattice in a special way. In this case, by taking the weighted digraph equivalent to the 2-skeleton (only vertices and edges) of the discretized sphere, the lattice action is also obtained by the bilinear form of the anni-symmetrized adjacency matrix for the weighted digraph and the vector of the vector of fermion fields. And the maximum number of fermion species can be derived as two, even in arbitrary dimensions.

Therefore, once we have a certain weighted digraph and an anti-symmetrized adjacency matrix associated with the digraph, we can obtain a lattice action corresponding to the graph and derive the number of fermion species.

We now discuss further application of the novel formulation of lattice fermions in term of spectral graph theory;

1. Applications of spheres discretised in other ways:

   In this thesis, we had taken the method of discretising spherical coordinates. However, as there are many other discretization methods, we will discuss these methods and investigate lattice fermions on discretised spheres by using them in the future.

2. Lattice fermions with the gauge field:

   One may ask a question whether we introduce the gauge field into our setups. Lattice fermion operator with the $U(1)$ background link variable giving a non-zero winding number (topological charge) in two dimensions is regarded as the antii-symmetrized adjacency matrix with the link variable as the components in spectral graph theory. By use of this fact, we may be able to re-interpret the index theorem connecting the topological charges and the Dirac zero-modes in terms of graph theory.

3. Novel lattice fermions:

   We can propose novel lattice fermions by translating a matrix with desirable properties (minimal zero modes, hermiticity or chirality) to a spectral graph, which corresponds to the lattice fermion. A fermion obtained by this procedure may correspond to a lattice fermion defined on the lattice with various topology.

6.2 The number of fermion species based on topology

In this paper, we have studied operators in lattice field theory using spectral graph theory proposed new conjecture claiming that the maximal number of exact Dirac zero-modes of free fermions on the finite lattices we formulate in the paper is equal to the summation of the Betti numbers of the D-dimensional manifold from which the lattice is constructed. Our conjecture is summarized as

$$\max\left[\,\#\text{species}({}^{*}\mathcal{M})\,\right] \;=\; \sum_{r=0}^{D}\beta_r(\mathcal{M})\,, \tag{6.9}$$

where #species($^*\mathcal{M}$) is the number of fermion species on the lattice, which is defined as a lattice-discretized version $^*\mathcal{M}$ of the manifold $\mathcal{M}$. In a sense that this conjecture relates the number of fermion species to the topology of spacetime manifold, it is complementary to the Nielsen–Ninomiya's no-go theorem which claims the emergence of pairs of fermion species as a result of the cancellation of chiral charges on torus.

Furthermore, we partially proved the conjecture on the relation between the fermion species and the Betti numbers of the graph. We have proved that the maximal number of fermion species of a free Dirac operator agrees with the sum of all the Betti numbers of the graph (lattice) structured as cartesian products of cycle digraphs (T^1 lattice) and simple directed paths (B^1 lattice).

We comment in the case of infinite-volume lattices things. For example, the number of zero-modes of naive fermion on the one-dimensional lattice hyperball $^*B^1$ approaches two in an infinite-volume limit, which is the same number as that on $^*T^1$. It is of great importance that our conjecture relates the topology of *a continuum manifold* and the zero-modes on *a finite lattice defined by discretizing the manifold*.

If the theorem is established for generic cases, it has impacts on the study of lattice field theory. For example, one can predict the number of exact Dirac zero modes of free fermions on non-standard lattices such as discretized double torus. Future works will be devoted to generalization and establishment of this conjecture.

Study on the connection between lattice field theory and graph theory leads to very rich understanding on both of them. In the upcoming work of ours, we will discuss the relation between lattice scalar field theory and topological graph theory, where the massless scalar operator on the lattice is exactly given by the graph Laplacian operator.

Acknowledgements

The author is grateful to his supervisors, Prof. Masaru Onoda in the Akita University and Prof. Tatsuhiro Misumi in the Kindai University, for guiding him and giving useful advice on this thesis. He appreciates hearty encouragement by his parents and grandmother during he has been enrolled in the graduate school. This work of J. Y. is supported by the Sasakawa Scientific Research Grant from The Japan Science Society.

Appendix A

Lattice field theory and graph Laplacian

A.1 Lattice boson and graph Laplacian

In this section, we show a relation between lattice boson and graph Laplacian. The graph Laplacian defined in Def. 9 corresponds to the Laplacian in the lattice field theory at least on the hypercubic lattices. Let G be the graphs corresponds to lattices: T^D-lattice, B^D-lattice or their cartesian products in D-dimensions. Therefore, the massless action of D-dimensional free lattice scalar field ϕ_n defined on N^D hypercubic-lattice sites is expressed as

$$S_{\rm b} = -\frac{1}{2}\sum_{n,\mu}\phi_n\left(2\phi_n - \phi_{n+\hat{\mu}} - \phi_{n-\hat{\mu}}\right) = -\frac{1}{2}\boldsymbol{\phi}L(G)\boldsymbol{\phi} \tag{A.1}$$

with $\boldsymbol{\phi} \equiv (\phi_{1,0,\cdots,1},\, \phi_{2,0,\cdots,1},\, \phi_{N,N,\cdots,N},\,)^{\rm T}$. The sum $\sum_{n,\mu}$ is the summation over lattice site $n = (n_1, n_2, ..., n_D)$ and $\mu = (1, 2, 3, ..., D)$ with the intervals being $1 \leq n_\mu \leq N$. $L(G)$ is the graph Laplacian matrix we defined in Def. 9. Thus, the spectrum of free and massless lattice boson agrees with that of the graph Laplacian matrix.

Indeed, the equivalence between the lattice scalar operator and the graph Laplacian matrix is not restricted to the above hypercubic lattices. In the continuum limit, in which the number of vertices approaches to an infinity with the graph topology being intact, the graph Laplacian results in the continuum Laplacian for an arbitrary lattice or graph G. Thus, the coincidence in Eq. (A.1) holds for generic lattices as

$$S_{\rm b} = \boldsymbol{\phi}\mathcal{B}\boldsymbol{\phi} = -\frac{1}{2}\boldsymbol{\phi}L(G)\boldsymbol{\phi} \tag{A.2}$$

where $\mathcal{B}$ stands for the lattice operator. As we have shown in Thm. 2, the number of zero modes of the Laplacian matrix is equivalent to 0-th Betti number $\beta_0(G)$. From this fact, we derive the following theorem.

Theorem 5 (Lattice scalar zero modes)**.** *The number of zero modes of a free and massless lattice scalar operator $\mathcal{B}$ is equivalent to the 0-th Betti number of the graph (lattice) $\beta_0(G)$, on which the lattice boson is defined.*

$$\dim(\mathrm{Ker}\mathcal{B}) \;=\; \dim(\mathrm{Ker}L(G)) \;=\; \beta_0(G)\,. \tag{A.3}$$

For any simply connected graphs (lattices), the free boson operator has a single zero mode.

This theorem holds for any graph (lattice) in any dimensions as long as the lattice boson operator is defined as the graph Laplacian. The assertion of this theorem for the connected graph is consistent with the results in the work [76].

A.2 Wilson term and graph Laplacian

By introducing graph Laplacian, we can well clarify the Wilson fermion in terms of spectral graph theory. We consider the finite volume four-dimensional hypercubic lattice imposed the periodic boundary condition in Eq. (2.2). Accordingly, the graph corresponding to the lattice is given by Eq. (4.34). From Sec. 2.3, the Wilson fermion action is given by

$$S_{\rm Wf} = S_{\rm nf} + S_{\rm W} \tag{A.4}$$

where $S_{\rm nf}$ is the lattice naive fermion action given by

$$S_{\rm nf} = \sum_n \sum_{\mu=1}^{4} \bar{\psi}_n \gamma_\mu D_\mu \psi_n = \frac{1}{2} \bar{\boldsymbol{\psi}} A_{\rm as}(G) \boldsymbol{\psi} \tag{A.5}$$

and $S_{\rm W}$ is the Wilson term given by

$$S_{\rm W} = \sum_n \sum_{\mu=1}^{4} \bar{\psi}_n \left(1 - C_\mu\right) \psi_n \ = \bar{\boldsymbol{\psi}} \mathcal{W} \boldsymbol{\psi}, . \tag{A.6}$$

$\mathcal{W}$ is the matrix-representation corresponding to the Wilson term. Then, by use of graph Laplacian the Wilson term can be rewritten as

$$S_{\rm W} = \frac{1}{2} \sum_n \sum_{\mu=1}^{4} \left(2\psi_n - \psi_{n+\hat{\mu}} - \psi_{n-\hat{\mu}}\right) = \frac{1}{2} \bar{\boldsymbol{\psi}} L(G) \boldsymbol{\psi} \tag{A.7}$$

where $L(G)$ is the Laplacian of the graph (lattice) G. It is notable that the added matrix $\mathcal{W}$ corresponding to the Wilson term is proportional to the graph Laplacian matrix as $\mathcal{W} = L/2$. Consequently, the Wilson fermion action in terms of graph theory is obtained as

$$S_{\rm Wf} = \frac{1}{2} \bar{\boldsymbol{\psi}} \left[A_{\rm as}(G) + L(G)\right] \boldsymbol{\psi} \, . \tag{A.8}$$

To discuss zero-modes of the anti-symmetrized adjacency matrix (matrix corresponding to the lattice Dirac operator) and the graph Laplacian (matrix corresponding to Wilson term), we focus the relation below

$$\left[A_{\rm as}(G),\, L(G)\right] = 0 \, . \tag{A.9}$$

It means that $A_{\rm as}(G)$ and $L(G)$ are simultaneously diagonalized. As we have shown, $L(G)$ has a single zero eigenvalue, which is equal to the 0-th Betti number $\beta_0 = 1$. This zero-eigenvector of $L(G)$ is also one of the zero eigenvectors of $A_{\rm as}(G)$, whose number

is $\sum_{r=0}^{4} \beta_r(T^4) = 16$. In this sense, *the Wilson term* $\mathcal{W} = L(G)/2$ *works to preserve a single zero-mode associated with* $\beta_0 = 1$ *out of the sixteen zero-modes of the naive fermion* $\mathcal{D} = A_{\rm as}(G)$. Therefore, the Wilson term, which is equivalent to the Laplacian matrix in arbitrary dimensions, works to preserve a single zero-mode associated with $\beta_0 = 1$ out of the 2^d zero-modes of the naive fermion. This is the graph-theoretical reason why the Wilson fermion extracts a single degree of freedom from the multiple doublers.

Appendix B

The diagonalization of $A_{\rm as}(G)$

The diagonalization of $A_{\rm as}(G)$ are obtained as

$$\begin{aligned}
\left(\mathcal{U}^\dagger A_{\rm as}(G)\mathcal{U}\right)_{mn} &= \sum_{\mu=1}^{D}\gamma_\mu\left\{\prod_{\nu=1}^{D-\mu}\prod_{\rho=1}^{\mu-1}\left(\mathbf{1}_{|V|_{D+1-\nu}}\right)_{m_{D+1-\nu}n_{D+1-\nu}}\left(\mathbf{1}_{|V|_\rho}\right)_{m_\rho n_\rho}\Lambda_{m_\mu n_\mu}\right\} \\
&= \sum_{\mu=1}^{D}\gamma_\mu\Lambda_{m_\mu n_\mu}\left(\prod_{\nu=1}^{D-\mu}\prod_{\rho=1}^{\mu-1}\delta_{m_{D+1-\nu}n_{D+1-\nu}}\delta_{m_\rho n_\rho}\right) \\
&= \sum_{\mu^{\rm c,e}\in S^{\rm c,e}}\gamma_{\mu^{\rm c,e}}\Lambda_{m_{\mu^{\rm c,e}}n_{\mu^{\rm c,e}}}\left(\prod_{\nu=1}^{D-\mu^{\rm c,e}}\prod_{\rho=1}^{\mu^{\rm c,e}-1}\delta_{m_{D+1-\nu}n_{D+1-\nu}}\delta_{m_\rho n_\rho}\right) \\
&\quad+\sum_{\mu^{\rm c,o}\in S^{\rm c,o}}\gamma_{\mu^{\rm c,o}}\Lambda_{m_{\mu^{\rm c,o}}n_{\mu^{\rm c,o}}}\left(\prod_{\nu=1}^{D-\mu^{\rm c,o}}\prod_{\rho=1}^{\mu^{\rm c,o}-1}\delta_{m_{D+1-\nu}n_{D+1-\nu}}\delta_{m_\rho n_\rho}\right) \\
&\quad+\sum_{\mu^{\rm p,e}\in S^{\rm p,e}}\gamma_{\mu^{\rm p,e}}\Lambda_{m_{\mu^{\rm p,e}}n_{\mu^{\rm p,e}}}\left(\prod_{\nu=1}^{D-\mu^{\rm p,e}}\prod_{\rho=1}^{\mu^{\rm p,e}-1}\delta_{m_{D+1-\nu}n_{D+1-\nu}}\delta_{m_\rho n_\rho}\right) \\
&\quad+\sum_{\mu^{\rm p,o}\in S^{\rm p,o}}\gamma_{\mu^{\rm p,o}}\Lambda_{m_{\mu^{\rm p,o}}n_{\mu^{\rm p,o}}}\left(\prod_{\nu=1}^{D-\mu^{\rm p,o}}\prod_{\rho=1}^{\mu^{\rm p,o}-1}\delta_{m_{D+1-\nu}n_{D+1-\nu}}\delta_{m_\rho n_\rho}\right),
\end{aligned} \tag{B.1}$$

where $\Lambda_{m_\mu n_\mu} \equiv \left(U_\mu^\dagger A'_{\rm as}(G_\mu)U_\mu\right)_{m_\mu n_\mu}$ and n_α, m_α range from 1 to $|V|_\alpha$. Furthermore, m and n are

$$m = m_1 + \sum_{\mu=2}^{D}\left(\prod_{\nu=1}^{\mu-1}|V|_\nu\left(m_\mu-1\right)\right), \quad n = n_1 + \sum_{\mu=2}^{D}\left(\prod_{\nu=1}^{\mu-1}|V|_\nu\left(n_\mu-1\right)\right), \tag{B.2}$$

respectively. Note that these two equations denote a replacement from the label of each site to the new labels m, n. Here we used $\left(\mathbf{1}_{|V|_\alpha}\right)_{m_\alpha n_\alpha} = \delta_{m_\alpha n_\alpha}$ and the properties of Kronecker product, which is $(A\otimes B)_{Q(i-1)+k,Q(j-1)+l} = A_{ij}B_{kl}$ for P-square matrix A and Q-square matrix B.

To derive the diagonal components of $\mathcal{U}^\dagger A_{\rm as}(G)\mathcal{U}$, we need to derive $U_\mu^\dagger A'_{\rm as}(G_\mu)U_\mu$ for $G_\mu \in \left\{D_\mu^{(\rm cycle)}, D_\mu^{(\rm path)}\right\}$. In the case of $A'_{\rm as}(D_\mu^{(\rm cycle)})$, A unitary matrix U_μ is $(U_\mu)_{jk} \equiv$

$\xi^{(j-1)(k-1)}/\sqrt{|V|_\mu}$ with $\xi = \exp(-2i\pi/N)$ for $j,k \in V(D_\mu^{(\mathrm{cycle})})$. By contrast, A unitary matrix U_μ that diagonalizes the matrix $A'_{\mathrm{as}}(D_\mu^{(\mathrm{path})})$ is $(U_\mu)_{jk} \equiv i^j \cos\left(\frac{jk\pi}{|V|_\mu+1}\right)/\sqrt{|V|_\mu+1}$ for $j,k \in V(D_\mu^{(\mathrm{path})})$. Accordingly, the components of $\Lambda_{m_\mu n_\mu}$ are obtained as

$$\begin{aligned}\Lambda_{m_\mu n_\mu} &= \left(U_\mu^\dagger A'_{\mathrm{as}}(G_\mu) U_\mu\right)_{m_\mu n_\mu} \\ &= \begin{cases} 2i\sin\left(\frac{2\pi(m_\mu-1)}{|V|_\mu}\right)\delta_{m_\mu n_\mu} & \left(G_\mu = D_\mu^{(\mathrm{cycle})}\right) \\ 2i\cos\left(\frac{m_\mu\pi}{|V|_\mu+1}\right)\delta_{m_\mu n_\mu} & \left(G_\mu = D_\mu^{(\mathrm{path})}\right) \end{cases}. \end{aligned} \tag{B.3}$$

By use of these results, the diagonalization of $A_{\mathrm{as}}(G)$ are

$$\begin{aligned}&\left(\mathcal{U}^\dagger A_{\mathrm{as}}(G)\,\mathcal{U}\right)_{mn} \\ &= 2i\left\{\sum_{\mu^{\mathrm{c,e}}\in S^{\mathrm{c,e}}} \gamma_{\mu^{\mathrm{c,e}}}\sin\left(\frac{2\pi(m_{\mu^{\mathrm{c,e}}}-1)}{|V|_{\mu^{\mathrm{c,e}}}}\right)\left(\prod_{\nu=1}^{D-\mu^{\mathrm{c,e}}}\prod_{\rho=1}^{\mu^{\mathrm{c,e}}-1}\delta_{m_{D+1-\nu}n_{D+1-\nu}}\delta_{m_{\mu^{\mathrm{c,e}}}n_{\mu^{\mathrm{c,e}}}}\delta_{m_\rho n_\rho}\right)\right. \\ &\quad + \sum_{\mu^{\mathrm{c,o}}\in S^{\mathrm{c,o}}} \gamma_{\mu^{\mathrm{c,o}}}\sin\left(\frac{2\pi(m_{\mu^{\mathrm{c,o}}}-1)}{|V|_{\mu^{\mathrm{c,o}}}}\right)\left(\prod_{\nu=1}^{D-\mu^{\mathrm{c,o}}}\prod_{\rho=1}^{\mu^{\mathrm{c,o}}-1}\delta_{m_{D+1-\nu}n_{D+1-\nu}}\delta_{m_{\mu^{\mathrm{c,o}}}n_{\mu^{\mathrm{c,o}}}}\delta_{m_\rho n_\rho}\right) \\ &\quad + \sum_{\mu^{\mathrm{p,e}}\in S^{\mathrm{p,e}}} \gamma_{\mu^{\mathrm{p,e}}}\cos\left(\frac{m_{\mu^{\mathrm{p,e}}}\pi}{|V|_{\mu^{\mathrm{p,e}}}+1}\right)\left(\prod_{\nu=1}^{D-\mu^{\mathrm{p,e}}}\prod_{\rho=1}^{\mu^{\mathrm{p,e}}-1}\delta_{m_{D+1-\nu}n_{D+1-\nu}}\delta_{m_{\mu^{\mathrm{p,e}}}n_{\mu^{\mathrm{p,e}}}}\delta_{m_\rho n_\rho}\right) \\ &\quad \left. + \sum_{\mu^{\mathrm{p,o}}\in S^{\mathrm{p,o}}} \gamma_{\mu^{\mathrm{p,o}}}\cos\left(\frac{m_{\mu^{\mathrm{p,o}}}\pi}{|V|_{\mu^{\mathrm{p,o}}}+1}\right)\left(\prod_{\nu=1}^{D-\mu^{\mathrm{p,o}}}\prod_{\rho=1}^{\mu^{\mathrm{p,o}}-1}\delta_{m_{D+1-\nu}n_{D+1-\nu}}\delta_{m_{\mu^{\mathrm{p,o}}}n_{\mu^{\mathrm{p,o}}}}\delta_{m_\rho n_\rho}\right)\right\} \\ &= 2i\left\{\sum_{\mu^{\mathrm{c,e}}\in S^{\mathrm{c,e}}} \gamma_{\mu^{\mathrm{c,e}}}\sin\left(\frac{2\pi(m_{\mu^{\mathrm{c,e}}}-1)}{|V|_{\mu^{\mathrm{c,e}}}}\right) + \sum_{\mu^{\mathrm{c,o}}\in S^{\mathrm{c,o}}} \gamma_{\mu^{\mathrm{c,o}}}\sin\left(\frac{2\pi(m_{\mu^{\mathrm{c,o}}}-1)}{|V|_{\mu^{\mathrm{c,o}}}}\right)\right. \\ &\quad \left. + \sum_{\mu^{\mathrm{p,e}}\in S^{\mathrm{p,e}}} \gamma_{\mu^{\mathrm{p,e}}}\cos\left(\frac{m_{\mu^{\mathrm{p,e}}}\pi}{|V|_{\mu^{\mathrm{p,e}}}+1}\right) + \sum_{\mu^{\mathrm{p,o}}\in S^{\mathrm{p,o}}} \gamma_{\mu^{\mathrm{p,o}}}\cos\left(\frac{m_{\mu^{\mathrm{p,o}}}\pi}{|V|_{\mu^{\mathrm{p,o}}}+1}\right)\right\}\delta_{mn}\,. \end{aligned} \tag{B.4}$$

Appendix C

Numerical analysis for D-dimensional spheres

C.1 Two-dimensional sphere

In this appendix, we show that there are up to two fermion species, or four zero-eigenvalues in the anti-symmetrized adjacency matrix, on the discretized 2-sphere (graphs like 2-sphere) labeled by (M, N)[1] by numerical calculations:

- If both the number of sites on the longitude direction M and the number of sites on the latitude direction N are even, there is no fermion species of the matrix-representation of lattice Dirac matrix. For instance, we consider the discretized 2-sphere labeled by $(4, 4)$, which is depicted in Fig. C.1.

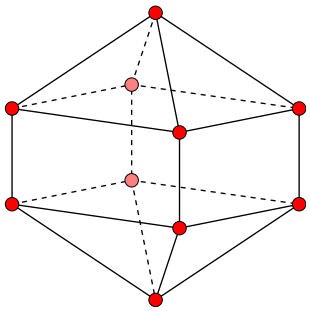

Figure C.1: Discretized 2-sphere labeled by $(4, 4)$.

The anti-symmetrized adjacency matrix of the $(4, 4)$ sphere is

$$A_{\rm as}(G^{(4,4)}_{S^2}) = \begin{pmatrix} I_2 \otimes A'_{\rm as}(D^{(\rm cycle)})_4 & \\ & O_2 \end{pmatrix} \otimes \sigma_1 + \begin{pmatrix} A'_{\rm as}(D^{(\rm path)})_2 \otimes I_4 & V_{8,2} \\ -V^\dagger_{8,2} & O_2 \end{pmatrix} \otimes \sigma_2 \,, \tag{C.1}$$

[1]Hereafter, we consider the number of sites on the latitude direction N is $N > 3$. We set the weights of all edges in the longitude direction to σ_1 and the weights of all edges in the latitude direction to σ_2.

with

$$V_{8,2} = \begin{pmatrix} 1 & 0 \\ 0 & -1 \end{pmatrix}_{2,2} \otimes \begin{pmatrix} 1 \\ 1 \\ 1 \\ 1 \end{pmatrix} . \tag{C.2}$$

where $A'_{\rm as}(D^{(\rm cycle)})_4$, $A'_{\rm as}(D^{(\rm path)})_2$ are the 4-square matrix in Eq. (3.26) and the 2-square matrix in Eq. (3.27) respectively. The matrix-representation of lattice Dirac operator on the $(4,4)$ sphere is given by $\mathcal{D}^{(4,4)} = A_{\rm as}(G^{(4,4)}_{S^2})/2$. The eigenvalues of this matrix are depicted in Fig. C.2. There is no zero-eigenvalue in $\mathcal{D}^{(4,4)}$, which means that there is no fermion species.

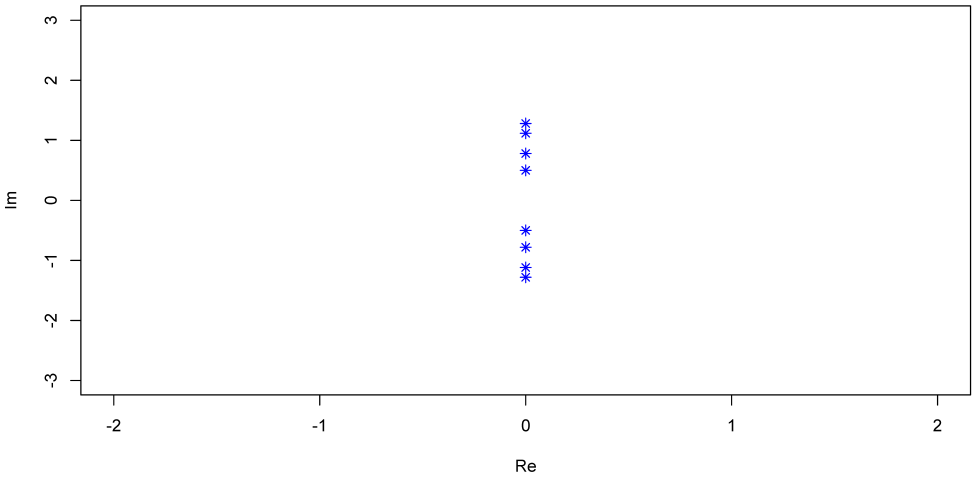

Figure C.2: Eigenvalue distribution of the matrix-representation of lattice Dirac matrix $\mathcal{D}^{(4,4)}$. There is no Dirac zero-modes, or equivalently no zero-eigenvalue.

- If M is odd and N is even, there is again no fermion species (no zero-eigenvalue). For instance, we take the discretized 2-sphere labeled by $(5,4)$. We numerically find that the number of zero-modes or the number of femrion species is zero as shown in Fig. C.3.

- If both of M and N are odd, there is a single fermion (two zero-eigenvalues). For instance, we consider the discretized 2-sphere labeled by $(5,5)$. Then, we numerically find that the number of fermion species (two zero-eigenvalues) is one as shown in Fig. C.4 and Fig. C.5. We note that a pair of eigenvalues corresponds to *a single fermion* since the two-dimensional γ matrices are 2×2 matrices. Thus, the existence of the pair of zero-eigenvalues shown in Fig. C.4 and Fig. C.5 means that there is a single fermion.

- If M is even and N is odd, there are two fermion species (four zero-eigenvalues) on the discretized 2-sphere. For instance, we take two cases, $(4,5)$ and $(6,9)$. The discretized 2-sphere $(4,5)$ is depicted in Fig. C.6.

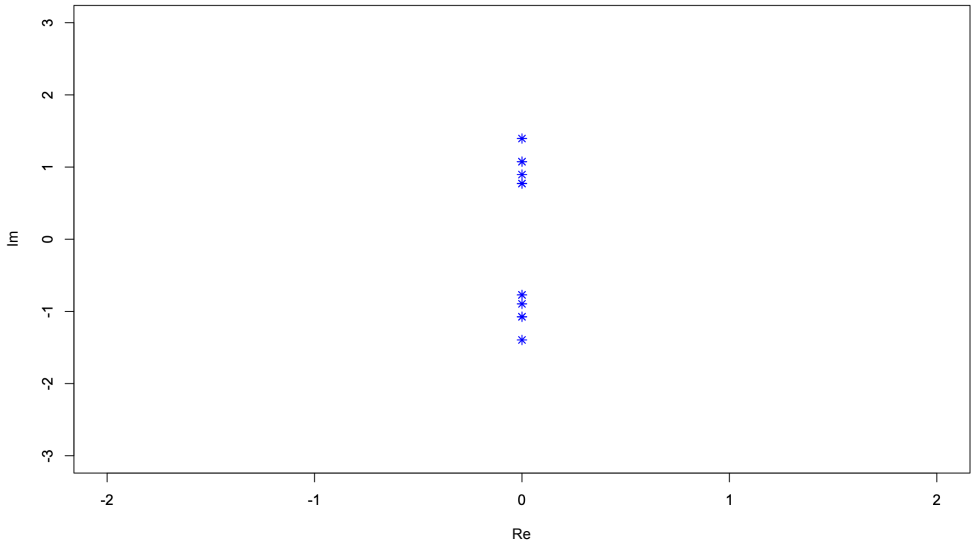

Figure C.3: Eigenvalue distribution of the matrix-representation of lattice Dirac matrix $\mathcal{D}^{(5,4)}$. There is no fermion species (no zero-eigenvalue) in $\mathcal{D}^{(5,4)}$.

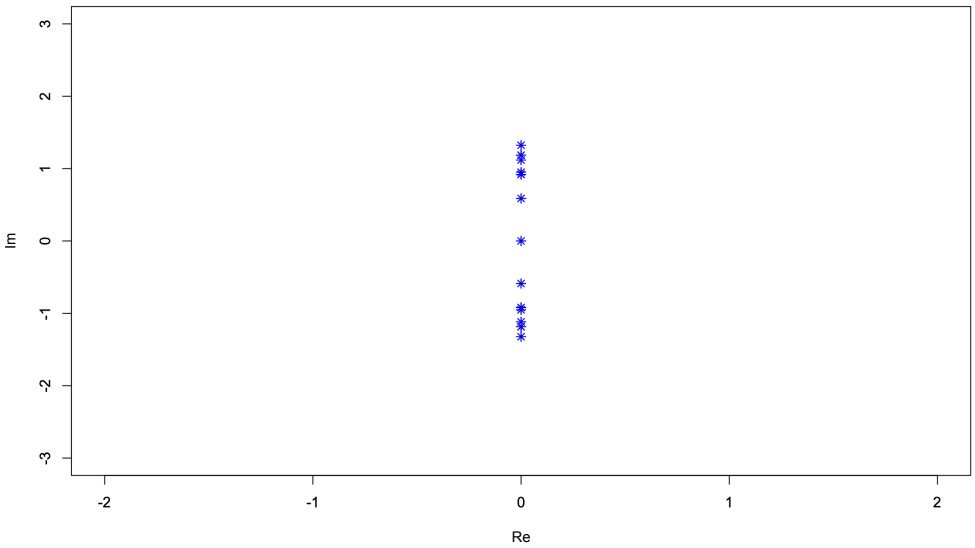

Figure C.4: Eigenvalue distribution of the matrix-representation of lattice Dirac matrix $\mathcal{D}^{(5,5)}$. The pair of zero eigenvalues corresponds to a single fermion.

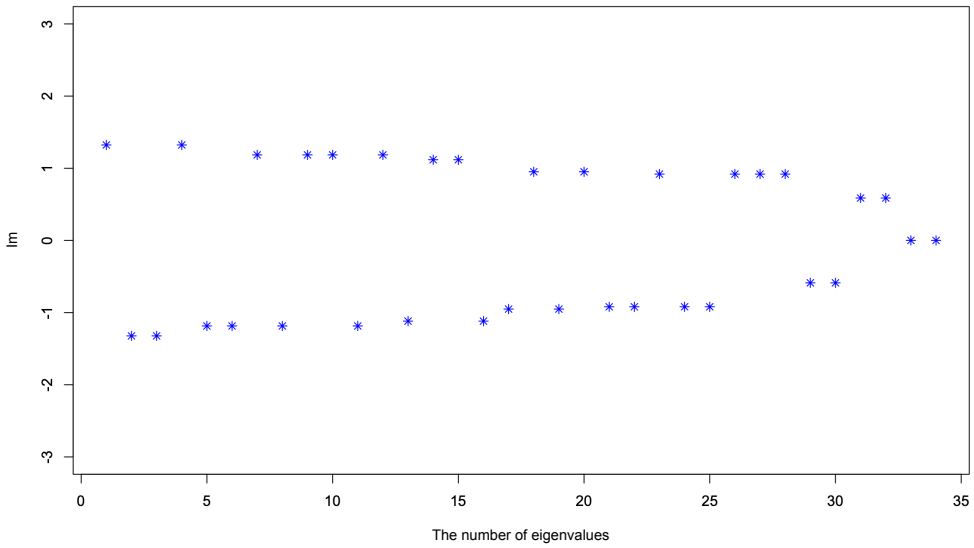

Figure C.5: Eigenvalue distribution is depicted, where the vertical axis represents the imaginary part of the Dirac matrix $\mathcal{D}^{(5,5)}$ and the horizontal axis represents the serial number of eigenvalues. The pair of zero eigenvalues corresponds to a single fermion.

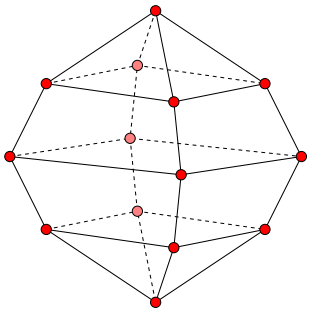

Figure C.6: Discretized 2-sphere labeled by $(4, 5)$.

The anti-symmetrized adjacency matrix of the $(4,5)$ sphere is

$$A_{\rm as}(G^{(4,5)}_{S^2}) = \begin{pmatrix} I_3 \otimes A'_{\rm as}(D^{(\rm cycle)})_4 & \\ & O_2 \end{pmatrix} \otimes \sigma_1 + \begin{pmatrix} A'_{\rm as}(D^{(\rm path)})_3 \otimes I_4 & V_{12,2} \\ -V^\dagger_{12,2} & O_2 \end{pmatrix} \otimes \sigma_2 \,, \tag{C.3}$$

with

$$V_{12,2} = \begin{pmatrix} 1 & 0 \\ 0 & 0 \\ 0 & -1 \end{pmatrix}_{3,2} \otimes \begin{pmatrix} 1 \\ 1 \\ 1 \\ 1 \end{pmatrix} . \tag{C.4}$$

The matrix-representation of lattice Dirac operator on the $(4,5)$ sphere is given by $\mathcal{D}^{(4,5)} = A_{\rm as}(G^{(4,5)}_{S^2})/2$. The eigenvalues of this matrix are depicted in Fig. C.7. There are two fermion species on 2-sphere $(4,5)$ since there are four zero-eigenvalues as seen from Fig. C.8.

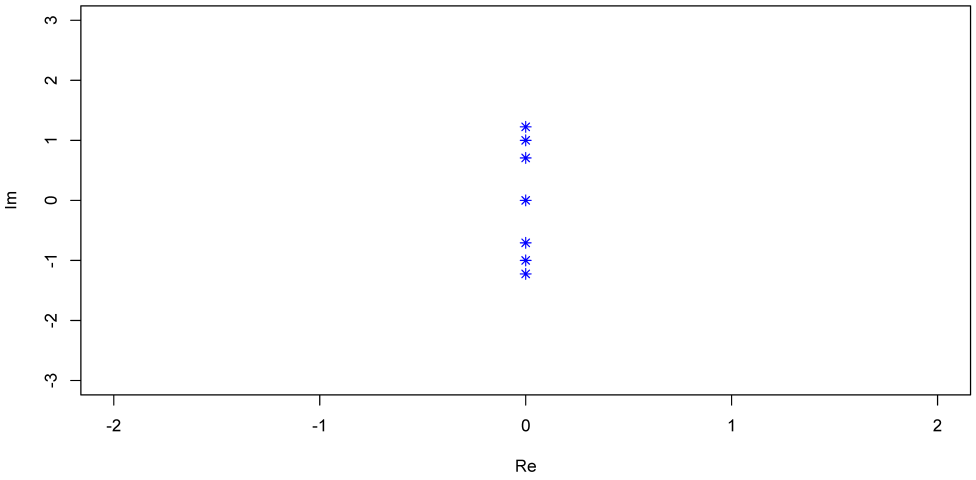

Figure C.7: Eigenvalue distribution of the matrix-representation of lattice Dirac operator $\mathcal{D}^{(4,5)}$. There are four zero-eigenvalues corresponding to two fermion species in two dimensions.

In the case of the $(6,9)$ 2-sphere, the anti-symmetrized adjacency matrix is

$$A_{\rm as}(G^{(6,9)}_{S^2}) = \begin{pmatrix} I_7 \otimes A'_{\rm as}(D^{(\rm cycle)})_6 & \\ & O_2 \end{pmatrix} \otimes \sigma_1 + \begin{pmatrix} A'_{\rm as}(D^{(\rm path)})_7 \otimes I_6 & V_{42,2} \\ -V^\dagger_{42,2} & O_2 \end{pmatrix} \otimes \sigma_2 \,, \tag{C.5}$$

with

$$V_{42,2} = \begin{pmatrix} 1 & 0 \\ 0 & 0 \\ 0 & 0 \\ 0 & 0 \\ 0 & 0 \\ 0 & 0 \\ 0 & -1 \end{pmatrix}_{7,2} \otimes \begin{pmatrix} 1 \\ 1 \\ 1 \\ 1 \\ 1 \\ 1 \end{pmatrix} . \tag{C.6}$$

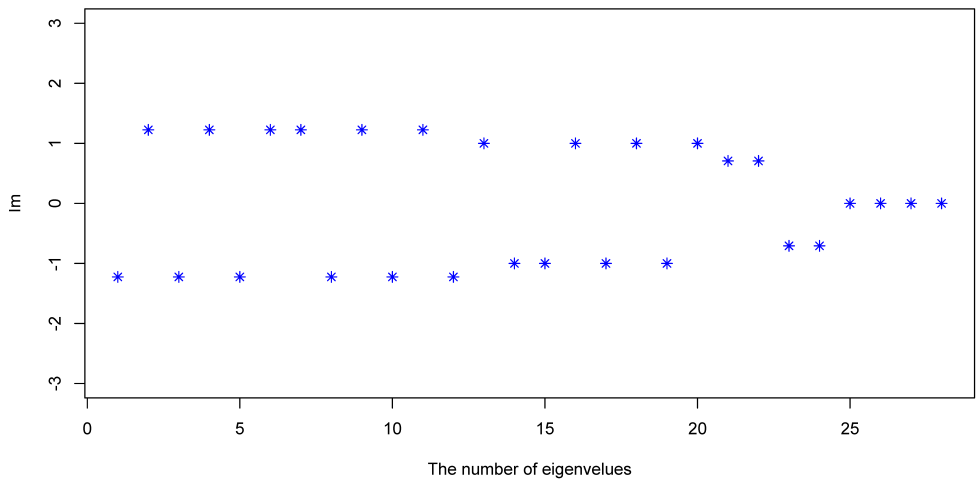

Figure C.8: Eigenvalue distribution is depicted, where the vertical axis represents the imaginary part of the matrix-representation of lattice Dirac operator $\mathcal{D}^{(4,5)}$ and the horizontal axis represents the serial number of eigenvalues. There are four zero-eigenvalues corresponding to two fermion species in two dimensions.

The matrix-representation of lattice Dirax operator on the $(6, 9)$ sphere is given by $\mathcal{D}^{(6,9)} = A_{\rm as}(G^{(6,9)}_{S^2})/2$. The eigenvalues of this matrix $\mathcal{D}^{(6,9)}$ are depicted in Fig. C.9. There are again two fermion species as there are four zero-eigenvalues in $\mathcal{D}^{(6,9)}$ as seen from from Fig. C.10.

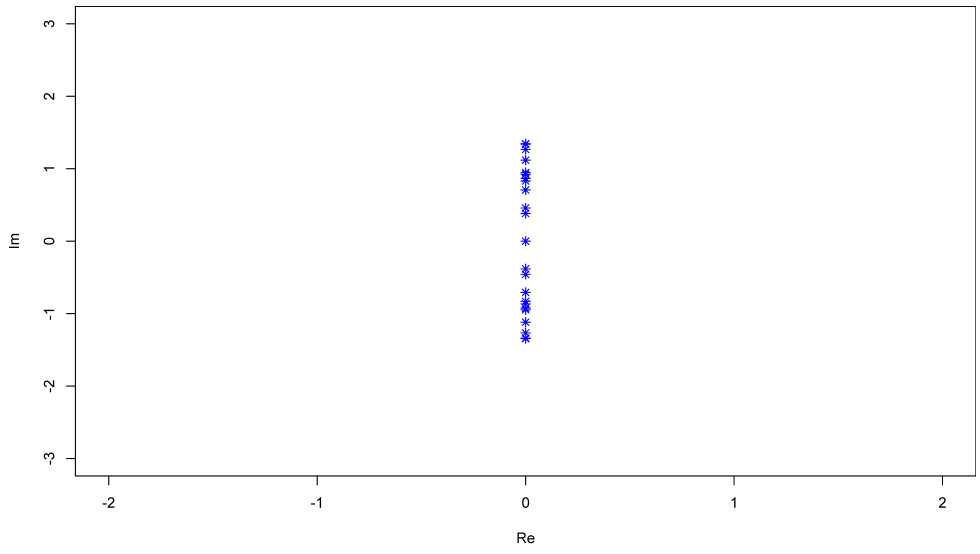

Figure C.9: Eigenvalue distribution of the matrix-representation of lattice Dirac operator $\mathcal{D}^{(6,9)}$. There are two fermion species (four zero-eigenvalues).

We summarize our results in Table. C.1.

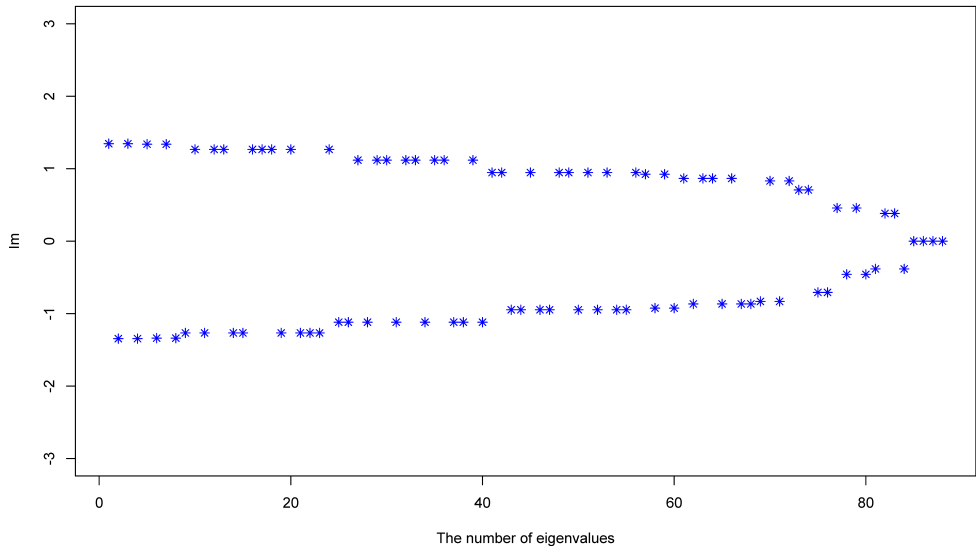

Figure C.10: Eigenvalue distribution is depicted, where the vertical axis represents the imaginary part of the matrix-representation of lattice Dirac operator $\mathcal{D}^{(6,9)}$ and horizontal axis represents the serial number of eigenvalues. There are four zero-eigenvalues corresponding to two fermion species in two dimensions.

Table C.1: Maximal number of the fermion species on 2-sphere (M, N)

the number of M	the number of N	maximal # of fermion species
even	even	0
odd	even	0
odd	odd	1
even	odd	2

C.2 Four-dimensional sphere

We discuss the discretized four-dimensional sphere. We first consider the discretized four-dimensional spherical-coordinate system for 4-sphere labeled by four integers (N_1, N_2, N_3, N_4) as

$$x_5 = r\cos\theta_4, \qquad x_4 = r\sin\theta_4\cos\theta_3, \qquad x_3 = r\sin\theta_4\sin\theta_3\cos\theta_2, \tag{C.7}$$

$$x_2 = r\sin\theta_4\sin\theta_3\sin\theta_2\cos\theta_1, \qquad x_1 = r\sin\theta_4\sin\theta_3\sin\theta_2\sin\theta_1 \tag{C.8}$$

where r is a radial distance and the four angles are discretized as $\theta_1 \equiv \frac{2\pi}{N_1}(n_1 - 1)$, $\theta_i \equiv \frac{\pi}{N_i - 1}(n_i - 1)$ for $i = 2, 3, 4$. $n_1, n_i \in \mathbb{N}$ run as $n_1 \in [1, N_1]$, $n_i \in [1, N_i]$. For simplicity, we fix a radial distance as $r = 1$. In a parallel manner to the discussion for 2-sphere, we label the lattice sites as (n_1, n_2, n_3, n_4). And we set the weights of all edges in the n_μ-direction to γ_μ.

For instance, we take $N_1 = 4$ and $N_i = 3$ for $i = 2, 3, 4$. A graph corresponding to the $(4, 3, 3, 3)$ 4-sphere is depicted in Fig. C.11. The anti-symmetrized adjacency matrix of

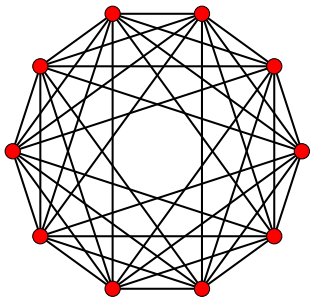

Figure C.11: A graph corresponding to the $(4,3,3,3)$ 4-sphere is the 5-orthoplex inside Petrie polygon ($G^{(4,3,3,3)}_{S^4}$).

the graph is given as

$$A_{\rm as}(G^{(4,3,3,3)}_{S^4}) = \begin{pmatrix} A'_{\rm as}(D^{(\rm cycle)})_4 & & \\ & O_6 & \end{pmatrix} \otimes \gamma_1 + \begin{pmatrix} O_4 & V_{4,2} & \\ -V^\dagger_{4,2} & O_2 & \\ & & O_4 \end{pmatrix} \otimes \gamma_2 + \begin{pmatrix} O_6 & V_{6,2} & \\ -V^\dagger_{6,2} & O_2 & \\ & & O_2 \end{pmatrix} \otimes \gamma_3 + \begin{pmatrix} O_8 & V_{8,2} \\ -V^\dagger_{8,2} & O_2 \end{pmatrix} \otimes \gamma_4 \quad . \tag{C.9}$$

The matrix-representation of lattice Dirac operator is given by $\mathcal{D}^{(4,3,3,3)} = A_{\rm as}(G^{(4,3,3,3)}_{S^4})/2$ This matrix $\mathcal{D}^{(4,3,3,3)}$ is 10×10 square matrix, apart from the γ matrix structure.

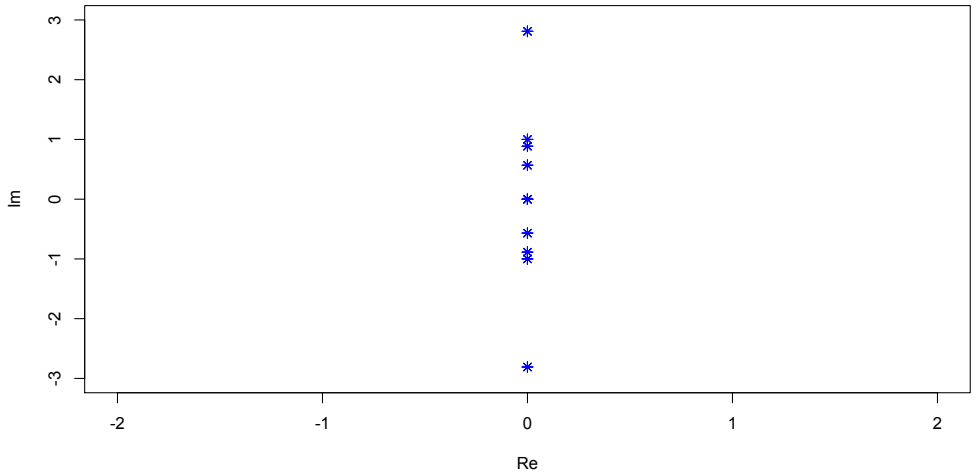

Figure C.12: Eigenvalue distribution of the matrix-representation of lattice Dirac operator $\mathcal{D}^{(4,3,3,3)}$. There are two fermion species in four dimensions, which emerge as eight zero-eigenvalues in the figure.

Fig. C.12 and Fig. C.13 shows the eigenvalue distributions of the matrix-representtion of lattice Dirac operator $\mathcal{D}^{(4,3,3,3)}$. For the dicretized 4-sphere $(4,3,3,3)$, we find that there are two fermion species as there are eight zero-eigenvalues of the matrix-representation of lattice Dirac operator $\mathcal{D}^{(4,3,3,3)}$.

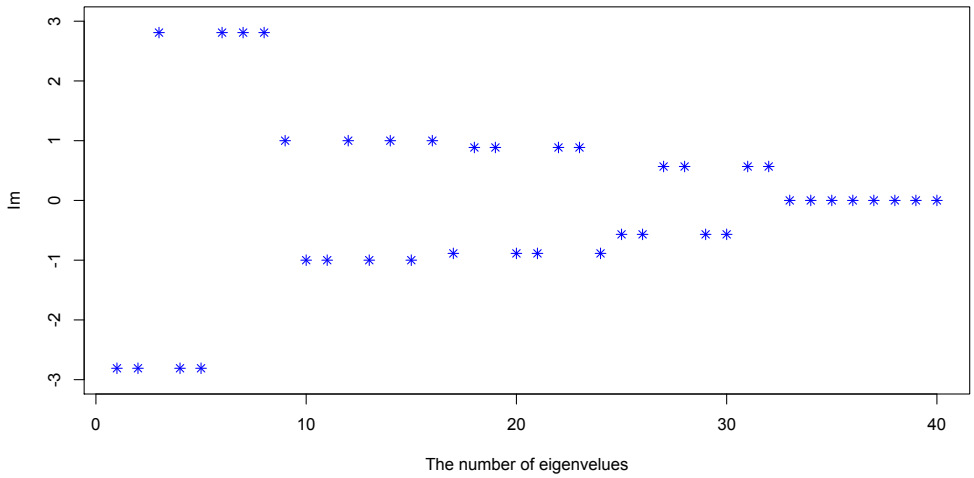

Figure C.13: Eigenvalues of the matrix-representation of lattice Dirac operator $\mathcal{D}^{(4,3,3,3)}$. There are eight zero-eigenvalues corresponding to two fermion species in four dimensions.

By studying other cases, we find that the number of femrion species on the discretized 4-sphere (N_1, N_2, N_3, N_4) is two when the number of sites N_1 is even and the number of sites N_i for i from 2 to 4 are odd, as with the case on the discretized 2-sphere (M, N). We could not find any example where the number of femrion species goes beyond two in four dimensions too.

Bibliography

[1] K. G. Wilson, "Confinement of Quarks," *Phys. Rev.* **D10** (1974) 2445–2459.

[2] M. Creutz, "Monte Carlo Study of Quantized SU(2) Gauge Theory," *Phys. Rev.* **D21** (1980) 2308–2315.

[3] H. B. Nielsen and M. Ninomiya, "Absence of Neutrinos on a Lattice. 1. Proof by Homotopy Theory," *Nucl. Phys.* **B185** (1981) 20.

[4] H. B. Nielsen and M. Ninomiya, "Absence of Neutrinos on a Lattice. 2. Intuitive Topological Proof," *Nucl. Phys.* **B193** (1981) 173–194.

[5] H. B. Nielsen and M. Ninomiya, "No Go Theorem for Regularizing Chiral Fermions," *Phys. Lett.* **105B** (1981) 219–223.

[6] H. Hopf, "Vektorfelder in n-dimensionalen-mannigfaltigkeiten," *Mathematische Annalen* **96** (1927) 225–250. `http://eudml.org/doc/159166`.

[7] K. G. Wilson, "Quarks and Strings on a Lattice," in *New Phenomena in Subnuclear Physics: Proceedings, International School of Subnuclear Physics, Erice, Sicily, Jul 11-Aug 1 1975. Part A*, pp. 69–142. 1975. `https://doi.org/10.1007/978-1-4613-4208-3_6`.

[8] D. B. Kaplan, "A Method for simulating chiral fermions on the lattice," *Phys. Lett.* **B288** (1992) 342–347, `arXiv:hep-lat/9206013 [hep-lat]`.

[9] Y. Shamir, "Chiral fermions from lattice boundaries," *Nucl. Phys.* **B406** (1993) 90–106, `arXiv:hep-lat/9303005 [hep-lat]`.

[10] V. Furman and Y. Shamir, "Axial symmetries in lattice QCD with Kaplan fermions," *Nucl. Phys. B* **439** (1995) 54–78, `arXiv:hep-lat/9405004`.

[11] H. Neuberger, "More about exactly massless quarks on the lattice," *Phys. Lett.* **B427** (1998) 353–355, `arXiv:hep-lat/9801031 [hep-lat]`.

[12] P. H. Ginsparg and K. G. Wilson, "A Remnant of Chiral Symmetry on the Lattice," *Phys. Rev.* **D25** (1982) 2649.

[13] J. B. Kogut and L. Susskind, "Hamiltonian Formulation of Wilson's Lattice Gauge Theories," *Phys. Rev.* **D11** (1975) 395–408.

[14] L. Susskind, "Lattice Fermions," *Phys. Rev.* **D16** (1977) 3031–3039.

[15] N. Kawamoto and J. Smit, "Effective Lagrangian and Dynamical Symmetry Breaking in Strongly Coupled Lattice QCD," *Nucl. Phys. B* **192** no. 1, (1981) 100–124. https://www.sciencedirect.com/science/article/pii/0550321381901966.

[16] H. S. Sharatchandra, H. J. Thun, and P. Weisz, "Susskind Fermions on a Euclidean Lattice," *Nucl. Phys.* **B192** (1981) 205–236.

[17] M. F. Golterman and J. Smit, "Selfenergy and Flavor Interpretation of Staggered Fermions," *Nucl. Phys. B* **245** (1984) 61–88.

[18] M. F. Golterman, "STAGGERED MESONS," *Nucl. Phys. B* **273** (1986) 663–676.

[19] G. Kilcup and S. R. Sharpe, "A Tool Kit for Staggered Fermions," *Nucl. Phys. B* **283** (1987) 493–550.

[20] W. Bietenholz and I. Hip, "The Scaling of exact and approximate Ginsparg-Wilson fermions," *Nucl. Phys. B* **570** (2000) 423–451, arXiv:hep-lat/9902019.

[21] M. Creutz, T. Kimura, and T. Misumi, "Index Theorem and Overlap Formalism with Naive and Minimally Doubled Fermions," *JHEP* **12** (2010) 041, arXiv:1011.0761 [hep-lat].

[22] S. Dürr and G. Koutsou, "Brillouin improvement for Wilson fermions," *Phys. Rev. D* **83** (Jun, 2011) 114512, arXiv:1012.3615 [hep-lat]. https://link.aps.org/doi/10.1103/PhysRevD.83.114512.

[23] S. Dürr, G. Koutsou, and T. Lippert, "Meson and Baryon dispersion relations with Brillouin fermions," *Phys. Rev. D* **86** (2012) 114514, arXiv:1208.6270 [hep-lat].

[24] T. Misumi, "New fermion discretizations and their applications," *PoS* **LATTICE2012** (2012) 005, arXiv:1211.6999 [hep-lat].

[25] Y.-G. Cho, S. Hashimoto, J.-I. Noaki, A. Juttner, and M. Marinkovic, "$O(a^2)$-improved actions for heavy quarks and scaling studies on quenched lattices," *PoS* **LATTICE2013** (2014) 255, arXiv:1312.4630 [hep-lat].

[26] Y.-G. Cho, S. Hashimoto, A. Juttner, T. Kaneko, M. Marinkovic, J.-I. Noaki, and J. T. Tsang, "Improved lattice fermion action for heavy quarks," *JHEP* **05** (2015) 072, arXiv:1504.01630 [hep-lat].

[27] S. Dürr and G. Koutsou, "On the suitability of the Brillouin action as a kernel to the overlap procedure," arXiv:1701.00726 [hep-lat].

[28] D. H. Adams, "Theoretical foundation for the index theorem on the lattice with staggered fermions," *Phys.Rev.Lett.* **104** (2010) 141602, arXiv:0912.2850 [hep-lat].

[29] D. H. Adams, "Pairs of chiral quarks on the lattice from staggered fermions," *Phys.Lett.B* **699** (2011) 394–397, arXiv:1008.2833 [hep-lat].

[30] C. Hoelbling, "Single flavor staggered fermions," *Phys.Lett.B* **696** (2011) 422–425, arXiv:1009.5362 [hep-lat].

[31] P. de Forcrand, A. Kurkela, and M. Panero, "Numerical properties of staggered overlap fermions," *PoS* **LATTICE2010** (2010) 080, arXiv:1102.1000 [hep-lat].

[32] M. Creutz, T. Kimura, and T. Misumi, "Aoki Phases in the Lattice Gross-Neveu Model with Flavored Mass terms," *Phys. Rev.* **D83** (2011) 094506, arXiv:1101.4239 [hep-lat].

[33] T. Misumi, M. Creutz, T. Kimura, T. Z. Nakano, and A. Ohnishi, "Aoki Phases in Staggered-Wilson Fermions," *PoS* **LATTICE2011** (2011) 108, arXiv:1110.1231 [hep-lat].

[34] E. Follana, V. Azcoiti, G. Di Carlo, and A. Vaquero, "Spectral Flow and Index Theorem for Staggered Fermions," *PoS* **LATTICE2011** (2011) 100, arXiv:1111.3502 [hep-lat].

[35] P. de Forcrand, A. Kurkela, and M. Panero, "Numerical properties of staggered quarks with a taste-dependent mass term," *JHEP* **04** (2012) 142, arXiv:1202.1867 [hep-lat].

[36] T. Misumi, T. Z. Nakano, T. Kimura, and A. Ohnishi, "Strong-coupling analysis of parity phase structure in staggered-wilson fermions," *Phys.Rev.D* **86** (2012) 034501, arXiv:1205.6545 [hep-lat].

[37] S. Dürr, "Taste-split staggered actions: eigenvalues, chiralities and Symanzik improvement," *Phys. Rev. D* **87** (Jun, 2013) 114501, arXiv:1302.0773 [hep-lat]. https://link.aps.org/doi/10.1103/PhysRevD.87.114501.

[38] C. Hoelbling and C. Zielinski, "Spectral properties and chiral symmetry violations of (staggered) domain wall fermions in the Schwinger model," *Phys. Rev. D* **94** no. 1, (2016) 014501, arXiv:1602.08432 [hep-lat].

[39] C. Zielinski, *Theoretical and Computational Aspects of New Lattice Fermion Formulations*. PhD thesis, Nanyang Technol. U., 2016. arXiv:1703.06364 [hep-lat].

[40] L. H. Karsten, "Lattice Fermions in Euclidean Space-time," *Phys. Lett. B* **104** (1981) 315–319.

[41] F. Wilczek, "ON LATTICE FERMIONS," *Phys. Rev. Lett.* **59** (1987) 2397.

[42] M. Creutz, "Four-dimensional graphene and chiral fermions," *JHEP* **04** (2008) 017, arXiv:0712.1201 [hep-lat].

[43] A. Borici, "Creutz fermions on an orthogonal lattice," *Phys. Rev. D* **78** (2008) 074504, arXiv:0712.4401 [hep-lat].

[44] P. F. Bedaque, M. I. Buchoff, B. C. Tiburzi, and A. Walker-Loud, "Broken Symmetries from Minimally Doubled Fermions," *Phys. Lett. B* **662** (2008) 449–455, arXiv:0801.3361 [hep-lat].

[45] P. F. Bedaque, M. I. Buchoff, B. C. Tiburzi, and A. Walker-Loud, "Search for Fermion Actions on Hyperdiamond Lattices," *Phys. Rev. D* **78** (2008) 017502, arXiv:0804.1145 [hep-lat].

[46] S. Capitani, J. Weber, and H. Wittig, "Minimally doubled fermions at one loop," *Phys. Lett. B* **681** (2009) 105–112, arXiv:0907.2825 [hep-lat].

[47] T. Kimura and T. Misumi, "Characters of Lattice Fermions Based on the Hyperdiamond Lattice," *Prog. Theor. Phys.* **124** (2010) 415–432, arXiv:0907.1371 [hep-lat].

[48] T. Kimura and T. Misumi, "Lattice Fermions Based on Higher-Dimensional Hyperdiamond Lattices," *Prog. Theor. Phys.* **123** (2010) 63–78, arXiv:0907.3774 [hep-lat].

[49] M. Creutz and T. Misumi, "Classification of Minimally Doubled Fermions," *Phys. Rev. D* **82** (2010) 074502, arXiv:1007.3328 [hep-lat].

[50] S. Capitani, M. Creutz, J. Weber, and H. Wittig, "Renormalization of minimally doubled fermions," *JHEP* **09** (2010) 027, arXiv:1006.2009 [hep-lat].

[51] B. C. Tiburzi, "Chiral Lattice Fermions, Minimal Doubling, and the Axial Anomaly," *Phys. Rev. D* **82** (2010) 034511, arXiv:1006.0172 [hep-lat].

[52] S. Kamata and H. Tanaka, "Minimal Doubling Fermion and Hermiticity," *PTEP* **2013** (2013) 023B05, arXiv:1111.4536 [hep-lat].

[53] T. Misumi, "Phase structure for lattice fermions with flavored chemical potential terms," *JHEP* **08** (2012) 068, arXiv:1206.0969 [hep-lat].

[54] T. Misumi, T. Kimura, and A. Ohnishi, "QCD phase diagram with 2-flavor lattice fermion formulations," *Phys. Rev. D* **86** (2012) 094505, arXiv:1206.1977 [hep-lat].

[55] S. Capitani, "Reducing the number of counterterms with new minimally doubled actions," *Phys. Rev. D* **89** no. 1, (2014) 014501, arXiv:1307.7497 [hep-lat].

[56] S. Capitani, "New chiral lattice actions of the Borici-Creutz type," *Phys. Rev. D* **89** no. 7, (2014) 074508, arXiv:1311.5664 [hep-lat].

[57] T. Misumi, "Fermion Actions extracted from Lattice Super Yang-Mills Theories," *JHEP* **12** (2013) 063, arXiv:1311.4365 [hep-lat].

[58] J. H. Weber, S. Capitani, and H. Wittig, "Numerical studies of Minimally Doubled Fermions," *PoS* **LATTICE2013** (2014) 122, arXiv:1312.0488 [hep-lat].

[59] J. H. Weber, *Properties of minimally doubled fermions*. PhD thesis, Mainz U., 2015. arXiv:1706.07104 [hep-lat].

[60] S. Dürr and J. H. Weber, "Dispersion relation and spectral range of Karsten-Wilczek and Borici-Creutz fermions," *Phys. Rev. D* **102** (Jul, 2020) 014516, arXiv:2003.10803 [hep-lat]. https://link.aps.org/doi/10.1103/PhysRevD.102.014516.

[61] T. Kimura, S. Komatsu, T. Misumi, T. Noumi, S. Torii, and S. Aoki, "Revisiting symmetries of lattice fermions via spin-flavor representation," *JHEP* **01** (2012) 048, arXiv:1111.0402 [hep-lat].

[62] A. Chowdhury, A. Harindranath, J. Maiti, and S. Mondal, "Many avatars of the wilson fermion: A perturbative analysis," *JHEP* **02** (2013) 037, arXiv:1301.0675 [hep-lat].

[63] J. Yumoto and T. Misumi, "Lattice fermions as spectral graphs," *JHEP* **02** (2022) 104, arXiv:2112.13501 [hep-lat].

[64] J. Yumoto and T. Misumi, "New conjecture on exact Dirac zero-modes of lattice fermions," *PTEP* **2023** no. 9, (2023) 093B01, arXiv:2301.09805 [hep-lat].

[65] D. West, *Introduction to Graph Theory*. Featured Titles for Graph Theory. Prentice Hall, 2001. https://books.google.co.jp/books?id=TuvuAAAAMAAJ.

[66] J. Bondy and U. Murty, *Graph Theory with Applications*. American Elsevier Publishing Company, 1976. https://books.google.co.jp/books?id=4bwrAAAAYAAJ.

[67] P. v. Mieghem, *Graph Spectra for Complex Networks*. Cambridge University Press, 2010.

[68] D. J. Watts and S. H. Strogatz, "Collective dynamics of 'small-world' networks," *Nature* **393** no. 6684, (1998) 440–442. https://doi.org/10.1038/30918.

[69] A. Kaveh and H. Rahami, "A unified method for eigendecomposition of graph products," *Communications in Numerical Methods in Engineering* **21** no. 7, (2005) 377–388, https://onlinelibrary.wiley.com/doi/pdf/10.1002/cnm.753. https://onlinelibrary.wiley.com/doi/abs/10.1002/cnm.753.

[70] G. Sabidussi, "Graph multiplication," *Mathematische Zeitschrift* **72** no. 1, (1959) 446–457. https://doi.org/10.1007/BF01162967.

[71] F. Aurenhammer, J. Hagauer, and W. Imrich, "Cartesian graph factorization at logarithmic cost per edge," *computational complexity* **2** no. 4, (1992) 331–349. https://doi.org/10.1007/BF01200428.

[72] W. N. Anderson and T. D. Morley, "Eigenvalues of the laplacian of a graph," *Linear and Multilinear Algebra* **18** no. 2, (1985) 141–145. https://doi.org/10.1080/03081088508817681.

[73] S. Kamata, S. Matsuura, T. Misumi, and K. Ohta, "Anomaly and sign problem in $\mathcal{N} = (2, 2)$ SYM on polyhedra: Numerical analysis," *PTEP* **2016** no. 12, (2016) 123B01, arXiv:1607.01260 [hep-th].

[74] S. Kamata, S. Matsuura, T. Misumi, and K. Ohta, "Numerical Analysis of Discretized $\mathcal{N} = (2, 2)$ SYM on Polyhedra," *PoS* **LATTICE2016** (2016) 210, arXiv:1612.01968 [hep-lat].

[75] R. C. Brower, E. S. Weinberg, G. T. Fleming, A. D. Gasbarro, T. G. Raben, and C.-I. Tan, "Lattice dirac fermions on a simplicial riemannian manifold," *Phys. Rev. D* **95** (Jun, 2017) 114510. https://link.aps.org/doi/10.1103/PhysRevD.95.114510.

[76] K. Ohta and S. Matsuura, "Supersymmetric Gauge Theory on the Graph," arXiv:2111.00676 [hep-th].